6-1-2023

Enabling Energy Efficiency in Connected and Automated Vehicles through Predictive Control Techniques

Farhang Motallebiaraghi
Western Michigan University

ENABLING ENERGY EFFICIENCY IN CONNECTED AND AUTOMATED VEHICLES THROUGH PREDICTIVE CONTROL TECHNIQUES

Farhang Motallebiaraghi, Ph.D.

Western Michigan University, 2023

The transportation sector is a significant contributor to global energy consumption and emissions, necessitating the development of sustainable transportation systems. In this regard, connected and automated vehicles (CAVs) have emerged as a potential solution to transform the transportation industry. By harnessing advanced mapping and location technologies, Vehicle-to-Vehicle (V2V) and Vehicle-to-Infrastructure (V2I) communication, CAVs offer the promise of improving efficiency, reducing traffic congestion, and enhancing safety and comfort. However, the adoption of CAVs also brings about various challenges, including energy efficiency concerns that need to be addressed to fully realize their potential benefits. This dissertation investigates energy-efficient control techniques for transportation vehicles using connected and automated vehicles. The primary research question driving this study is: How can energy-efficient controls be implemented with consideration of current and near future CAV technologies? By exploring this question, the study aims to examine the practical implementation of energy-efficient control techniques specifically within the context of connected and automated vehicles. The research hypothesis posits that the implementation of energy-efficient control techniques in transportation vehicles, leveraging the capabilities of connected and automated technologies, will lead to significant reductions in energy consumption and emissions while maintaining or improving overall vehicle performance. This hypothesis will be empirically tested through comprehensive data analysis and evaluation. By addressing this research question and hypothesis, this dissertation seeks to contribute to the development of effective energy-efficient control strategies for transportation vehicles. The investigation will provide insights and recommendations for integrating energy-efficient controls in connected and automated vehicles, with the ultimate goal of promoting sustainability and reducing energy consumption within the transportation sector. Artificial neural networks (ANNs), predictive optimal energy management strategies (POEMS), and autonomous eco-driving control are studied to improve fuel economy, energy efficiency, drivability, and safety. The study compares optimal energy management strategies and evaluates predictive optimal energy management strategies in hybrid electric vehicles and connected vehicles.

It also integrates POEMS with optimal traffic management to enhance system efficiency and develops accurate models for predicting emissions and fuel economy in light-duty vehicles. The research identifies research gaps in energy-efficient control of electrified autonomous vehicle eco-driving and evaluates the energy-saving potential of autonomous eco-driving control. The findings demonstrate that connected and automated vehicles offer new prospects for energy-efficient driving, and the application of these methods can significantly improve energy efficiency and reduce emissions in transportation vehicles. The results have implications for the development of energy-efficient control strategies for future transportation systems. By addressing the challenges of energy efficiency and sustainability in transportation, this dissertation contributes to the development of more sustainable transportation systems.

ENABLING ENERGY EFFICIENCY IN CONNECTED AND AUTOMATED VEHICLES THROUGH PREDICTIVE CONTROL TECHNIQUES

by

Farhang Motallebiaraghi

A dissertation submitted to the Graduate College
in partial fulfillment of the requirements
for the degree of Doctor of Philosophy
Mechanical Engineering
Western Michigan University
June 2023

Dissertation Committee:

Zachary D. Asher, Ph.D., Chair
Richard T. Meyer, Ph.D.
Alvis C Fong, Ph.D.
Damon Miller, Ph.D.

Acknowledgments

I extend my heartfelt thanks to my advisor, Dr. Zachary D. Asher, for their invaluable guidance and support. Their unwavering dedication and expert mentorship have been crucial throughout my study journey.

I also express my gratitude to my dissertation committee members, Dr. Alvis Fong, Dr. Damon Miller, and Dr. Richard Meyer, for their insightful comments and constructive criticism, which have helped shape and refine this dissertation.

Furthermore, I am deeply thankful to my collaborators from Colorado State University, including Dr. Thomas Bradley, Aaron Rabinowitz, Yao Kaisen, and researchers at the National Renewable Energy Lab, Dr. Jake Holden, Dr. Venu Garikapati, and Dr. Christopher Hoehne, for their invaluable contributions to this research project.

I would also like to acknowledge the members of the EEAV lab, past and present, for their support and input, which has helped shape my thinking and approach.

Finally, I extend my deepest appreciation to my friends and family for their unwavering love, encouragement, and support throughout this journey. Without your support, this dissertation would not have been possible.

To all those who have supported me on this journey, I extend my sincere gratitude. Your support has been integral to the success of this research project.

Farhang Motallebiaraghi

Table of Contents

List of Tables

List of Figures

Chapter 1

Connected and Automated Vehicles Technology and Energy Management

1.1 Introduction

Autonomous driving and Connected and Automated Vehicles (CAVs) have received significant attention due to their potential to revolutionize transportation systems. CAVs offer various benefits such as improved safety, traffic control, and energy-efficient driving. However, it is crucial to consider the power consumption of CAVs' equipment. Therefore, this dissertation focuses on enhancing energy efficiency in CAVs through a control and planning architecture. The chapter provides an overview of key components of CAV technology, including vehicle automation, connectivity, and powertrains, highlighting their interconnectedness. Additionally, the chapter delves into the topic of CAV technology and energy management, discussing current developments and challenges that need to be addressed.

1.2 CAV Technology

CAVs are a type of vehicle equipped with advanced technologies that enable them to operate with minimal driver input or no human intervention at all. CAVs are equipped with a range of sensors, cameras, radar, lidar, and other technologies that allow them to perceive their environment and make decisions based on this information. These sensors enable CAVs to detect and respond to other vehicles, pedestrians, and road infrastructure, making them safer and more efficient.

In addition to advanced sensing technologies, CAVs are also equipped with advanced communication systems that allow them to connect with other vehicles, traffic infrastructure, and control centers. This connectivity enables CAVs to share information about traffic conditions, road hazards, and other pertinent information, en-

hancing their safety and efficiency. For example, CAVs can receive real-time information about traffic conditions, weather, and road closures, allowing them to adjust their routes and speeds to avoid congestion and potential hazards.

1.2.1 Vehicles Automation

CAVs can operate in a range of driving modes, including fully autonomous, semi-autonomous, and driver-assisted modes. In fully autonomous mode, the vehicle can operate without any human input, while in semi-autonomous mode, the vehicle requires some human input but can also operate autonomously. In driver-assisted mode, the vehicle provides assistance to the driver but does not operate autonomously.

To regulate the impact of AVs on traditional road users, it's crucial to understand their level of autonomy. The National Highway Traffic Safety Administration (NHTSA) and the Society of Automotive Engineers (SAE) both define levels of automation. The SAE's six levels range from 0 (no automation) to 5 (fully self-driving). Most AV development is at Level 3, where drivers can take control in specific situations. The NHTSA used the SAE's definitions and has identified five levels of automation. Level 0 is manual control, Level 1 is driver assistance, and Level 2 is partial automation. Level 3 is conditional automation, Level 4 is high automation, and Level 5 is full automation. Figure 1.1 [6] depicts the various levels of driving automation for autonomous vehicles (AVs) as defined by NHTSA [7].

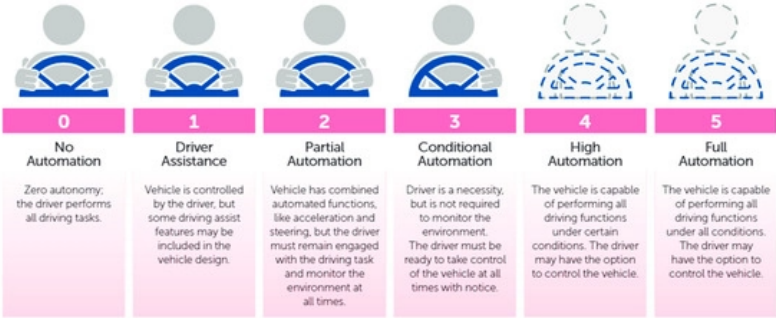

Figure 1.1: Levels of autonomous driving.

1.2.2 Vehicles Connectivity

Intelligent transportation systems (ITS) involve integrating various technologies and services to improve transportation efficiency and safety. Vehicle connectivity is a key aspect of ITS, enabled by technologies such as Dedicated Short-Range Communications (DSRC) and cellular communications. DSRC enables Vehicle-to-vehicle (V2V) and Vehicle-to-infrastructure (V2I) communication, but has limitations in range and bandwidth. Cellular communications provide internet connectivity to access cloud-based data and services, enabling more sophisticated applications, such as predictive maintenance and personalized advertising. However, cellular connectivity

poses challenges, such as security and reliability concerns. Therefore, a combination of DSRC and cellular communications is often used to achieve optimal vehicle connectivity in ITS.

- **DSRC:** A wireless communication technology that allows vehicles to communicate with each other and with roadside infrastructure for V2V and V2I communication.
- **V2V:** A wireless communication technology that enables vehicles to exchange information about their location, speed, and other data relevant to traffic safety and efficiency.
- **V2I:** A wireless communication technology that enables vehicles to exchange information with roadside infrastructure, such as traffic lights, signs, and cameras.
- **V2X:** A wireless communication technology that enables vehicles to exchange information with any other entity, including other vehicles, infrastructure, pedestrians, and cloud-based services.
- **Wi-Fi:** Allows vehicles to create a wireless local area network (WLAN) or connect to an existing Wi-Fi network for passenger internet access and media streaming.
- **Cellular communications:** Enables vehicles to connect to the internet via a cellular network for access to cloud-based data and services.

1.2.3 Vehicle Powertrains

Vehicle powertrain types have varying energy efficiency and environmental impacts. Internal combustion engines (ICEs) remain prevalent, but newer powertrain types, such as hybrid electric vehicles (HEVs) and electric vehicles (EVs), are increasingly popular due to their improved energy efficiency and reduced emissions. However, auxiliary loads, such as air conditioning, lights, and infotainment systems, can significantly increase overall energy consumption in all powertrain types. CAVs can improve energy efficiency in each powertrain type by optimizing vehicle motion control and energy management. CAVs can optimize ICEs by reducing idle time and managing engine efficiency. In HEVs, CAVs can manage the electric motor and internal combustion engine more efficiently. In EVs, CAVs can optimize battery use and recharging by managing driving behavior and traffic patterns. By better controlling and managing driving behavior and energy use, CAVs can help improve energy efficiency and reduce emissions in all powertrain types.

1.2.4 CAV Systematic Overview

The proceeding section provides a comprehensive systems-level perspective on the implementation of CAVs. The proposed systems model shown in Figure 1.2 comprises four core elements, namely vehicle perception, remote planning and routing, real-time vehicle running planning and control, and the vehicle plant.

The first component, vehicle perception, involves leveraging a suite of sensors to detect and interpret environmental data, which serves as the foundation for generating a worldview of the vehicle surroundings and ultimately predicting vehicle operation.

The second component, remote planning and routing, is responsible for developing a route plan for the vehicle that accounts for various factors such as traffic, road conditions, and destination. This element also ensures that the vehicle adheres to the prescribed route and incorporates necessary adjustments when required.

The third component, real-time vehicle running planning and control, relies on the operation prediction generated in the first component to optimize fuel efficiency through vehicle optimal control. The running controller receives the control request and is responsible for enforcing component constraints while adapting to control disturbances such as vehicle operation or environmental disruption.

The fourth component, the vehicle plant, encompasses the powertrain and steering interface, which actuates the running controller output. Subsequently, the energy consumption or fuel efficiency can be assessed to evaluate the effectiveness of the control system.

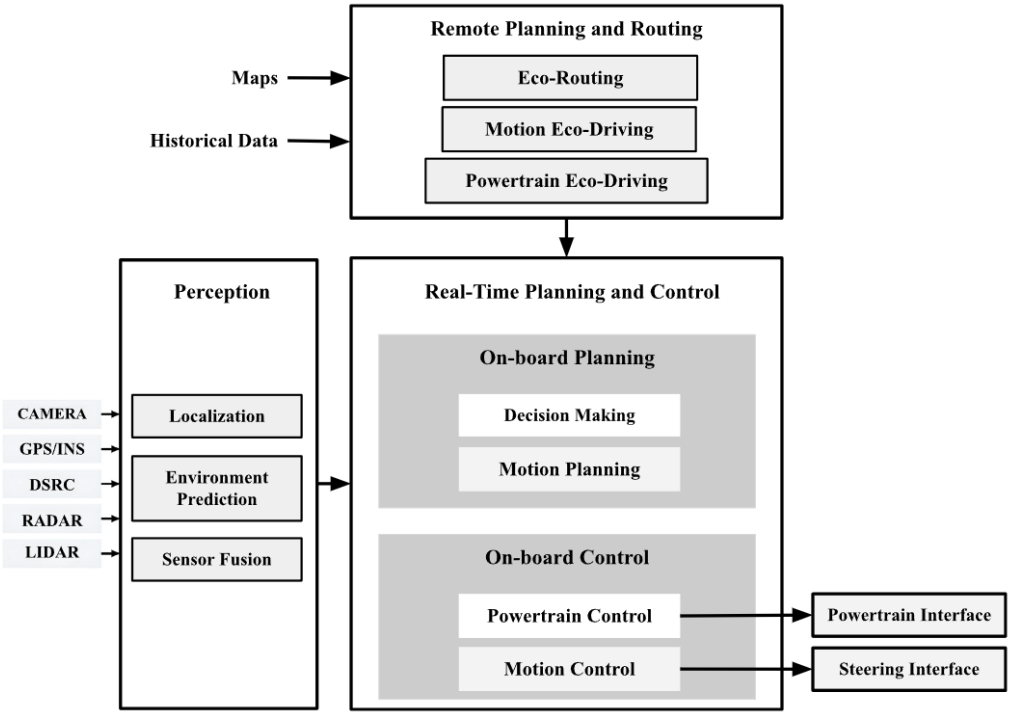

Figure 1.2: System Level of CAV.

1.3 CAV Technology and Energy Management

There are three primary types of vehicle control that can reduce fuel consumption for a fixed drive cycle: eco-routing, eco-driving, and improved energy management. Eco-routing and eco-driving decrease fuel consumption

by modifying the drive cycle, while improved energy management seeks to increase the efficiency of the vehicle powertrain without altering the drive cycle. Eco-routing finds alternate routes between a fixed starting and ending location to minimize fuel consumption and travel time, enabling vehicle powertrain efficiency while maintaining social efficiency. Eco-driving implements fuel-efficient driving behaviors along a fixed route, such as removing stops, traveling at a fuel-efficient speed, and limiting acceleration and deceleration magnitudes. Improved energy management strategies seek to reduce energy consumption over a fixed drive cycle by using mathematical optimization to minimize fuel consumption. Optimal energy management strategies can be formulated as either an instantaneous optimization, such as selecting the optimal transmission gear, or as a predictive optimization that uses data prediction to minimize fuel consumption over a window of time. Ongoing research in these areas aims to further optimize fuel efficiency in modern and future vehicles.

1.3.1 Current Energy Management Development of CAV Technology

The development of energy management strategies for CAV technology is an ongoing area of research and development. Energy management strategies for CAVs can be broadly categorized into hardware and software-based solutions.

Hardware-based solutions aim to optimize the energy efficiency of CAVs by improving the design and engineering of vehicle components, such as batteries, power electronics, and motors. For example, the development of advanced battery chemistries, high-efficiency power electronics, and lightweight materials can improve the energy efficiency of CAVs.

Software-based solutions, on the other hand, leverage data analytics, machine learning, and optimization algorithms to optimize energy use in CAVs. For instance, predictive energy management systems can optimize battery use and charging by analyzing driving behavior and traffic patterns. Other software-based solutions include eco-routing, which optimizes routes for energy efficiency, and ITS, which optimize traffic flow and reduce congestion.

Efforts are also being made to integrate hardware and software-based solutions to create holistic energy management strategies for CAVs. These integrated solutions aim to maximize the energy efficiency of CAVs while maintaining safety and reliability. Overall, the development of energy management strategies for CAVs is critical for enabling sustainable and efficient transportation systems of the future.

1.3.2 Energy Management Challenges of CAV Technology

The adoption of CAV technology presents new challenges for energy management in the transportation sector. CAVs rely on advanced sensors, communication technologies, and data processing capabilities to enable real-time decision making and control of vehicle motion. However, these technologies also increase the energy consumption of CAVs and introduce new energy management challenges. For instance, the computation and communication

needs of CAVs require high power and create additional energy consumption. Moreover, CAVs must maintain a stable and reliable energy supply to ensure safety and reliability. To address these challenges, energy-efficient hardware and software designs, as well as advanced power management strategies, are being developed to optimize energy use in CAVs. These efforts aim to improve energy efficiency, reduce energy waste, and enable more sustainable transportation systems. Velocity prediction is a crucial aspect of optimal energy management in CAVs. Predictive energy management systems rely on real-time predictions of vehicle speed and acceleration to optimize energy use. Velocity prediction algorithms leverage a combination of sensor data, such as cameras, lidar, and radar, along with contextual information from maps, traffic data, and weather forecasts to forecast vehicle future speed and acceleration.

Accurate and reliable velocity predictions are essential for optimizing energy use in real-time. Predictive energy management systems use velocity predictions to adjust vehicle speed, acceleration, and regenerative braking to maximize energy efficiency and reduce energy waste. Furthermore, these systems optimize the use of the vehicle battery, charging, and power distribution systems to ensure optimal energy use while maintaining safety and reliability.

1.4 Research Gaps

–Despite the fact that there have been many advancements in energy management strategies for CAVs, there are still research gaps that need to be addressed. One area that requires further investigation is the development of real-time optimization algorithms for CAVs. While current optimization algorithms are effective in managing energy consumption, they are limited in their ability to handle complex driving scenarios and user preferences. To overcome this limitation, more research is needed in developing advanced optimization algorithms that can handle a wide range of driving scenarios and optimize energy consumption while considering user preferences. Additionally, the development of these algorithms needs to take into account the computational limitations of on-board vehicle systems and the availability of real-time data. By addressing these research gaps in real-time optimization algorithms, CAVs can achieve even greater efficiency and sustainability, contributing to a greener future for transportation.

1.4.1 Research Gap 1: Optimal EMS with Actual Velocity Predictions

The lack of performance of optimal EMS (Energy Management Systems) with actual velocity predictions is a critical issue in the field of energy management. These systems use predictive algorithms to optimize energy use by predicting the optimal velocity for a given operation based on various factors such as load, ambient temperature, and equipment condition. The goal is to achieve energy savings and reduce environmental impact. However, the actual velocity of the operation can often deviate from the optimal prediction due to unforeseen

circumstances such as changes in weather conditions, equipment failures, or unexpected loads.

When the actual velocity deviates from the optimal prediction, the optimal EMS system may not be able to achieve the predicted energy savings, and in some cases, it may even result in higher energy consumption. For instance, if an optimal EMS system predicts a low load and operates at a slow velocity, but the actual load is much higher, then the system may consume more energy to compensate for the difference in load. This can lead to inefficient energy usage and higher energy costs, defeating the purpose of using an optimal EMS system.

To overcome this issue, EMS developers must consider potential deviations from predicted velocities and develop more robust and adaptable systems that can adjust to changes in real-time. One approach could be to use artificial intelligence and machine learning algorithms to learn from the historical data and continuously improve the predictive models based on actual velocities. Additionally, developers could integrate real-time monitoring and feedback mechanisms into the EMS system that can adjust the velocity in response to changes in real-time.

Moreover, it is essential to consider the human element in the optimization process. Optimal EMS systems are designed to be fully automated, but in practice, human operators may need to intervene and make adjustments to the velocity to address unforeseen circumstances or operational inefficiencies. Thus, the system should have a user-friendly interface that enables operators to adjust the velocity quickly and efficiently to maintain optimal performance.

In conclusion, the lack of performance of optimal EMS with actual velocity predictions is a critical issue that can lead to inefficient energy usage and higher energy costs. By implementing the strategies discussed, optimal EMS systems can achieve their intended goals of reducing energy consumption and lowering environmental impact. With the use of artificial intelligence and machine learning algorithms, real-time monitoring and feedback mechanisms, and a user-friendly interface for human intervention, EMS developers can design systems that can adapt to changes in real-time and maintain optimal performance. By doing so, these systems can contribute to a sustainable and energy-efficient future.

1.4.2 Research Gap 2: Optimal EMS and Traffic Optimization, and Vehicle Emission Modeling

The advancement of transportation systems towards improved efficiency and sustainability requires addressing several critical research gaps. Firstly, the integration of POEMS and ITS holds significant potential but remains understudied. While these mechanisms have been treated as independent entities, their combined effect on system efficiency remains unexplored. Comprehensive studies are needed to quantify the synergistic benefits and optimize the integration of POEMS and ITS. Such investigations would contribute to reducing energy consumption, enhancing travel time, and minimizing environmental impact, thus fostering more sustainable transportation systems.

Secondly, the development of high-fidelity emission models using deep neural networks (DNNs) offers promise, yet key research gaps persist. Understanding the complex interactions among vehicle characteristics, driving conditions, and emissions is crucial for accurate modeling. Moreover, the scalability and generalizability of DNN-based models across diverse scenarios and regions require further exploration. Addressing these gaps necessitates the development of novel algorithms, improved data collection methodologies, and validation of DNN-based emission models in real-world scenarios. This will enable effective control development, real-time optimization of energy management systems, and contribute to more environmentally friendly transportation practices.

Furthermore, the integration of optimal energy management strategies with traffic management optimization presents an opportunity to enhance transportation efficiency and sustainability. However, the interactions and trade-offs between these domains lack comprehensive investigation. Future research should focus on developing advanced algorithms that effectively combine energy management strategies and traffic optimization, considering real-time traffic conditions, vehicle characteristics, and network constraints. Bridging this gap would pave the way for integrated solutions that maximize system efficiency, reducing energy consumption and improving travel time.

To ensure the practical implementation of these advancements, it is essential to develop comprehensive frameworks and guidelines for policymakers and stakeholders. Clear guidelines are needed to facilitate the implementation and evaluation of integrated approaches. These frameworks would provide actionable insights for optimizing transportation systems, thereby supporting the transition towards sustainable and efficient practices. By addressing these research gaps, the field of transportation engineering can contribute significantly to the development of environmentally conscious and technologically advanced transportation systems.

1.4.3 Research Gap 3: Lack of Real Vehicle Autonomous Eco-Driving Control Evaluation

Research in the field of energy efficient control of electrified AV eco-driving necessitates addressing several critical research gaps. One of the primary gaps is understanding the critical sensors and signals required for effective vehicle control through autonomous eco-driving (AED). Currently, there is a lack of comprehensive understanding regarding these specific sensors and signals that optimize energy efficiency in vehicles. Research is needed to identify the essential sensors and signals for perception and sensor fusion, which will enable the development of improved energy-efficient control strategies.

Another important research gap pertains to the impact of faults or missing data from perception systems on vehicle control in terms of energy efficiency. Investigating the types of faults or missing data from perception that may hinder effective vehicle control is crucial. Understanding how these issues impact the implementation of AED will facilitate the development of strategies to mitigate their effects. By addressing this gap, researchers can ensure reliable and robust energy-efficient control, even in the presence of perception system errors or missing

data.

Additionally, the operational and real-world challenges associated with implementing AED control need to be addressed. Real-world deployment poses various challenges that require thorough understanding and solutions. These challenges include integrating AED with a physical vehicle plant and evaluating the performance of the planning subsystem equipped with AED in real-world conditions. Research is needed to overcome these challenges, enabling the successful implementation and practical application of AED control strategies in real-world scenarios.

In addition to the previously mentioned research gaps, there is a notable gap in the identification of research gaps specifically for autonomous eco-driving controls in electrified vehicles. Currently, no research has conducted an evaluation of system maturity based on the Department of Defense (DoD) approach to derive research gaps in this particular area [8].

The DoD approach to evaluating system maturity involves assessing the readiness and capability of technologies for deployment. By applying this approach to autonomous eco-driving controls in electrified vehicles, researchers can systematically identify gaps in knowledge, technology, and implementation that hinder the maturity and widespread adoption of such systems. This evaluation can provide valuable insights into the specific areas where further research is needed to enhance the effectiveness and efficiency of autonomous eco-driving controls in electrified vehicles.

Through a thorough evaluation using the DoD approach, researchers can develop a comprehensive understanding of the readiness levels and identify potential research gaps related to the implementation of eco-driving in electrified autonomous vehicles. This will enable targeted research efforts to address the identified gaps and accelerate the development and deployment of energy-efficient autonomous driving technologies in electrified vehicles.

in conclusion, by addressing these research gaps, studies can significantly advance the field of Energy Efficient Control of Electrified AV Eco-driving. Understanding critical sensors and signals will facilitate the development of optimized perception and sensor fusion systems. Investigating the impact of perception faults or missing data will lead to strategies that ensure robust control even in imperfect conditions. Overcoming operational and real-world challenges will pave the way for the practical implementation of AED control, contributing to enhanced energy efficiency in autonomous vehicles operating in real-world environments.

1.5 Conclusions

This dissertation aims to explore energy-efficient control techniques for transportation vehicles by leveraging connected and automated vehicles. This work will answer the following research questions:

- *How effective are actual velocity predictive optimal energy management strategies in improving energy efficiency and reducing emissions in hybrid electric vehicles, and how do they compare to other EMS ap-*

proaches?

- *How can the integration of predictive optimal energy management strategies, intelligent traffic systems, and deep neural networks enhance transportation vehicle energy efficiency, reduce travel time, minimize environmental impact, and develop accurate emission models for individual vehicles?*
- *How can the performance of autonomous eco-driving control differ from simulations when it is operated with a real vehicle?*

1.5.1 Dissertation Organization

This dissertation comprises a series of interrelated studies, presented across Chapters 3-9, that collectively address the overarching research objectives.

- Chapter 1: Connected and Automated Vehicles Technology and Energy management
- Chapter 2: Research Questions and Definition of Research Scope
- Chapter 3: Research Question 1 Study 1 - Vehicle velocity prediction using artificial neural network and effect of real world signals on prediction window
- Chapter 4: Research Question 1 Study 2 - Comparison of Optimal Energy Management Strategies Using Dynamic Programming, Model Predictive Control, and Constant Velocity Prediction
- Chapter 5: Research Question 1 Study 3 - Development and evaluation of velocity predictive optimal energy management strategies in intelligent and connected hybrid electric vehicles
- Chapter 6: Research Question 2 Study 1 - Mobility energy productivity evaluation of prediction-based vehicle powertrain control combined with optimal traffic management
- Chapter 7: Research Question 2 Study 2 - High-fidelity modeling of light-duty vehicle emission and fuel economy using deep neural networks
- Chapter 8: Research Question 3 Study 1 - Identifying and Assessing Research Gaps for Energy Efficient Control of Electrified AV Eco-driving
- Chapter 9: Research Question 3 Study 2 - Autonomous Eco-Driving Evaluation of an Electric Vehicle on a Chassis Dynamometer
- Chapter 10: Conclusions

Chapter 2

Research Questions and Definition of Research Scope

2.1 Primary Research Question

Based on the research gaps presented in chapter 1, the primary research question is:

"How can energy efficient controls be implemented with consideration of current and near future CAV technologies?"

Hypothesis: The integration of energy efficient controls with current and near future CAV technologies can lead to reduced energy consumption and operational costs in transportation systems, while improving safety and mobility.

To answer this question, this dissertation is divided into 3 more focused questions. The first research question focuses on the application of machine learning in POEMS, second research question revolves around applicaiton fo DNNs and TMS for FE and emission modeling and evaluation for CAVs. The last question focuses on the autonomous eco-driving control evaluation. Future work will allow improvements of the overall system energy efficiency for CAVs.

2.2 Research Question 1 - Optimal EMS with Actual Velocity Predictions

Research Question 1: *How effective are actual velocity predictive optimal energy management strategies in improving energy efficiency and reducing emissions in hybrid electric vehicles, and how do they compare to other EMS approaches?*

Hypothesis: Real-time, actual velocity predictive optimal energy management strategies, are implementable.

Task 1.1: Conduct a performance evaluation of velocity prediction using artificial neural networks (ANN) when real-world data is utilized.

Task 1.2: Conduct a performance evaluation and comparison of predictive optimal energy management strategies in HEVs for different velocity prediction windows.

Task 1.3: Integrate the best velocity predictions obtained from the machine learning (ML) and ANN methods into fuel economy (FE) simulations to assess the effectiveness of practically implementable predictive optimal energy management strategies.

2.3 Research Question 2 - Optimal EMS and Traffic Optimization, and Vehicle Emission Modeling

Research Question 2: *How can the integration of predictive optimal energy management strategies, intelligent traffic systems, and deep neural networks enhance transportation vehicle energy efficiency, reduce travel time, minimize environmental impact, and develop accurate emission models for individual vehicles?*

Hypothesis: There are promising synergistic benefits to travel time and energy efficiency when POEMS and Optimal TMS are combined.Also, Accurate and simple emission modeling and characterization can be used to inform energy management control developments.

Task 2.1: Integrate previously developed and published research on Predictive Optimal Energy Management Strategies (POEMS) with optimal TMS, to address the need for quantifying improvement in system efficiency resulting from simultaneous vehicle and network optimization.

Task 2.2: Development and assessment of deep neural network (DNN) architectures, specifically recurrent neural networks (RNN) and convolutional neural networks (CNN), for predicting vehicle emissions.

This study will result in a comprehension of how to establish the overall resilience of the perception subsystem and a technical analysis of the resilience measures used to evaluate simulation and real-world localization algorithms.

2.4 Research Question 3 - Lack of Real Vehicle Autonomous Eco-Driving Control Evaluation

Research Question 3: *How can the performance of autonomous eco-driving control differ from simulations when it is operated with a real vehicle?*

Hypothesis: Autonomous Eco-driving control can be implemented in CAVs.

Task 3.1: First Identify and assess research gaps for energy efficient control of electrified AV eco-driving.

Task 3.2: Conduct a performance evaluation and comparison of various autonomous eco-driving control methods using a real vehicle.

2.5 Definition of Research Scope

The overall goal of this research is to enhance energy efficiency in connected and automated vehicles through the application of predictive control techniques. This includes investigating artificial neural networks (ANNs), predictive optimal energy management strategies (POEMS), and autonomous eco-driving control. The research also aims to integrate POEMS with optimal traffic management and develop accurate models for predicting emissions and fuel economy in light-duty vehicles.

By addressing the challenges of energy efficiency and sustainability in transportation, this dissertation contributes to the development of more sustainable transportation systems. It explores the potential benefits of connected and automated vehicles and their impact on energy-efficient driving. The findings have implications for the development of energy-efficient control strategies in future transportation systems.

Chapter 3

Vehicle Velocity Prediction Using Artificial Neural Network and Effect of Real-World Signals on Prediction Window

This study evaluated the effectiveness of using V2I data and ANN for vehicle velocity prediction. This study was published at SAE World Congress and it is considered as Task 1.1 of research question No. 1 [9]. My unique contribution was helping with data analysis, specifically contributing to the analysis of vehicle velocity data. Participated in the writing, review, and editing process of the manuscript.

3.1 Introduction

The rise of ITS is predicted to be a major disruption, on par with the early days of automobiles [10]. ITS technology, such as Advanced Driver Assistance Systems (ADAS), V2V, and V2I communication, has the potential to revolutionize transportation by enabling safer and more efficient movement of people and goods [11, 12]. ITS can provide vital information, such as vehicle position and velocity, and infrastructure-level transit time, leading to significant improvements in fuel economy, transportation efficiency, and safety [13].

One emerging and important application of velocity prediction is developing energy management strategies to improve fuel economy in HEVs and plug-In hybrid electric vehicles (PHEVs). Automation and future prediction horizons can increase vehicle operation efficiency by enabling control over vehicle operations. Accurate prediction of future driving conditions is crucial in determining the constraints of the energy optimization problem. Thus,

detection algorithms based on the speed profile are being developed to aid in this task [14, 15]. However, an inaccurate prediction can lead to decreased energy savings or even safety concerns. Hence, there is a pressing need to develop accurate and robust approaches for predicting vehicle speed and understanding which input signals can produce better predictions.

One promising technique for modeling complex prediction problems and patterns is ANN. ANNs have the ability to extract unseen features and relationships, making them reliable for complex prediction tasks. Moreover, their ability to predict future output allows for the use of optimal control principles to derive an optimal solution [16]. Several researchers have recognized the potential of self-driving vehicle technology to inform ANN prediction models, whose outputs can derive control strategies to improve fuel economy [17–25]. It is important to note that each study uses "Intelligent Vehicle" technology inputs to the prediction model to inform optimal control.

Vehicle speed prediction has been extensively studied and addressed in various publications. For instance, Lefèvre et al. compared parametric and non-parametric models for predicting ego vehicle velocity over a 1-10 second horizon [26]. The study results revealed that simple models performed well for short-term prediction while advanced models performed better for long-term prediction. Olabiyi et al. employed DNNs for vehicle speed prediction [27]. Similarly, Lemieux et al. used deep learning networks to predict both ego vehicle velocity and route [28]. On the other hand, Zhang et al. utilized V2V and V2I communications for future vehicle velocity prediction and developed an energy management strategy based on the predictions [29]. In another study, Sun et al. used Radial Basis Function neural networks to predict vehicle speed performance on four standard driving cycles [30]. Meanwhile, Hellström and Jankovic proposed a model for predicting the acceleration behavior of human drivers [31].

Liu Kuan's study [32] specifically aimed to compare different approaches for predicting 10-second forward vehicle speed. The study found that among all the approaches, the Long Short-Term Memory (LSTM) deep neural network performed the best. LSTM is a powerful neural network used in deep learning because it can successfully train very large architectures. Despite the previous studies on vehicle speed prediction, the issue of the dependency of prediction on different groups of signals still needs to be further understood. Therefore, there is still a need for ongoing research to determine the most important input signals that can produce more accurate predictions.

To explore the potential applications and accuracy of vehicle velocity predictions, we utilized LSTM to predict ego vehicle velocity based on various signals gathered along the roads of Fort Collins, Colorado. We created different input groups from these signals to better understand their effect on prediction horizon. Additionally, we tested the deployment of our prediction algorithm on fast processing hardware, specifically the NVIDIA Drive PX2, which is designed for developing algorithms for autonomous vehicles.

This chapter is organized into several sections. Section 3.2 describes the problem statement, introduces the collected dataset, and provides an overview of LSTM deep NNs. We also discuss the NVIDIA Drive PX2

hardware and its functions in this section. Section 3.3 outlines the assessment methods used and presents the results obtained under different scenarios. Finally, section 3.4 summarizes our conclusions and highlights the direction of future research, specifically the implementation of our approach using the NVIDIA Drive PX2.

3.2 Methodology

In this study, our goal is to assess the potential of different signals, including radar signal, ego vehicle sensor data, ADAS-derived near-neighbor relative position, infrastructure-level transit time (Segment Speed), and signal phase and timing (SPaT), in improving vehicle velocity prediction accuracy. Specifically, we will investigate the effect of these signals on various forward prediction windows. To extract features for our velocity prediction analysis, we collected drive cycles using a sensor-equipped vehicle in Fort Collins, Colorado. This approach allows us to obtain a comprehensive understanding of how the selected signals impact the accuracy of vehicle velocity prediction across different forward prediction windows.

3.2.1 Drive Cycle Development and Signal Recording

The Fort Collins dataset was collected in August 2019 and consists of data obtained from repeated drives along a fixed route by the same driver. The route follows a round trip, which includes the following segments:

1. Parking Lot
2. West on Mulberry St. until Shields St.
3. South on Shields St. until Prospect Rd.
4. East on Prospect Rd. until College Ave.
5. North on College Ave. until Mulberry St.
6. West on Mulberry St. until the Parking Lot
7. Parking Lot

The birds-eye view of this route is shown in Figure 3.1. In the figure, the black arrows indicate the driving directions, the black circle represents the start and endpoint of the route, the red targets correspond to traffic signals, and the blue lines represent traffic segments. The route covers a total distance of 4 miles and takes approximately 10-12 minutes per cycle, depending on traffic.

The test will generate data from two sources: the ADAS data from the vehicle forward cone, obtained through a smart radar system typical of production vehicle ADAS, and V2I data in the form of traffic signal information

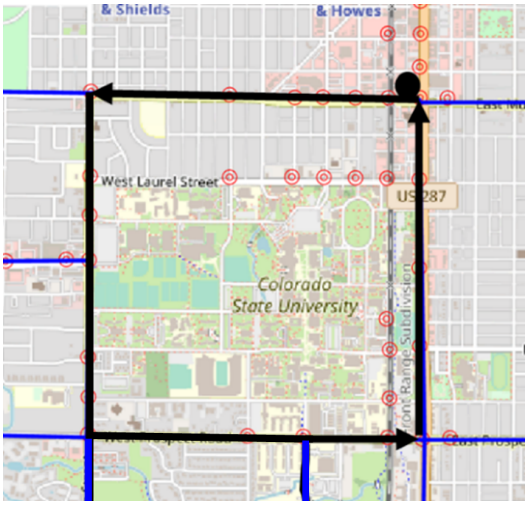

Figure 3.1: Drive cycle map of the Fort Collins dataset.

and segment travel times. The ego vehicle used for the test was a specially instrumented research vehicle equipped with the aforementioned ADAS sensors, a stereo camera, and a Freematics logger.

Several feature plots are presented in this section. Figure 3.2 displays the velocity vs. time plot for one drive instance, while the longitude vs. latitude vs. time plot for the same drive instance is shown in Figure 3.3. The velocity profiles for three drive instances are compared in a map terrain in Figure 3.3a.

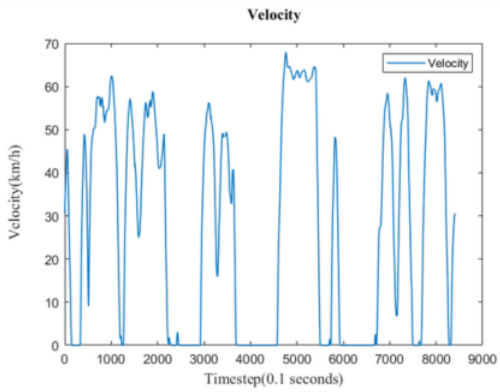

Figure 3.2: Drive cycle map of the Fort Collins dataset.

The objects detected by the radar system in the area immediately in front of the vehicle are plotted in Figure 3.3b, showing their positions relative to the vehicle. Finally, Figure 3.3c presents the longitude vs. latitude vs. altitude plot, with velocity displayed on the map terrain.

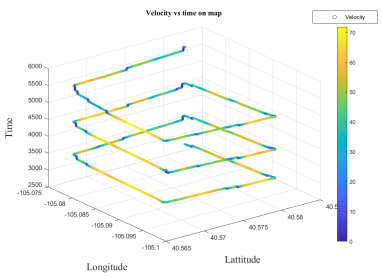

(a) Velocity on the longitude vs. latitude vs. time

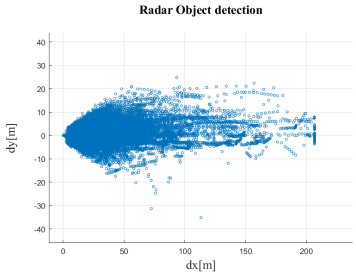

(b) Radar object detections immediately in front

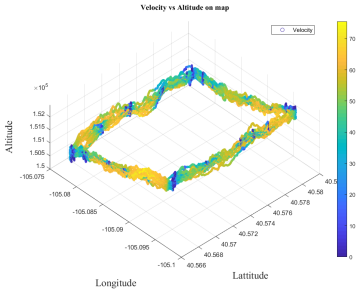

(c) Velocity on the map terrain

Figure 3.3: dataset

3.2.2 Prediction Model Derivation: Long Short- Term Memory (LSTM) Deep Neural Network

Introduction to LSTM Model

LSTM is a type of Recurrent Neural Network (RNN) designed to handle long-term dependencies in large datasets, while avoiding problems like gradient vanishing/exploding that traditional RNNs encounter. It is the most commonly used deep learning model for sequential data analysis. An RNN consisting of LSTM units is called LSTM network.

Unlike conventional RNNs, which have only one activation function in their repeating parts, LSTMs have three gates with different activation functions that interact with each other. The memory cell, memory block, or cell is a typical LSTM unit, which consists of a cell and three gates - forget gate, input gate, and output gate. The cell can remember values over arbitrary time intervals, and the gates regulate the flow of information into and out of the cell.

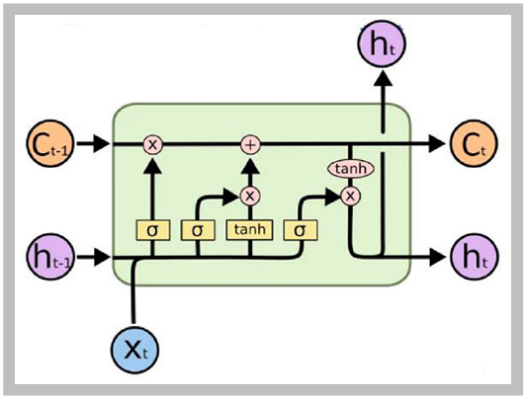

Figure 3.4: LSTM Cell internal structure

Figure 3.4 shows the typical internal structure of an LSTM cell, which includes three gates. The computation details can be found in the literature [23–35]. The gate computations can be summarized using the following

equations.

1. Forget Gate: Decides what information to discard from the cell.

$$f_t = \sigma(W_f[h_{t-1}^T, X_t^T]^T + b_f) \tag{3.1}$$

2. Input Gate: Decides which values from the input to update the memory state.

$$i_t = \sigma(W_i[h_{t-1}^T, X_t^T]^T + b_i) \tag{3.2}$$

$$\tilde{C}_t = \tanh(W_c[h_{t-1}^T, X_t^T]^T + b_c) \tag{3.3}$$

3. Output Gate: Decides what to output based on input and the memory of the cell.

$$o_t = \sigma(W_o[h_{t-1}^T, X_t^T]^T + b_o) \tag{3.4}$$

$$C_t = f_t * C_{t-1} + i_t * \tilde{C}_t \tag{3.5}$$

$$h_t = o_t * \tanh C_t \tag{3.6}$$

where W_f, W_i, W_C, W_o and b_f, b_i, b_C, b_o designate vectors (matrices) of weights and biases for forget gate, input gate, cell state, and output gate, respectively. In the above expressions, σ is a sigmoid function.

LSTM Applied to Fort Collins Data Set

The LSTM development was based on Keras 1.0 using Python 3.7. After experimenting with different structures, a 2-layer neural network with 3 hidden layers was selected, with 50, 30, 15 neurons in each of the hidden layers. To speed up the training process and avoid gradient vanishing, the "ReLu" activation function was chosen. To prevent overfitting, both regularization and dropout layers were included.

The 10 sec ahead prediction results are shown in Figure 3.5. The resulting LSTM model shows very promising prediction results. The effect of different signals on the prediction window is further explained in the Result section.

Assessment

To ensure accurate assessment of the prediction results, two assessment criteria were introduced: Mean Absolute Error (MAE) and Timeshift. MAE measures the average magnitude of the errors in a set of predictions without considering their direction, while Timeshift measures the difference between the time when the predicted

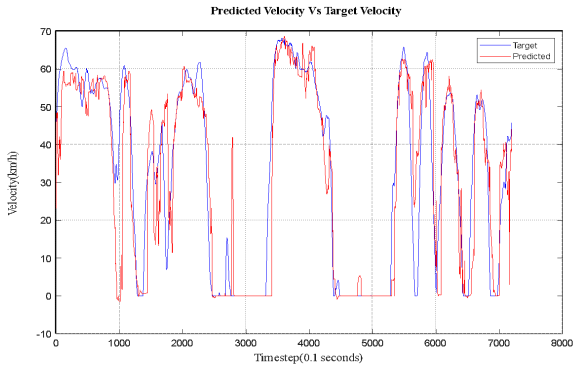

Figure 3.5: LSTM model 10 sec ahead prediction results on Fort Collins dataset (Group D)

value is observed and the time when the actual value is observed. These criteria provide a comprehensive evaluation of the predictive performance and the temporal accuracy of the model.

- **MAE:** Mean Absolute Error (MAE) is a measure of the difference between two continuous variables. Assume y_{t1}, ..., y_{tn} are prediction results and Z_{t1}, ..., Z_{tn} are target values at time instance t. The MAE is given by,

$$MAE(Y_t, Z_t) = \frac{\sum_{i=1}^{n} \mid y_{ti} - Z_{ti} \mid}{n}. \tag{3.7}$$

Smaller MAE means smaller errors between prediction results and target values.

- **Time Shift:** The time shift is a measure of the time lag between the predicted time series and target time series. It uses a cross-correlation technique for finding the time shift error. A smaller time shift means a smaller time lag between the prediction results and target values. It can be expressed as

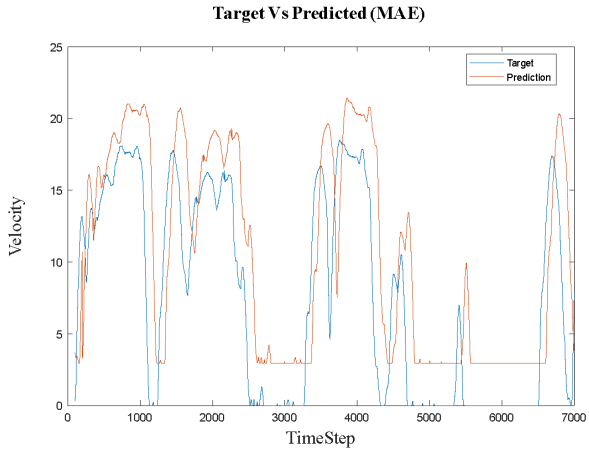

Figure 3.6: Hypothetical example of prediction consisting of both errors

$$Timeshift = arg_{\delta} max \sum_{0}^{n} \mid y_{t-\delta} * Z_{t1} \mid. \tag{3.8}$$

To illustrate the importance of using both assessment criteria, Figure 3.6 showed a hypothetical prediction example with both errors.

3.2.3 Implementation of Prediction Model Using In-Vehicle Hardware

The automated driving system employs specialized driving mode algorithms to optimize performance across all aspects of dynamic driving tasks. To achieve this, the use of artificial intelligence in autonomous vehicles requires a supercomputer capable of handling Level 3 to Level 4 operations. The NVIDIA Drive PX2 offers the added capability of handling Level 5 operations, as depicted in Figure 3.7. This hardware can also be used for neural network training and porting algorithms or applications from a PC or system to an embedded platform. With these capabilities, it is possible to simulate a driving environment and operate a simulated vehicle [36]. With its ability to handle up to 8-12 cameras, radar, 2 Tegra processors, and 3 GPUs, the NVIDIA DRIVE PX2 is an ideal hardware platform for implementing these strategies, consuming an average of 80W of power.

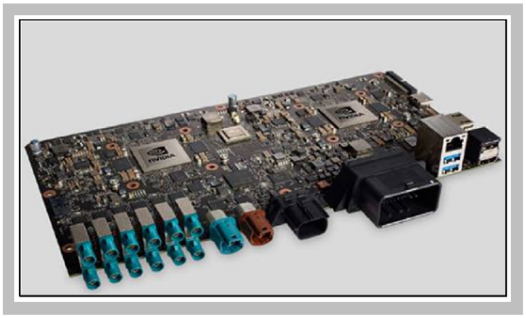

Figure 3.7: NVIDIA Drive PX2

3.3 Results and Discussion

3.3.1 Dataset Groups and Prediction Results

To compare different signals, we organized them into distinct groups. The prediction plots display a comparison between the predicted values and the target values, representing the next prediction horizon (e.g., 10, 15, 20, or 30 seconds).

Table 3.1 outlines the data included in Group A, which encompasses current velocity and GPS. Figure 3.8 illustrates the results for velocity prediction for the 10th second using the Group A signals, plotted against the target value. However, it is evident that the prediction results are not aligned with the target values.

Table 3.1: Signals Used in Group A

Data Group A	Current Velocity
	GPS

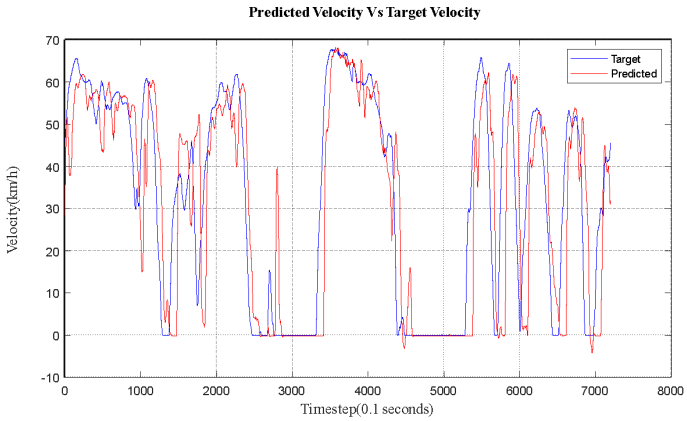

Figure 3.8: 10th-second Prediction Results using Group A signals

Figure 3.9 reveals that Group B signals yield superior results compared to Group A. This enhanced performance is attributed to the inclusion of additional data parameters, namely the previous 5 seconds of signals, as well as the EGO and Engine parameters dataset.

Table 3.2: Signals Used in Group B

Data Group B	Current Velocity
	GPS
	Previous 5 Seconds
	EGO and Engine Parameters

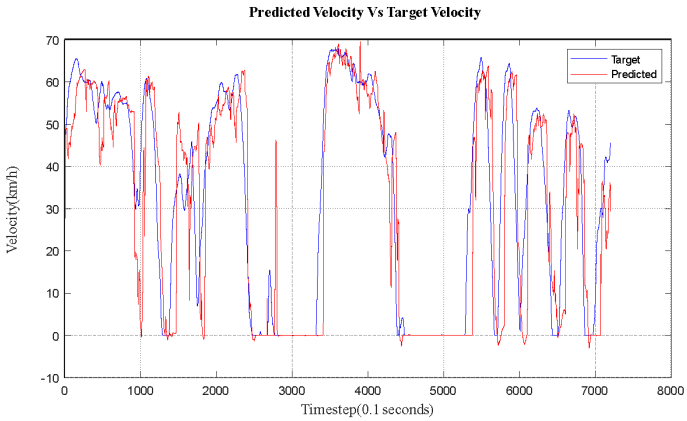

Figure 3.9: 10th-second Prediction Results using Group B signals

Figure 3.10 displays a plot that has been generated from the Group C dataset. This dataset comprises various signals, including Current Velocity, GPS, Previous 5 Seconds, EGO and Engine Parameters, and Radar Data.

Table 3.3: Signals Used in Group C

Data Group C	Current Velocity
	GPS
	Previous 5 Seconds
	EGO and Engine Parameters
	Radar Data

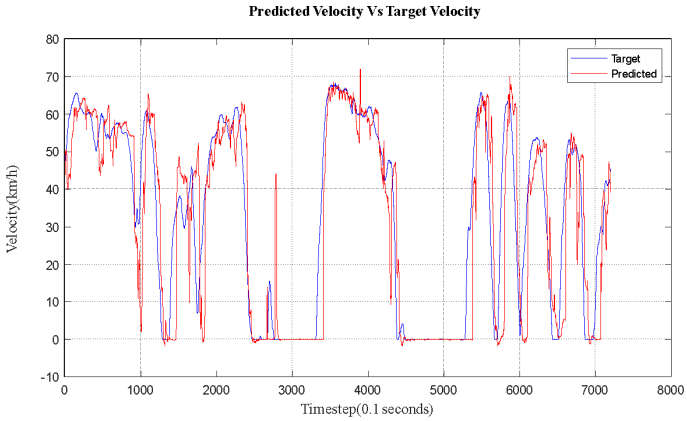

Figure 3.10: 10th-second Prediction Results using Group C signals

The prediction results obtained from the Group D dataset, which are tabulated in Table 3.4, are displayed in Figure 3.11. The results show significant improvement over the Group B and Group C datasets due to the inclusion of the SPaT signal.

Table 3.4: Signals Used in Group D

Data Group D	Current Velocity
	GPS
	Previous 5 Seconds
	EGO and Engine Parameters
	SPaT

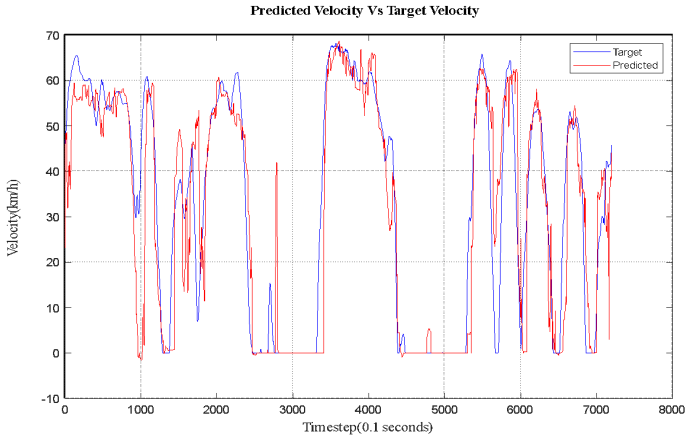

Figure 3.11: 10th-second Prediction Results using Group D signals

Figure 3.12 displays the prediction results obtained using the Group E dataset. While the results show improvement over the Group C dataset, they also reveal some mispredictions compared to the Group D dataset, which includes the SPaT signal.

The Group E dataset comprises several signals, including Current Velocity, GPS, Previous 5 Seconds, EGO and Engine Parameters, SPaT, and Segment Speed. The signals used in the Group E dataset are tabulated in Table 3.5.

Table 3.5: 10th-second Prediction Results using Group E signals

Data Group E	Current Velocity
	GPS
	Previous 5 Seconds
	EGO and Engine Parameters
	SPaT
	Segment Speed

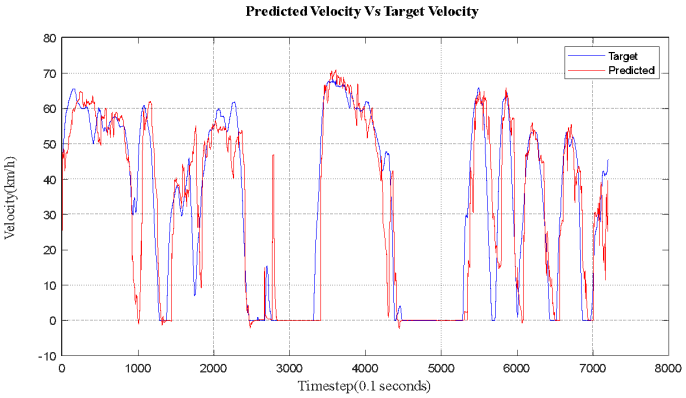

Figure 3.12: 10th-second Prediction Results using Group E signals

The mispredictions observed in the Group E dataset highlight the importance of considering relevant signals in predictive modeling. Possible reasons why the inclusion of the Segment Speed signal in the Group E dataset did not improve accuracy compared to the Group D dataset include noise in the data, insufficient relevance to the prediction task, model complexity, and interactions with other signals. It is likely that a combination of these factors contributed to the observed differences in performance.

The velocity prediction for the 10th second using Group F and Group G signals are shown in Figure 3.13 and Figure 3.14, respectively. Table 3.6 and Table 3.7 tabulate the signals used in Group F and Group G datasets, respectively. Both datasets include Current Velocity, GPS, Previous 5 Seconds, EGO and Engine Parameters, and Segment Speed. However, the Group G dataset does not include Radar data.

Table 3.6: 10th-second Prediction Results using Group F signals

Data Group F	Current Velocity
	GPS
	Previous 5 Seconds
	EGO and Engine Parameters
	Segment Speed
	Radar
	Radar

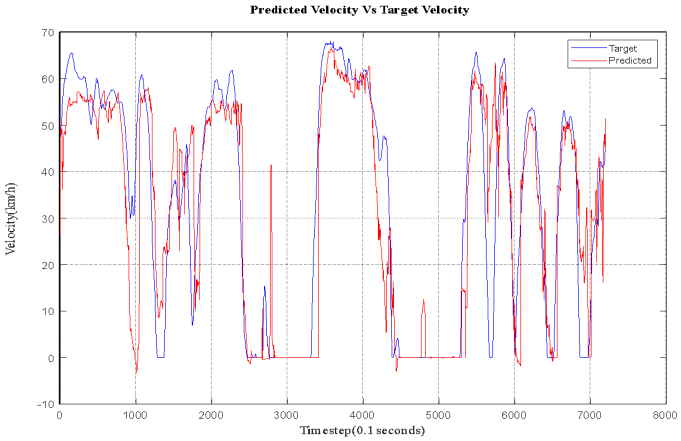

Figure 3.13: 10th-second Prediction Results using Group F signals

Table 3.7: 10th-second Prediction Results using Group G signals

Data Group G	Current Velocity
	GPS
	Previous 5 Seconds
	EGO and Engine Parameters
	Segment Speed

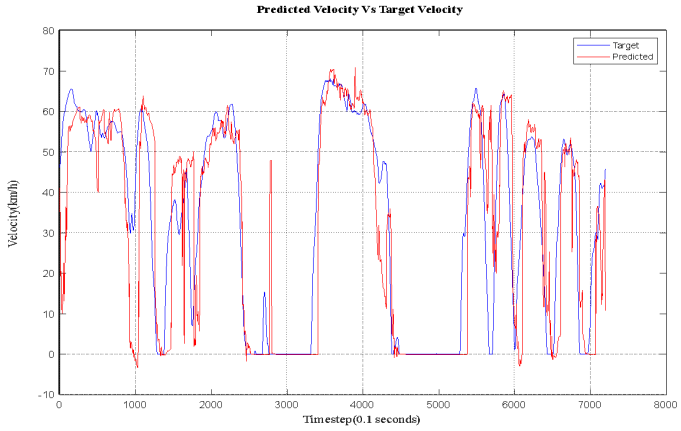

Figure 3.14: 10th-second Prediction Results using Group G signals

3.3.2 Effect on Prediction Horizon

Signal Groups are utilized to generate prediction results for the upcoming 10, 15, 20, and 30 seconds of forward projection, which are then evaluated based on their Mean Absolute Error (MAE). The plot displayed in Figure 3.15 illustrates the comparison of MAE values. Additionally, Table 3.8 provides the average MAE values for each

Signal Group results. In addition to the observations discussed previously, it is worth mentioning that the results presented in Table 3.8 indicate that the predictive performance of each Signal Group varies significantly based on the target horizon. This finding suggests that different Signal Groups may be more suitable for certain use cases depending on the desired prediction horizon.

Furthermore, the results obtained by Group D, which incorporates SPaT data, support the notion that real-time traffic information can significantly improve the accuracy of traffic flow predictions. This finding is consistent with prior research in the field, which has demonstrated the effectiveness of utilizing real-time data sources, such as connected vehicle technology, to improve traffic flow prediction accuracy.

It is also noteworthy that Group B, which incorporates additional vehicle-specific parameters, outperforms Group A. This finding suggests that incorporating vehicle-specific data into traffic flow prediction models can be beneficial in improving prediction accuracy. Moreover, it highlights the potential benefits of utilizing advanced sensor technologies, such as vehicle-to-infrastructure (V2I) communication systems, to collect and transmit this type of data in real-time.

Table 3.8: MAE Comparison: Velocity prediction of signal groups on different prediction windows (m/s)

Prediction Window	**Group A**	**Group B**	**Group C**	**Group D**	**Group E**	**Group F**	**Group G**
10 sec	2.45	2.14	2.18	1.78	1.86	1.85	2.14
15 sec	3.52	3.22	3.24	2.55	2.64	2.66	3.11
20 sec	4.32	4.02	4.02	3.09	3.24	3.28	3.71
30 sec	5.29	4.91	5.02	4.04	4.18	4.23	4.53

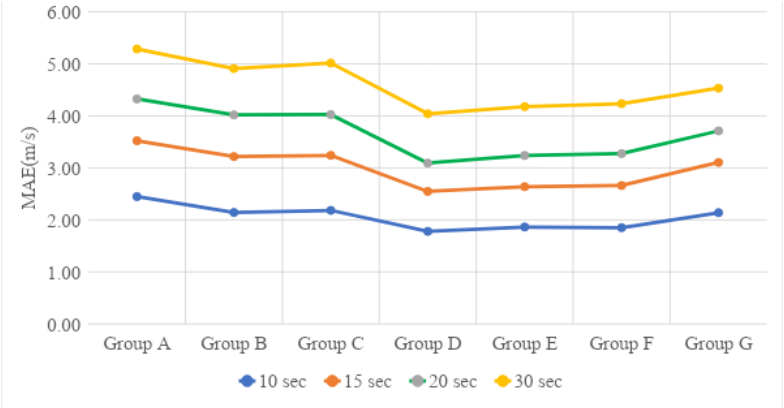

Figure 3.15: Effect of signal groups on MAE

Group D data comprises several inputs, including current velocity, GPS, the previous 5 seconds of velocity, EGO, and Engine parameters, and SPaT (Signal Phase and Timing). On the other hand, Groups E and F utilize segment speed, which appears to negatively impact prediction accuracy. As a result, these groups display some mispredictions when compared to Group D's performance. These findings align with previous research,

such as [37], which found that using Segment Speed for prediction led to lower fuel economy due to increased mispredictions. Overall, our results indicate that Group D outperforms Group A with a nearly 50% reduction in error. We utilized Group D data as an input to LSTM for 10-second prediction, resulting in a MAE of 1.78 m/s and a time shift of 2.25 seconds. These findings suggest that incorporating real-time data sources such as SPaT can significantly improve prediction accuracy, and the use of advanced machine learning techniques like LSTM can further enhance the accuracy of traffic flow predictions.

Figure 3.16 illustrates the impact of signal groups on time shift, while Table 3.9 summarizes the average result values. Our analysis has indicated that the time shift in predictions increases as the prediction window is expanded. This finding is consistent with prior research, which has shown that longer prediction horizons tend to be associated with greater time shifts. This may be due to the cumulative effects of errors in the prediction model, as well as external factors such as changes in traffic patterns and conditions.

Table 3.9: Effect of signal groups on prediction window time shift (s)

Prediction Window	Group A	Group B	Group C	Group D	Group E	Group F	Group G
10 sec	5.67	4.23	4.25	2.35	2.42	2.25	4.16
15 sec	9.65	7.59	7.55	3.68	3.23	3.44	6.77
20 sec	13.43	10.64	10.72	4.05	4.27	4.23	8.85
30 sec	22.19	17.31	17.48	7.07	7.45	7.46	13.01

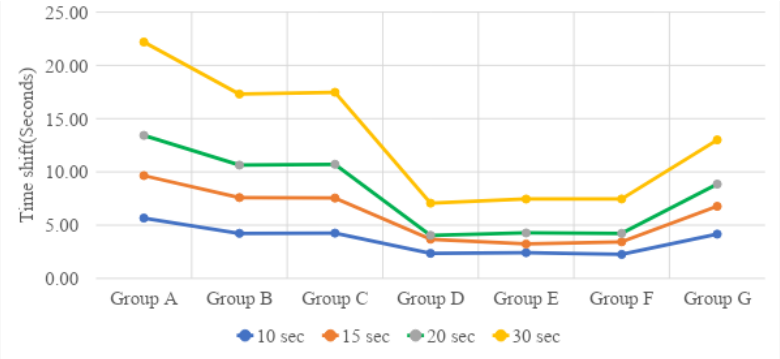

Figure 3.16: Effect of signal groups on prediction window Time shift

3.3.3 Velocity Prediction In-Vehicle Implementation

In simulations, desktop computer equipped with Python 3.7, Keras - TensorFlow, and an RTX 2060 GPU was used. The data was collected prior to analysis and used to derive results.

The performance of the algorithm was also investigated using the NVIDIA PX2 architecture, which could perform multiple complex computations and gather live data while mounted in a vehicle. The algorithm was implemented in a similar manner on this platform, and comparable results were observed to those obtained using

the desktop computer.

This finding indicates that our algorithm is robust and can be applied across different architectures and environments. Furthermore, it suggests that our approach has the potential to be implemented in actual vehicles, where it could provide real-time traffic flow predictions to support more effective traffic management and planning.

3.4 Conclusion

In this study, multiple signals were collected in Fort Collins, Colorado, which were used as input features for LSTM. LSTM showed good performance in predicting vehicle velocity and could be used for predicting different prediction horizons. The results were assessed using MAE and compared across different Groups, where an increase in error was observed with an increase in the prediction horizon. Group D dataset showed the best performance, with SPaT data proving to be very useful for prediction. Although Group E had more signals, the Segment speed did not improve the results. Group D used as input to LSTM for 10th-second prediction showed an MAE of 1.78 m/s, and a time shift of 2.25 seconds was observed. It was also observed that Group D showed almost a 50% reduction in error compared to Group A. Finally, the algorithm was implemented on the vehicle hardware NVIDIA Drive PX2, where similar results were obtained.

This study has demonstrated the importance of V2I data for significant improvement in vehicle velocity prediction, as well as the effectiveness of the LSTM neural network in predicting future velocity. However, there are still several areas for further research.

Firstly, the prediction method could be extended with different NN architectures that are better suited to handling time-series data, such as WaveNet or Convolutional Neural Networks. Additionally, the number of drive cycles used for training the models could be increased to improve their accuracy and generalizability.

Secondly, this study has focused on predicting vehicle velocity, but there are other important variables that could be predicted using similar techniques, such as vehicle acceleration, fuel efficiency, and emissions. Future work could investigate the effectiveness of different signal groups for predicting these variables, as well as the potential benefits of combining multiple prediction models.

Finally, this study has demonstrated the potential of using live signals collected on NVIDIA Drive PX2 for real-time prediction. Future work could explore the feasibility of implementing this algorithm in actual vehicles, and the potential benefits of using this technology for improving safety and efficiency on the roads.

3.5 Chapter Conclusion

This section of the research partially addresses research question 1, Task 1.1. Research question 1 is restated here:

Research Question 1: *How effective are actual velocity predictive optimal energy management strategies in improving energy efficiency and reducing emissions in hybrid electric vehicles, and how do they compare to other EMS approaches?*

Hypothesis: Real-time, actual velocity predictive optimal energy management strategies, are implementable.

The study effectively addresses the research question by examining the impact of V2I data and LSTM modeling on vehicle velocity prediction. The results indicate that LSTM demonstrates good performance in predicting vehicle velocity and can be utilized for various prediction horizons. The study compares different groups based on input features and reveals that Group D, which includes SPaT data, exhibits the best performance. Additionally, the research demonstrates that the use of V2I data significantly improves the accuracy of vehicle velocity prediction. The implementation of the algorithm on vehicle hardware further confirms the validity of the findings. Consequently, this study demonstrates that V2I data is crucial for achieving significant improvements in vehicle velocity prediction, supporting the hypothesis. Furthermore, it highlights the predictive capabilities of artificial neural networks (ANN) in forecasting future velocity.

Chapter 4

Comparison of Optimal Energy Management Strategies Using Dynamic Programming, Model Predictive Control, and Constant Velocity Prediction

This study investigates the use of velocity prediction for improving fuel economy in HEVs through optimal energy management strategies. The study evaluates the performance of MPC using velocity predictions and compares it to other strategies, such as constant velocity prediction and full drive cycle prediction using dynamic programming. This study was published at SAE World Congress and it is considered as Task 1.2 of research question No. 1 [38]. My unique contribution to this involves the analysis and interpretation of the data presented in the paper. I actively participated in the writing, review, and editing process.

4.1 Introduction

Transportation-related air pollution issues have gained increasing attention in recent years. Federal and state governments have mandated that new transportation projects conform to the Environmental Protection Agency (EPA) regulations. Advancement in novel vehicle control approaches that accomplish improved fuel economy (FE) is an ongoing topic of study due to the financial, environmental, and cultural impact of transportation [39, 40].

Improving FE is an important way to reduce the adverse effects of climate change, and it also reduces our energy footprint [41]. This FE improvement along with a significant reduction in emissions could be achieved using HEVs and plug-in hybrid electric vehicles (PHEVs).

Modern-day vehicles are equipped with an ability to comprehend the worldview with many sophisticated sensors and signals, and the industry is moving rapidly toward the "Intelligent Vehicle Era" [42]. An intelligent vehicle means a vehicle that can sense the environment around it, communicate with it, and execute the controls accordingly. The type of sensors/signals available is Vehicle to Vehicle (V2V)/Vehicle to Infrastructure (V2I) communication, Advanced Driver- Assistance Systems (ADAS; RADAR, LiDAR, camera), traffic data, Controller Area Network (CAN) data, and Global Positioning System (GPS) [43–46]. These modern-day technologies can tremendously improve vehicular safety along with reduced energy consumption and reduced environmental pollution.

There are two types of vehicle control strategies that can effectively improve the FE (1) driving behavior modification including eco-driving and eco-routing and (2) powertrain operation modification through optimal energy management strategy (EMS) [44, 47]. The optimal EMS can be classified as (1) instantaneous second-by-second optimization without prior knowledge of the whole drive-cycle (DC) and (2) predictive optimal EMS, which requires some trip information known beforehand [44, 48, 49].

Furthermore, predictive optimal EMS can be classified as:

1. Globally optimal EMS with perfect full DC knowledge and prediction by using numerical optimization methods like dynamic programming (DP) and Pontryagin's minimum principle (PMP) [6, 10, 12]. DP is a numerical optimization method, which aims to find the globally optimal solution subject to the chosen discretization.DP is considered a benchmark for evaluating the performance of other control strategies due to its complexity and sensitivity to prediction accuracy.

2. Nonglobally optimal EMS with stochastic prediction and computationally efficient nonglobal optimal EMS [44,50,51]. In [50] and [51] authors used equivalent consumption minimization methods that don't guarantee in the global solution but come with a less computational cost and are practically implementable.

When deriving a globally optimal EMS using deterministic prediction, DP has been the overwhelming favorite due to its ease of use and robustness and no need for knowledge of derivatives [44, 50, 52]. A globally optimal EMS with deterministic prediction is difficult to implement in practice because of the high computational cost, but it is still beneficial in simulation to define the upper practical limit on FE benefits for a given vehicle and DC [44, 53]. One novel research suggests that DP can be implementable in real time only during acceleration event portions of a DC [54].

For computationally efficient nonglobal optimal EMS, we can implement model predictive control (MPC), where the optimization is done over a moving finite horizon that is shorter than the DC. Also with the ad-

vancement in perception systems and associated computational improvements, MPC could be implementable in real-world vehicles [44, 51, 55]. When limited trip information is available, we can implement optimal EMS by assuming the velocity to be constant for that horizon [53]. This novel EMS strategy could be implementable in vehicle controllers with an MPC type of framework.

4.2 Methodology

4.2.1 DC Development

Three different instances of a real-world DC are employed to symbolize highway driving and city-highway driving to develop the prediction model [25, 32]. The main differences separating these DCs are velocities and acceleration through the path. The location of DCs shown in Figure 4.1 and Figure 4.2 is in Ann Arbor, MI.

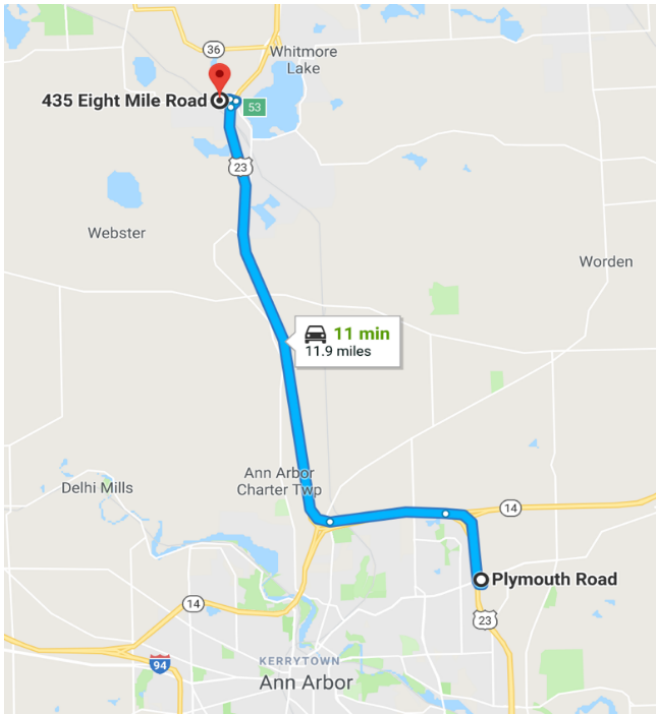

Figure 4.1: DC map: Highway DC (created with Google Maps).

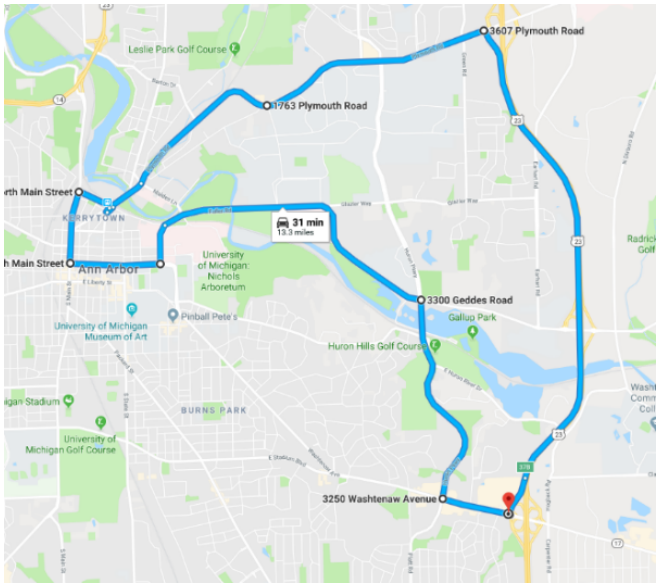

Figure 4.2: DC Map: City-Highway DC (created with Google Maps).

4.2.2 Baseline EMS

The Baseline EMS outlines the current performance of a 2017 Toyota Prius Prime in a rules-based, nonpredictive control strategy. Engine speed and engine torque through the whole DC are used as an input into a controls-oriented model. This controls-oriented model was developed using previously documented Toyota Prius operation equations [52, 53], integrated with MATLAB/Simulink but updated with vehicle parameters for the engine and motors to accurately represent a 2017 Toyota Prius Prime.

Comparison and validation between the controls oriented model used in this research and chassis dynamometer data are shown in Figure 4.3, where (a) is fuel consumption and (b) the initial state of charge (SOC_i) at the beginning of the DC and the final state of charge (SOC_f) at the end of the DC. These plots show a linear relationship between the controls-oriented model and the chassis dynamometer data for both fuel consumption and state of charge (SOC) across the industry-standard U.S. EPA DCs, including the Urban Dynamometer Driving Schedule (UDDS) and Highway Fuel Economy Test (HWY). The above DCs are only used for validation purposes, and the rest of the research utilizes two custom DCs to represent highway driving and city-highway driving. Because there is a linear relationship between the controls-oriented model and chassis dynamometer data over a variety of standard DCs, the model is validated [25].

In the blending approach, the engine gets utilized often during the charge depletion phase, thereby assisting the battery in meeting the total power demand as compared to charge depletion-charge sustenance. So, in blending, the battery charge depletes slowly and the engine operates efficiently because the engine operates on higher loads and consumes more fuel. As a result, blending and charge sustenance incur nearly the same total energy costs through the depletion phase [25, 56]. So, we considered the charge-sustaining approach. Also we

included adjusted accessory power loads to baseline EMS as well as to all Optimal EMS to avoid any unfair advantage over the baseline.

4.2.3 Optimal EMS

Developing and executing an optimal EMS has most generally been performed as an application of optimal control. A mathematical optimization problem is formulated by defining a dynamic equation that describes the current state of the vehicle, a cost function that penalizes fuel use, and constraints that ensure a desired final value of the battery SOC and powertrain component restrictions [51]. Optimal EMS system implementation can be broken down into distinctive subsystems as shown in Figure 4.4, perception (worldview computation), planning (optimal energy control computation), and implementation of the optimal EMS in the vehicle (vehicle plant subsystem, which includes a vehicle running controller) [25, 44, 57]. The following subsections identify each self-governing subsystem used in this research.

- Perception Subsystem

  The input data to the predictive optimal EMS is a series of sensors and signals such as CAN data, Radio Detection and Ranging (RADAR), GPS, V2V, V2I, and traffic data that recognize environmental information, thus defining vehicular surroundings. This can be used to produce a forecast of future vehicle states through a deep neural network, stochastic modeling, regression analysis [32, 44, 58]. The perception subsystem deals with the velocity prediction as well as the error between the desired and actual speeds.

- Planning Subsystem

  As shown in Figure 4.4, the input of this subsystem is vehicle operation prediction, which is velocity data derived from the first subsystem (perception) [37, 44]. From the desired velocity, the total desired power at each time instant can be computed. Using this total desired power (addition of internal combustion [IC] engine power and battery power), the control values that can deliver the desired IC engine power can be subsequently calculated. The main role of this subsystem is to compute the optimal control and issue a control request, which is the input for the final subsystem.

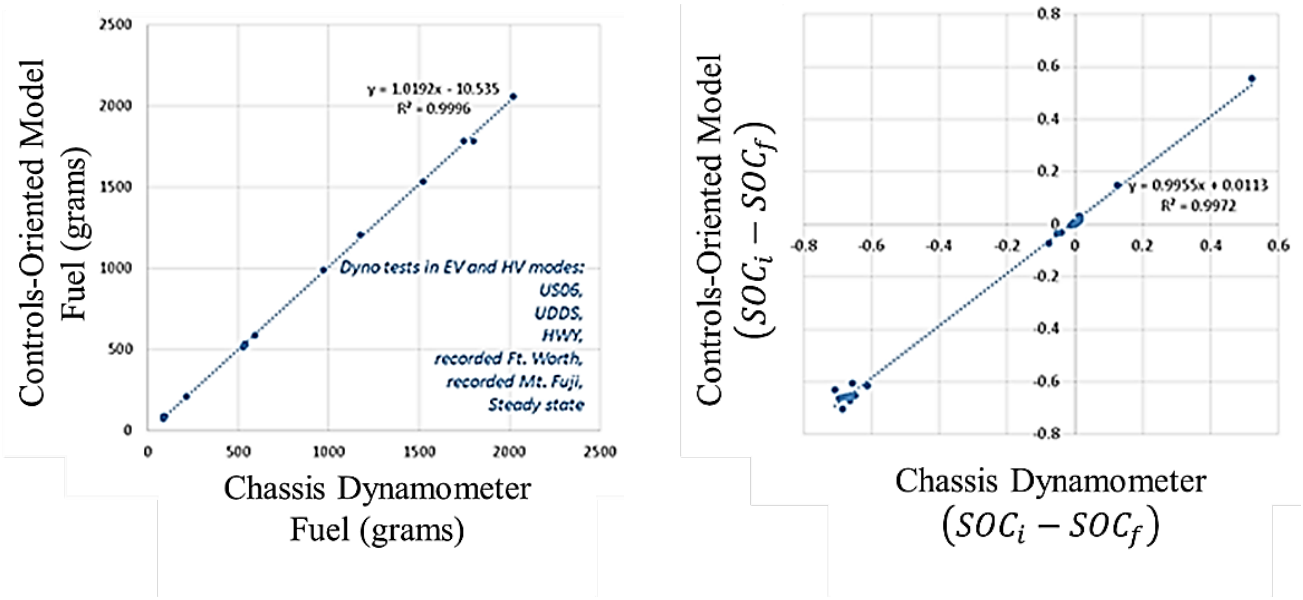

(a) (b)

Figure 4.3: A comparison between (a) the controls-oriented model used in this research and chassis dynamometer data of fuel consumption (b) and the initial SOC_i at the beginning of the DC and the final SOC_f at the end of the DC

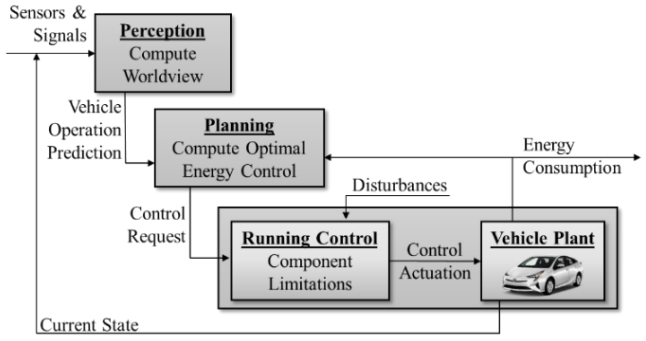

Figure 4.4: The system-level viewpoint of predictive optimal energy management

Dynamic Programming

Based on Bellman's principle of optimality, DP is a numerical method that solves multistage decision-making problems and finds the global optimal solution by operating backward in time [10, 25, 26]. We assumed that the desired future speed of the entire DC is obtained from the perception subsystem. To solve any problem with DP, first the dynamic equation and the cost function must be discretized. This can be done most conveniently by dividing the total time into N equal intervals of Δt. So time can be expressed as t=k Δt, where k is the time index. The speed data can be used to calculate the total desired power and subsequently the control values that can deliver the desired IC engine torque [53, 59]. Fuel consumption rates are calculated based on this data along with IC engine speed. Whereas, the SOC of the battery is also calculated for each power-split ratio and each time

index to make sure the total desired power demand gets satisfied without violating the SOC constraints. The detailed DP planning subsystem is shown in Figure 4.5. It takes future velocity as an input to calculate optimal controls by proceeding backward in time and provides optimal EMS decision matrix (engine power, SOC, and fuel consumption) [25]. Figure 4.6 shows the principle of backward recursive DP optimization, where it takes full DC prediction as an input and applies DP optimizer backward to calculate optimal control and the next state.

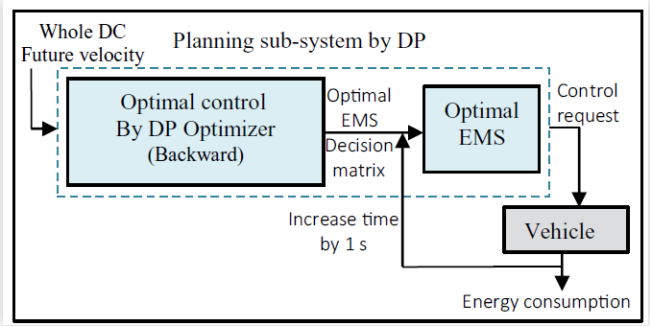

Figure 4.5: Detailed view of the planning subsystem by DP

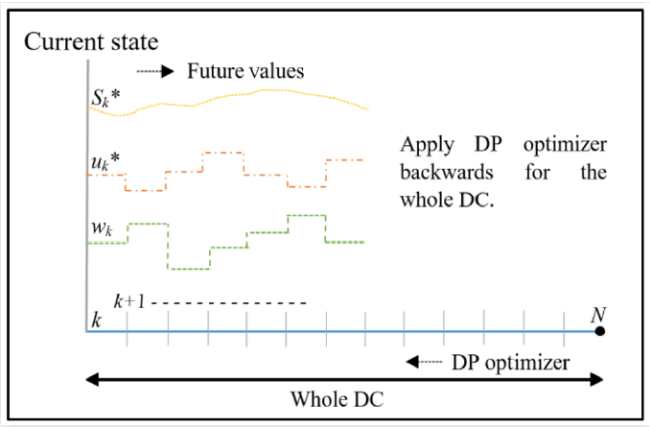

Figure 4.6: Working principle of DP

In general, the DP technique consists of a dynamic equation, a cost function (J), and state (S) and control variables (U) with feasibility constraints. In our study, we implemented DP on a 2017 Toyota Prius Prime by setting SOC as a state variable (S), engine speed ($u1$) and engine torque ($u2$) as the control variables, vehicle velocity as an exogenous input ($w1$), propulsion torque as another exogenous input ($w2$), and the summation of the mass of fuel used and charge sustention penalty as a cost function, which is to be minimized.

Dynamic Equation:

The overall DP formulation for the 2017 Toyota Prius Prime model is

$$s(k+1) = f(s, u_1, u_2, w_1, w_2, k)\Delta t. \tag{4.1}$$

The simplified DP equation consisting (please see [60] for derivation) of all dynamic equations of the vehicle, wheel, and SOC of power-split architecture with planetary gear train arrangement is

$$s(k+1) = s(k) - C_1 + \sqrt{C_2 - [C_3 * u_2 * ((C_4 * u_1) - (C_5 w_1))] - [C_6 w_1((C_7 w_2) - (C_8 * u_2))]}. \tag{4.2}$$

where k is the time index, *s(k)* is the current SOC, *s(k+1)* is the derived next SOC after applying control, and C values are constant and used to display the equation in a simple way (please see [60]).

Cost Function:

The cost function is the addition of the mass of fuel used and charge sustaining penalty. Though the penalty weight selection process is arbitrary, we kept in mind the strict charge-sustaining condition as well while selecting.

$$Cost = m_{fuel}(u_1, u_2) + W(SOC_f - SOC_{f,BaselineEMS}). \tag{4.3}$$

where m_{fuel} is mass of fuel used, which is a function of engine speed and engine torque derived using engine map. W is a penalty weight $(1665 - 1670)$ and SOC_f, Baseline EMS is the final SOC of the baseline EMS.

Constraints:

As the vehicle operates in strict charge-sustaining mode, an increase in the initial battery SOC above 20an extra advantage to FE improvement. On the other hand, if we reduce the initial SOC below 10%, it penalizes the FE improvement. So the constraints selected here show relevant and feasible operation of the 2017 Toyota Prius Prime in charge-sustaining mode as follows:

$$S_{min}(k) \leq s(k) \leq S_{max}(k) = 10\% \leq SOC(k) \leq 20\%. \tag{4.4}$$

$$u_{1min}(k) \leq u_1(k) \leq u_{1max}(k) = 0Nm \leq te(k) \leq 140 \text{ Nm}. \tag{4.5}$$

$$u_{2min}(k) \leq u_2(k) \leq u_{2max}(k) = 0rpm \leq ne(k) \leq 5200 \text{ rpm}. \tag{4.6}$$

Optimal Control Formulation by DP:

Start with defining inputs (constants, exogenous inputs) and discretizing the state and control variables:

$$\bar{s} = \{s_{min}, s_{min} + \delta s, ...s_{max}\} \quad (\delta s = 0.01\%) \tag{4.7}$$

$$\bar{u_1} = \{u_{1min}, u_{1min} + \delta u_1, ...u_{1max}\} \quad (\delta u_1 = 1Nm) \tag{4.8}$$

$$\bar{u_2} = \{u_{2min}, u_{2min} + \delta u_2, ...u_{2max}\} \quad (\delta u_2 = 10rpm) \tag{4.9}$$

Now from three-dimensional (3-D) matrix of *s , u1, u2* for simplicity and to reduce computational time. The new control and state variables are

$$S = [s]_{\bar{s},\bar{u1},\bar{u2}} \tag{4.10}$$

$$U_1 = [u_1]_{\bar{s},\bar{u1},\bar{u2}} \tag{4.11}$$

$$U_2 = [u_2]_{\bar{s},\bar{u1},\bar{u2}} \tag{4.12}$$

Now evaluate the vehicle model by backward recursive DP to calculate the next state as in 4.7.

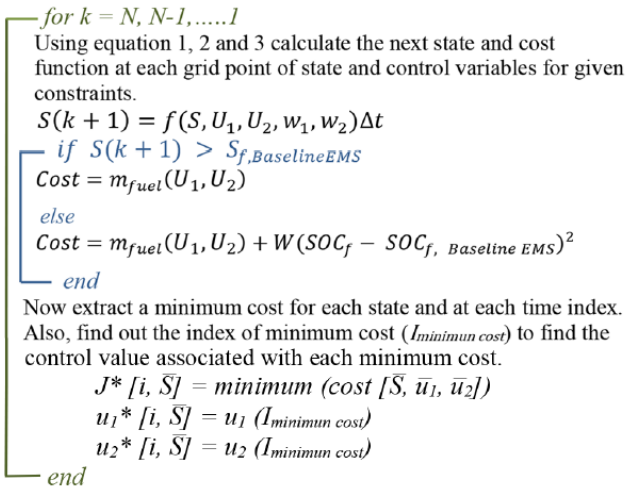

Figure 4.7: Dynamic Programming Algorithm Structure

While solving the DP algorithm, introduce the “tic” and “toc” functions to record the computational time. The total time recorded with the above DP algorithm using a Dell Inspiron 17 7000 for Highway DC is 31,703 s.

Optimal EMS Using Optimal Control:

Figure 4.8 and Figure 4.9 show the optimal control (u_1^* and u_2^*) matrix obtained by full DC prediction using DP with Highway and City-Highway DC, respectively. Using these controls, engine power, SOC, and fuel consumption have been calculated, which is globally optimal.

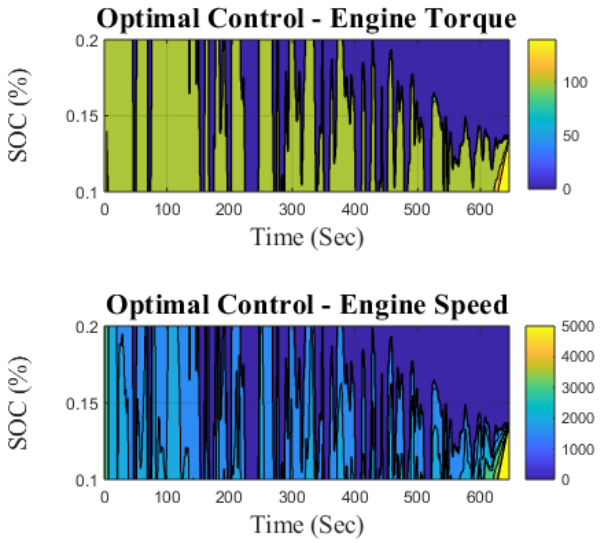

Figure 4.8: The optimal control matrix obtained using DP for the Highway DC

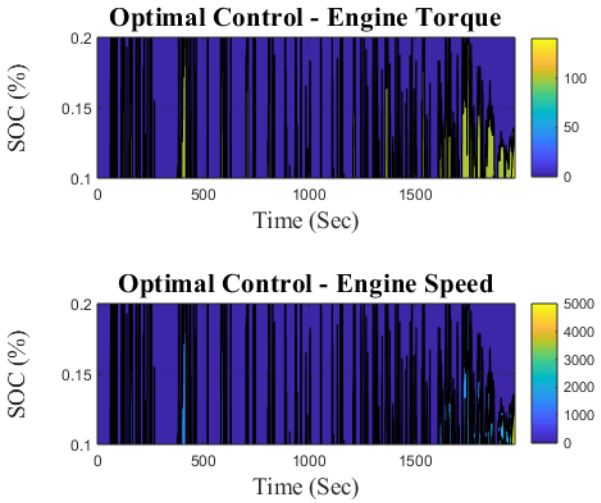

Figure 4.9: The optimal control matrix obtained using DP for the City-Highway DC

Model Predictive Control

Even though DP gives globally optimal EMS, it is very difficult to implement in practice because full DC cannot be predicted currently.

Nowadays, many researchers are exploring the optimal EMS, which can be implemented practically. MPC is a prospective strategy that can deliver optimal controls with practical considerations [19, 61–64].

Control inputs that are applied from the current time to a future time result in minimization of a cost function subject to the system dynamics and additional constraints [65–67].

Concept of MPC are shown in Figure 4.10 and Figure 4.11, respectively. Since the full DC prediction is not readily available beforehand, our knowledge is limited to the velocity predictions for the desired horizon at each time index as we progress. So MPC takes the predicted velocity of the desired horizon as an input to calculate optimal controls only for that selected horizon using DP optimizer backward in time, as shown in Figure 4.11. This process provides us optimal control for the entire horizon. But for further optimal EMS calculation, just select the controls of the desired time index.

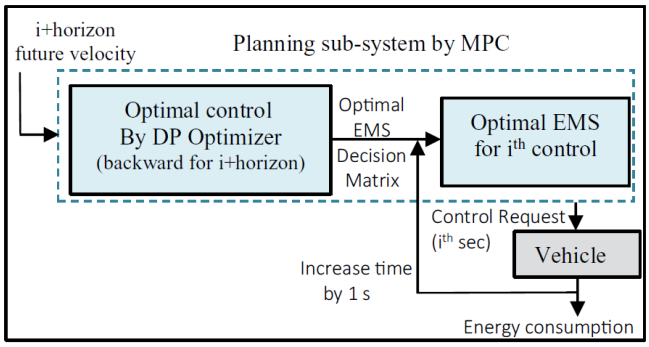

Figure 4.10: Detailed view of the planning subsystem by MPC

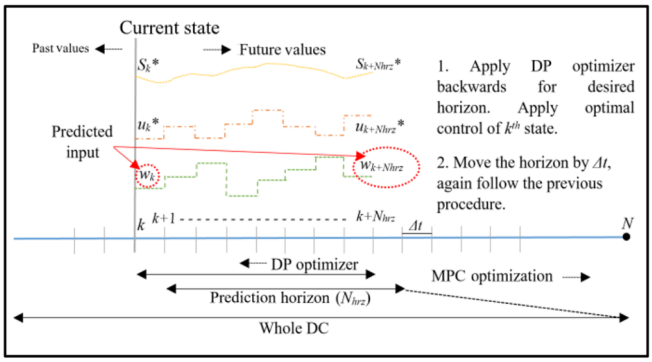

Figure 4.11: Working principle of MPC.

In general, MPC consists of a control equation, a cost function (J), and state (S) and control variables (U) with feasibility constraints. In our study, we have implemented MPC with a 10 s prediction horizon and keeping DP as the optimizer.

Control Equation:

The overall MPC formulation for the 2017 Toyota Prius Prime model is as follows:

$$s(k+1) = f(s, u_1, u_2, w_1, w_2, k)\Delta t \tag{4.13}$$

where k is the time index, $SOC(k)$ is the current SOC, $SOC(k+1)$ is the derived next SOC after applying control, u_1 is engine speed, u_2 is engine torque, and w_1, w_2 are an exogenous input - velocity, and propulsion torque.

Cost Function:

The cost equation is the same as DP. The only difference considered is horizon time, not the whole DC.

$$Cost = m_{fuel}(u_1, u_2) + W(SOC_f - SOC_{f,BaselineEMS})^2 \tag{4.14}$$

where $N_{horizon}$ is the number of the horizon time-step.

Constraints:

Constraints are the same as those used in DP. Only the horizon is considered.

Optimal Control Formulation by MPC:

To derive optimal controls, DP has been used as an optimizer in MPC. Start with the defining inputs (all constants, exogenous inputs. It starts from the first time state as shown in 4.12

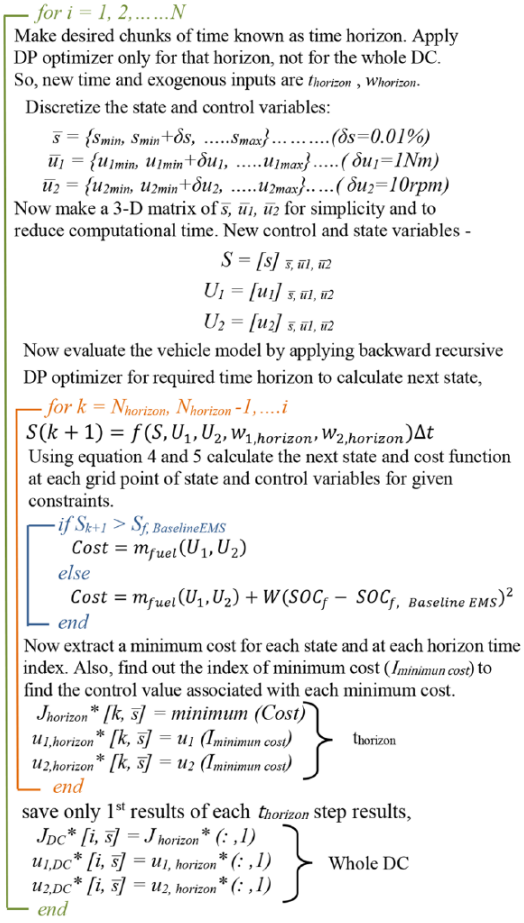

Figure 4.12: MPC Algorithm Structure

The total time recorded with the MPC algorithm of 4.12 on a Dell Inspiron 17 7000 for the Highway DC is 307,325 s (475 s for 1 time-step).

Optimal EMS Using Optimal Control:

Figure 4.13 and Figure 4.14 show the engine power, SOC, and fuel consumption calculated with the optimal control (u_1^* and u_2^*) matrix obtained by MPC over a 10s horizon prediction with Highway and City-Highway DC, respectively.

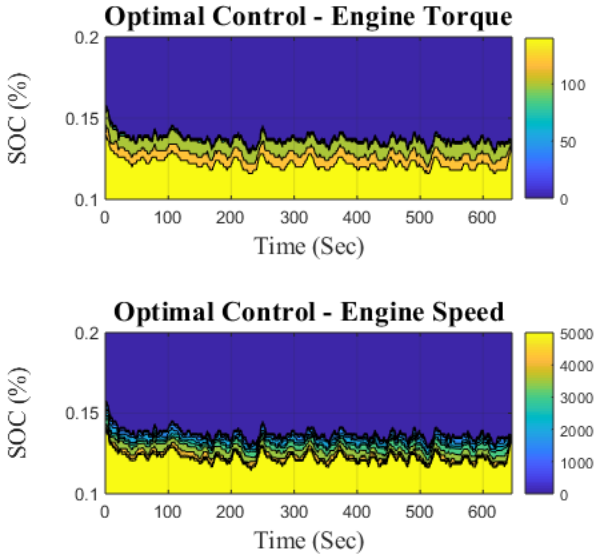

Figure 4.13: The optimal control matrix obtained using MPC for the Highway DC

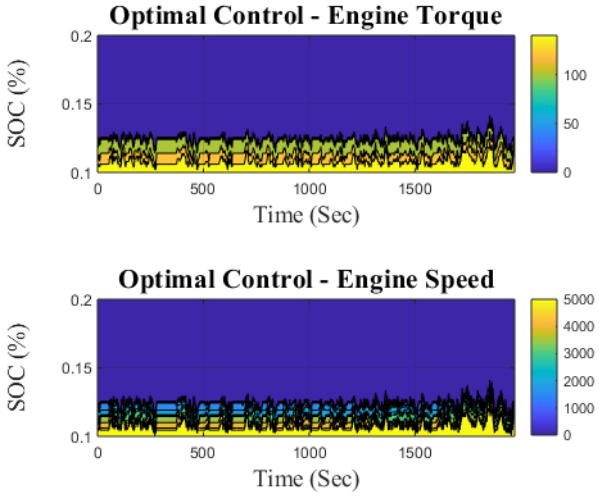

Figure 4.14: The optimal control matrix obtained using MPC for the City-Highway DC

Constant Velocity Prediction

Due to limitations on the perception subsystem, in the near term with limited trip information available or with no trip information available,we can calculate the optimal controls by assuming a constant speed for an assumed finite time horizon [53].

The planning subsystem responsible for detailed constant velocity prediction is depicted in 4.15 and its operational principle is illustrated in 4.16. In this subsystem, the input consists of the future velocity for a predetermined horizon (typically 10 seconds) assumed to be constant, matching the velocity of the present time-

step. Utilizing a backward-moving DP optimizer, the optimal controls for the selected horizon are calculated, as indicated in 4.16. This process yields optimal control throughout the horizon, with the horizon velocity remaining constant and equal to the velocity of the current time-step. However, for the purpose of further optimal EMS calculation, only the controls associated with the present time-step are selected. Given the advancements in current perception subsystems, this method proves advantageous for implementation in vehicle controllers employing a model predictive control (MPC) framework.

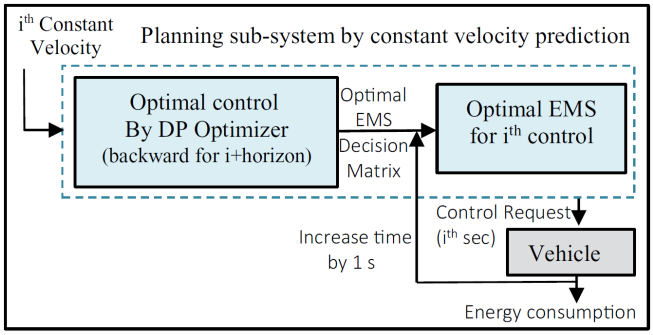

Figure 4.15: Detailed view of the planning subsystem by constant velocity prediction

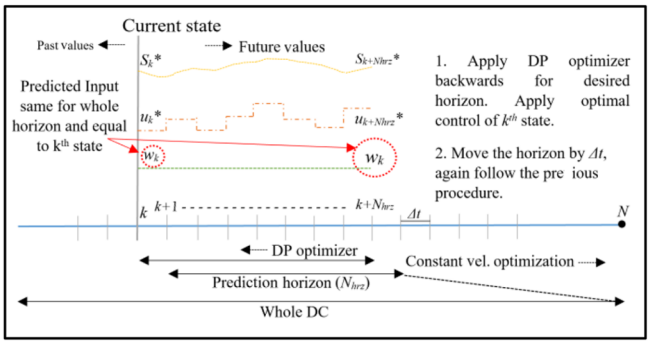

Figure 4.16: Working principle of constant velocity prediction

The control equation, cost equation, constraints, state, and control variables are the same as previously used in MPC. The only difference is in the horizon velocity.

Optimal control formulation by constant velocity prediction:

To derive optimal controls, use DP as an optimizer. This starts with defining inputs (all constants, exogenous inputs) Start from the first time state

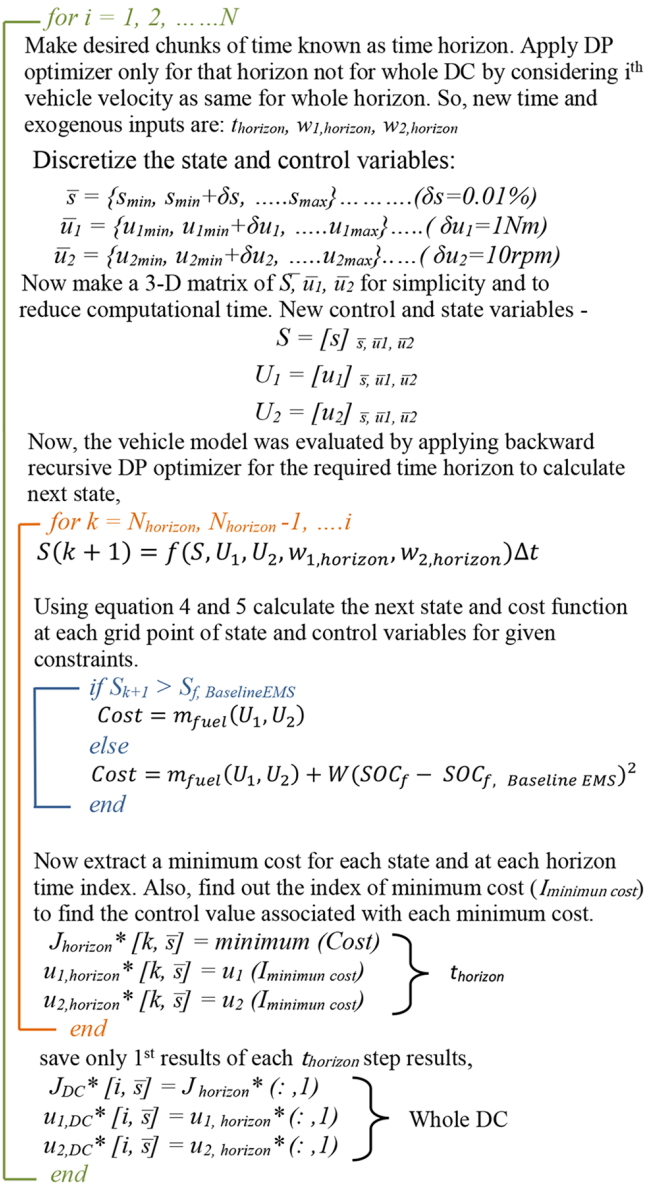

Figure 4.17: Constant Velocity (CV) prediction Algorithm Structure

The total time recorded with the constant velocity prediction algorithm of 4.17 on Dell Inspiron 17 7000 for Highway DC is 298,914 s (462 s for 1 time-step).

Optimal EMS Using Optimal Control:

Figure 4.18 and Figure 4.19 show the engine power, SOC, and fuel consumption calculated for the optimal control (u_1^* and u_2^*) matrix obtained by constant velocity prediction with Highway and City-Highway DC, respectively.

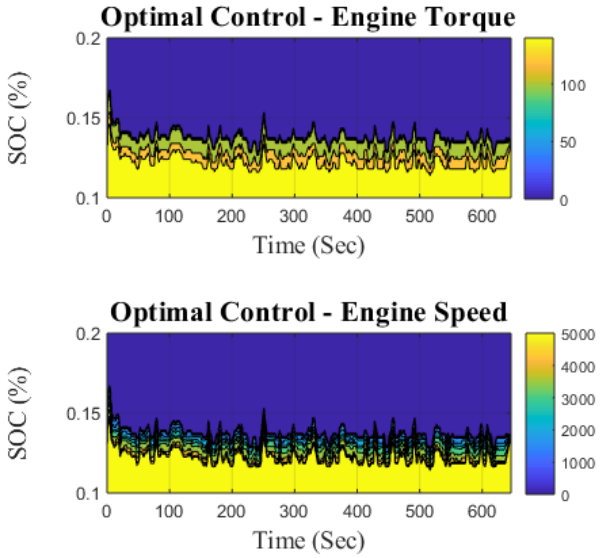

Figure 4.18: The optimal control matrix obtained using constant velocity prediction for the Highway DC

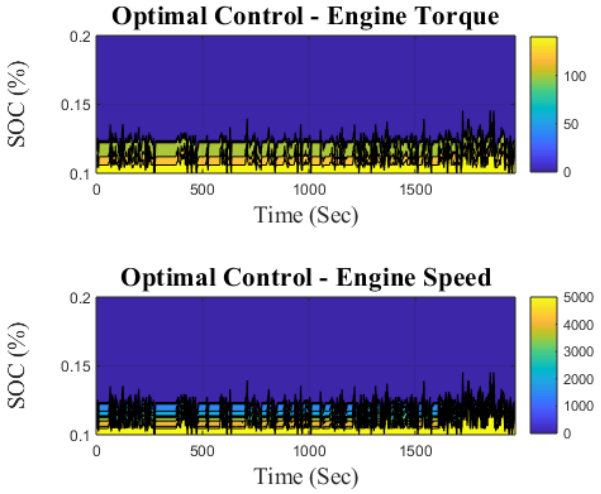

Figure 4.19: The optimal control matrix obtained using constant velocity prediction for the City-Highway DC

4.3 Results

We proposed three different strategies for optimal EMS analysis: (1) perfect full DC prediction using dynamic programming, (2) 10 s prediction horizon MPC, and (3) 10 s horizon constant velocity prediction. Figure 4.20 and Figure 4.21 show the comparative result of fuel consumption and SOC level with Highway DC and City-Highway DC, respectively, at each time index of all three strategies with baseline EMS, which outlines the current performance of a vehicle in a rules-based, nonpredictive control strategy. The percentage of FE improvement

with these three proposed strategies over baseline FE is calculated as

$$\%\Delta(FE) = \frac{(MPG_e)_{OptimalEMS} - (MPG_e)_{BaselineEMS}}{(MPG_e)_{BaselineEMS}} \tag{4.15}$$

where $(MPG_e)_{OptimalEMS}$ is miles per gallon of gasoline equivalent with optimal EMS and $(MPG_e)_{BaselineEMS}$ is miles per gallon of gasoline equivalent with baseline EMS.

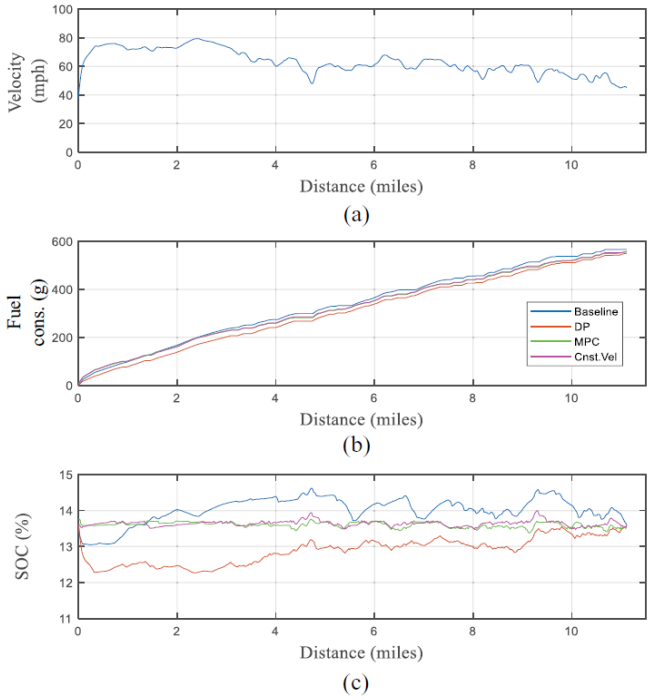

Figure 4.20: Baseline, DP, MPC, and constant velocity prediction EMS comparisons for the Highway DC

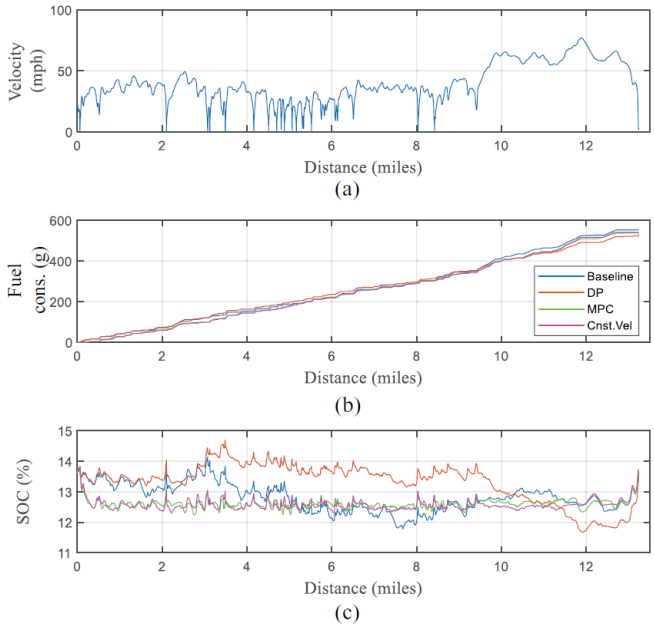

Figure 4.21: Baseline, DP, MPC, and constant velocity prediction EMS comparisons on the City-Highway DC

From Figures 4.20 to 4.21 (a)-(c), the overall fuel consumption trend from lowest to highest can be given as:

$$DP < MPC < ConstantVelocityPrediction < BaselineEMS \tag{4.16}$$

Perfect full DC prediction implemented with DP shows the best FE improvement and is considered as the upper limit on FE improvement. On the contrary, the baseline EMS shows the point of comparison for any FE improvements. Overall, the perfect full DC prediction implemented with DP showed 2.94% and 4.32% of FE improvement over baseline FE on the Highway and City-Highway DC, respectively.

Figure 4.20 (b) shows a constant velocity prediction fuel consumption trend that closely follows the MPC trend on highway driving. On the contrary, Figure 4.21 (b) shows a significant difference between constant velocity prediction and MPC fuel consumption trends. But it also shows that even with the limited prediction constant velocity, prediction strategy can provide a remarkable FE improvement. Overall, the 10 s prediction horizon MPC showed 1.85% and 3.32% of FE improvement over baseline FE on the Highway and City- Highway DC, respectively. While the 10 s horizon constant velocity prediction showed 1.59% and 2.47% of FE improvement over baseline FE on the Highway and City-Highway DC, respectively. Also, all EMS strategies start and end with the same SOC level, which aligns with our assumption(s) that a vehicle works in the "charge sustaining" mode.

From Figures 4.20-4.21 (c), SOC trends of DP strictly obey charge-sustaining operation, but in between the DC endpoints, the SOC fluctuates largely. This clearly indicates DP takes full advantage of the battery power with perfect full DC prediction. Due to this in both highway and city-highway driving, FE improvement is

highest. This is also justified by the DP fuel consumption trends shown in Figures 4.20-4.21 (b). This clearly shows that the DP fuel consumption trend is distinct from others, where fuel consumption is lowest with DP.

Figure 4.20 (c) indicates that, on highway driving, SOC trends of both MPC and constant velocity prediction at each timestep always stay close to the initial SOC level, which looks like the SOC level is constant for the whole DC. On the other hand, Figure 4.21 (c) indicates that, with city-highway driving, the SOC trends of both MPC and constant velocity prediction show some fluctuations, but their amplitude is much smaller than the DP SOC trend. This low SOC fluctuation results in a higher battery life.

Figure 4.22 and Figure 4.23 show the behavioral comparisons of the engine power trends of different EMS strategies on the highway and city-highway driving, respectively. When comparing the engine power from the Baseline EMS and the globally Optimal EMS in Figure 4.22 (a), there are few points, like at the 4th and 12th mile distances, where the Optimal EMS has turned off the engine and operated the engine at lower overall power with fewer fluctuations, resulting in 2.94% of FE improvement. Similarly, when comparing the engine power from the Baseline EMS and the globally Optimal EMS in Figure 4.23 (a), there are many points where the Optimal EMS has turned off the engine and operated the engine at lower overall power with fewer fluctuations, resulting in 4.3% of FE improvement.

Figures 4.22-4.23 (b) show the MPC engine power trend closely follows the DP engine power trend with some exceptions. The amplitude and number of fluctuations of the MPC engine power are higher than the DP engine power trends. Because of this engine behavior, MPC demonstrates a lower FE improvement than DP. Despite this, MPC has the potential to achieve 60%-65% and 70%-80% of global FE improvement levels on the highway and city-highway DC, respectively, as summarized in Figure 4.24.

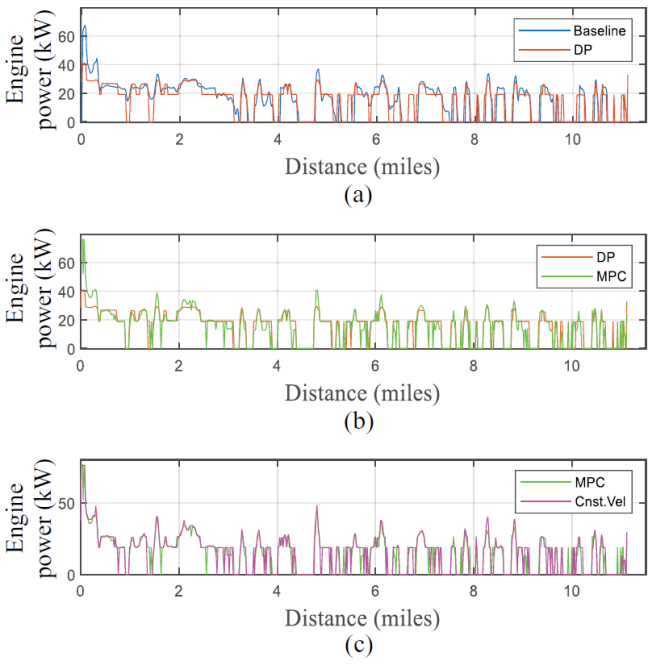

Figure 4.22: Baseline, DP, MPC, and constant velocity prediction engine power comparisons

Figure 4.22 (c) indicates a sharp increment in the engine power for the constant velocity prediction in some instances as compared to MPC engine power on the Highway DC. This indicates that constant velocity prediction can potentially achieve 80%-92% of MPC FE improvement. On the other hand, the engine power trend with constant velocity prediction shows multiple sharp increments over MPC engine power on the City-Highway DC, as shown in Figure 4.23 (c). This causes a drop in the FE improvement potential of constant velocity prediction over MPC FE improvement. Overall the constant velocity prediction has the potential to achieve 50%-60% of global FE improvement.

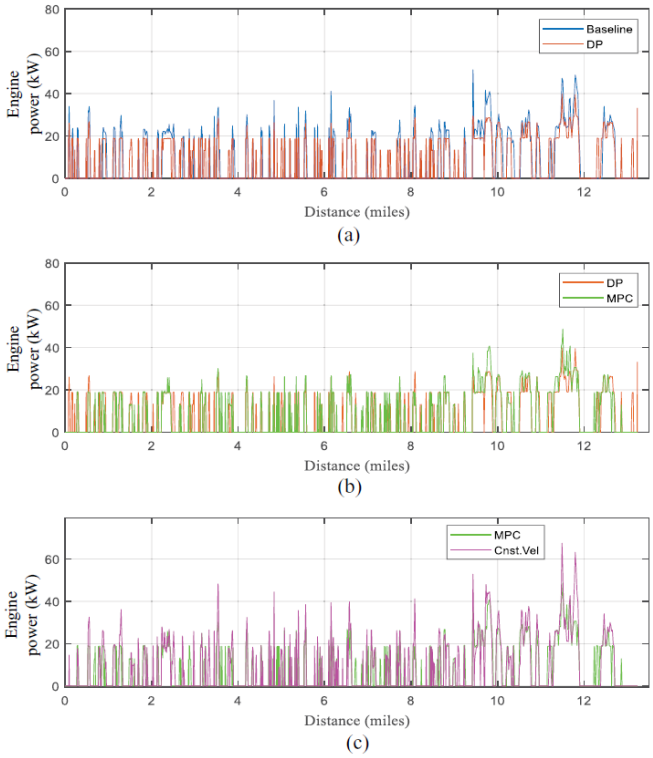

Figure 4.23: Baseline, DP, MPC, and constant velocity prediction engine power comparisons with City-Highway DC

Overall the FE improvement results of both highway and city-highway driving with all three strategies over baseline EMS are shown in Figure 4.24. The perfect full DC prediction along with DP has the largest average FE improvement, followed by the 10 s prediction horizon MPC, and then the 10 s horizon constant velocity prediction over baseline EMS.

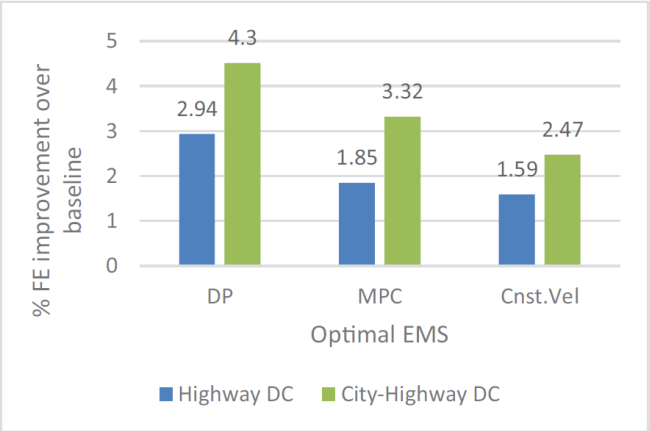

Figure 4.24: Summary of the FE improvement with all EMS on both Highway and City Highway DC

Figure 4.24 also provides evidence that on the Highway DC, constant velocity prediction can achieve nearly the same level of fuel efficiency improvement as MPC. Therefore, for highway driving scenarios, it may be more beneficial to utilize the simpler constant velocity prediction method rather than the more complex MPC method. This is because constant velocity prediction does not necessitate accurate horizon prediction, unlike MPC. In contrast, on the City-Highway DC, there is a substantial disparity between the fuel efficiency improvement achieved by MPC and constant velocity prediction. This indicates that MPC yields superior results on the City-Highway DC due to its consideration of accurate horizon velocity predictions.

4.4 Conclusion

In this study, we have investigated three different EMS in simulation using real-world Highway DC in a validated control-oriented 2017 Toyota Prius Prime model operating in charge-sustaining mode. The input to all EMS planning subsystems is velocity predictions obtained from the perception subsystem. The output of the given planning subsystem is the vehicle control matrix that realizes FE improvement with optimal engine power generation while maintaining the battery SOC level in the whole DC.

The perfect full DC prediction along with DP gives globally optimal EMS, which represents the upper limit of the achievable FE improvement. The 10 s prediction window MPC strategy provides the second-best FE improvement results in this study, which were found to be very significant. The MPC results suggest that it has the potential to achieve 60%-65% and 70%-80% of global FE improvement over Highway and City- Highway DC, respectively. This is good news because, with near-term advancements in perception systems, MPC can likely be implemented in near-future vehicles. The even simpler case of constant velocity prediction also shows promising results when implemented in vehicle controllers with an MPC type of framework. The constant velocity prediction results suggest that it has the potential to achieve 80%-90% and 75%-85% of MPC FE improvement over the Highway and City-Highway DC, respectively. Also, the MPC and constant velocity prediction results

suggest that FE improvement from the perfect 10 s MPC is only slightly higher than constant velocity 10 s, which means that a 10 s prediction window is not that beneficial for generating actual velocity predictions for MPC. The MPC and constant velocity SOC results corroborate the above claim(s) to achieve better battery performance. Overall, these results contribute to the mounting evidence that velocity prediction fidelity does not need to be as robust as initially suspected, thus contradicting more than a decade of previous research.

For future work, we seek to combine both perception and planning subsystem and integrate it with a real-world vehicle through NVIDIA PX2 and vehicle controller. Our near-term goal is to implement the constant velocity prediction strategy as it does not require a perfect horizon operation prediction. As the 10 s prediction window is not that beneficial for generating actual velocity predictions for MPC, we seek to explore more prediction windows and its effect on FE improvement. Also the total computational time with these MPC and constant velocity prediction methods are almost ten times higher than the DP computational time. But in an implementation perspective with the MPC and constant velocity prediction methods, at each time-step, we only need to optimize the next 10 s (not the entire DC as with DP). So this large computational time gets distributed over the entire DC. As high performance, energy-efficient computing like NVDIA PX2 is available, our long-term goal is to implement the MPC strategy as our perception research gets mature.

4.5 Chapter Conclusion

This section of the research partially addresses research question 1, Task 1.2. Research question 1 is restated here:

Research Question 1: *How effective are actual velocity predictive optimal energy management strategies in improving energy efficiency and reducing emissions in hybrid electric vehicles, and how do they compare to other EMS approaches?*

Hypothesis: Real-time, actual velocity predictive optimal energy management strategies, are implementable.

This study effectively addresses the research question by investigating three different energy management strategies (EMS) in a simulated real-world scenario using a Toyota Prius Prime model. The study utilizes velocity predictions obtained from the perception subsystem as inputs to the EMS planning subsystems. The results show that the globally optimal EMS, achieved through perfect full DC prediction and dynamic programming (DP), provides the highest fuel efficiency (FE) improvement. However, the study reveals that the 10-second prediction window model predictive control (MPC) strategy offers significant FE improvement, indicating its potential for implementation in near-future vehicles. Furthermore, even the simpler approach of constant velocity prediction shows promising results when implemented within an MPC framework. The constant velocity prediction approach demonstrates high FE improvement, suggesting its viability for achieving efficient energy management in hybrid electric vehicles. The results also indicate that the fidelity of velocity predictions does

not need to be as robust as previously believed, challenging previous research in the field. Overall, this research demonstrates the effectiveness of actual velocity predictive optimal energy management strategies in enhancing energy efficiency and reducing emissions in hybrid electric vehicles. It provides valuable insights into the performance of different EMS approaches, highlighting the potential of MPC and constant velocity prediction as viable alternatives for achieving significant FE improvement.

Chapter 5

Development and Evaluation of Velocity Predictive Optimal Energy Management Strategies in Intelligent and Connected Hybrid Electric Vehicles

The study evaluates the effectiveness of Predictive Optimal Energy Management Strategies (POEMS) for Hybrid Electric Vehicles (HEV) using predicted velocity data. This study was published in the "Energies" by MDPI (Multidisciplinary Digital Publishing Institute) and it is considered as Task 1.3 of research question No. 1 [68]. I shared the first authorship with Aaron Rabinowitz. My contributions encompassed the investigation process and the writing, review, and editing of the chapter. Together with Aaron Rabinowitz, I conducted the research, analyzed the data, and interpreted the results. Our collaborative effort in writing the original draft, as well as the subsequent review and editing stages, led to the successful publication of the journal paper and the inclusion of its key findings in Chapter 5.

5.1 Introduction

Improving FE is a critical goal to reducing climate change and air pollution. The transportation sector is responsible for 27% of all greenhouse gas emissions produced globally and more than 50% of nitrogen oxide emissions [69]. Recent studies show that greenhouse gas emissions are a significant contributor to global climate change [70] and lowered life expectancy in many countries [71]. Greenhouse gas emission levels are directly related to the FE of vehicles; reducing total miles driven is a difficult-to-implement and politically controversial goal,

thus much research into methods to improve vehicle Fuel Economy (FE) has been performed [72].

A critical component of improving FE is vehicle electrification. Recently, Hybrid Electric Vehicles (HEV) and Plug-in Hybrid Electric Vehicles (PHEV) have been widely researched because of their greater potential to increase Fuel Economy (FE) and emissions over that of conventional Internal Combustion Engine (ICE) vehicles [73]. However, currently available HEVs do not operate optimally [74].

In addition to advancements in powertrain technology, recent developments in the automotive industry have led to huge advancements in Intelligent and Connected Vehicle (ICV) technology. Advanced Driver Assistance System (ADAS) technology has seen rapid market penetration due to its potential to bring safety and convenience benefits to customers [75–77]. Automation (i.e. ADAS) and connectivity (i.e. ICV) technology are critical technologies not only for safety and commercialization of autonomous vehicles but also for energy efficiency through implementation of Predictive Optimal Energy Management Strategies (POEMSs) on HEVs and PHEVs which can increase their FE and reduce their emissions [78–82].

POEMSs use predicted vehicle velocity (enabled through ADAS [83] and connectivity) as an input to optimal control. The optimal solution output is then used as an input to the vehicle plant, ideally an HEV or PHEV due to the additional operational degrees of freedom [84]. This process has been the subject of active research since the first publication in 2001 [78]. Note that in the current transportation environment, perfect future velocity prediction is not possible. To address this issue, researchers have used Model Predictive Control (MPC) which, in this context, is the application of DP optimization to fixed length prediction windows. Research in this space has demonstrated that perfect velocity prediction is not required [85], and that even heuristic approaches which rely on acceleration event prediction can be used [80, 86] to achieve improvements in FE. Although it is worth noting that these FE improvements are modest compared to those theoretically achievable with prefect prediction of vehicle velocity. High-fidelity prediction of future vehicle velocity is presently achievable through the employment of Machine Learning (ML) and Artificial Neural Network (ANN) methods and ICV technology [17–20, 22–25, 87]. Despite all of this research, a thorough investigation of the datasets and prediction models effect on vehicle FE (the full system) has not been conducted. The latest research has explored the effect on velocity prediction error metrics rather than resultant vehicle FE [25, 88].In order to facilitate real world implementation, certain specific research gaps must be addressed; these research gaps are defined in [84] as:

1. Performance of Optimal EMS with Actual Velocity Predictions
2. Performance of Optimal EMS when Subjected to Disturbances
3. Performance of Optimal EMS in Real Vehicles

To the author's knowledge, this research represents the first comprehensive study fully addressing Research Gap 1. Previous research in the area of POEMS has focused on select aspects of Research Gap 1 but no

comprehensive study has been performed which concerns the use of real-world data and real-time prediction methods in POEMS. This study, being such a comprehensive analysis, allows for research to progress towards other aspects of implementation namely Research Gaps 2 and 3. Previous research in this area is summarized as follows. The efficacy of predictive Optimal EMS for improving efficiency in HEVs was first shown in 2001 in [78] utilizing perfect prediction. In 2008 velocity prediction was introduced to the literature in [21] which used an analytical traffic based velocity prediction model. In 2015, the advantages of ANN prediction were shown in [19,20]. In 2017 and 2018 a series of studies [37,83,85,89] experimented with different data streams to optimize prediction with a shallow ANN. In 2019 more modern machine learning techniques were introduced into the field in [90] where reinforcement learning was used along with traffic data to train an ANN to produce optimal controls for a power-split hybrid. Also in 2019, [25,91] showed that high fidelity predictions were possible through the use of deep Long-Short-Term-Memory (LSTM) ANNs. Finally, in 2020, a thorough analysis of various combinations of real world data streams and machine learning techniques [25,88,92] showed that the highest degree of prediction fidelity could be attained through the use of LSTM ANNs with the use of Signal Phase and Timing (SPaT) and Lead Vehicle data.

Thus, in order to close the gap, this study outlines a comprehensive system-level study addressing the interactions between groups of available real-world data, velocity prediction methods, and Optimal EMS methods with respect to the overall system output: FE.

This study rigorously evaluates the dataset and perception model for POEMS and evaluates performance using the FE for a validated HEV to enable full system performance insight, which to-date is missing from the literature. Cutting-edge AI technology is leveraged to generate high-fidelity future vehicle velocity predictions in 10 to 20 second windows. The predictions are fed into an MPC control method in order to determine the optimal instantaneous torque split for a power-split HEV. The FE achievable with the proposed POEMS will be compared to that achievable with perfect prediction Full drive-Cycle DP (FCDP), Perfect Prediction MPC (PP-MPC), Constant Velocity-prediction MPC (CV-MPC), and Autonomie baseline control. This study will further show that the proposed method is implementable on current vehicles with current technology and has the potential to provide significant FE improvements within the HEV fleet if implemented.

5.2 POEMS Methodology

5.2.1 Overall System

HEV POEMS uses predictions of future vehicle velocity to inform an optimal powertrain control strategy, thus achieving greater energy efficiency. Powertrain controls include torque split and gear shifting based on powertrain states such as battery State of Charge (SOC) and current gear in the case of a parallel power-train configuration or only torque split in the case of a parawhnllel configuration.

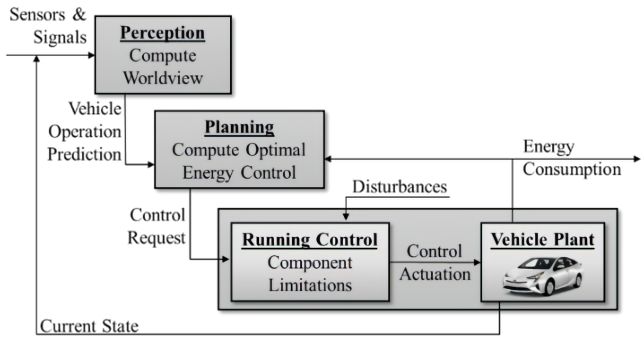

Figure 5.1: POEMS logic flow schematic

As shown in Figure 5.1, a POEMS consists of three major subsystems. The first is the perception system which predicts vehicle motion using information about previous and current vehicle motion, powertrain states, driver inputs, ADAS, and V2X data as inputs. The second is the planning subsystem which computes optimal controls based on the predicted vehicle velocity. And finally the third subsystem is the vehicle plant which can be either the physical vehicle or high-fidelity simulation model of the vehicle. The final system outputs are the actual vehicle velocity and powertrain states.

POEMS achieve greater FE by ensuring that the engine is used in regions of maximum efficiency as often as possible. This concept is shown in Figure 5.2 which includes a Brake Specific Fuel Consumption (BSFC) map for an example engine and different combinations of engine speed and torque which produce different engine efficiencies. Thus, most engine controllers attempt to operate the engine along its Ideal Operating Line (IOL) [93] which contains the most efficient torque for a given engine speed. POEMS utilizes future vehicle velocity information to ensure that the engine operates within the most efficient segment of the IOL. By considering an Ideal Operating Line Segment (IOLS), POEMS aims to optimize the engine's performance and achieve maximum efficiency.

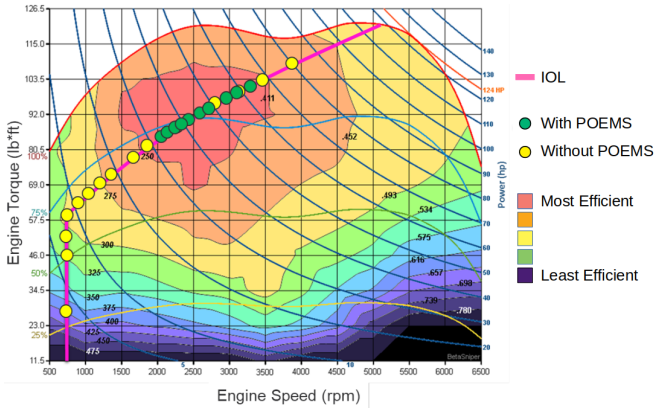

Figure 5.2: Example BSFC plot with IOL and operating points with and without POEMS

As shown in Figure 5.2, simply operating along the IOL (yellow dots) does not guarantee efficient operation.

POEMSs increase FE by guaranteeing operation within the IOLS (green dots).

Although this paper only concerns vehicle motion, the POEMS method can be extended to account for additional exogenous inputs such as cabin heating and cooling requirements [94–96] without fundamentally changing the method.

5.2.2 System Inputs

Data-Set Development

The first step in the development of practical and high-fidelity real world future vehicle speed prediction was to collect a sample generic data-set which would represent all data sources potentially available to a given ICV. All data sources selected are currently available to ICVs or will be available in the near future [97]. In this section a taxonomy for such a data-set is defined. This taxonomy defines data both in terms of its source form and its processed form and defines the process of transformation.

The first step in defining the data-set is to define the sources of the data. Three distinct source categories are proposed:

1. VEH: Vehicle operational data such as vehicle motion, performance, and driver inputs. This data concerns only the ego vehicle itself and its driver.

2. ADAS: Advanced Driver Assistance System (ADAS) data [98]. This consists of the data generated by external object sensors on the vehicle and concerns objects within the vehicle's line of sight.

3. V2I: Data which the vehicle receives through connectivity to infrastructure and other vehicles.

In order to be considered an ICV, a vehicle must receive information from all three of the above sources. Most modern vehicles receive data from the VEH and ADAS sources [99] and V2I is available in some regions [100]. These signals were obtained from the ego vehicle CAN bus and the City of Fort Collins, Colorado.

Within these source categories, signals of use in vehicle future velocity prediction are shown in Table 5.1.

Table 5.1: Data sources and associated signals

Data Source	Signal	Description
VEH	General Vehicle Signals	Signals such as speed, acceleration, throttle position, and steered angle which can be found via CAN on any vehicle
VEH	Historical Speeds (HS)	Historical speed data for the vehicle at the current location
ADAS	Lead Vehicle Track (LV)	Relative location of confirmed lead vehicle from ADAS system
V2I	Signal Phase and Timing (SPaT)	Signal phase and timing of next traffic signal
V2I	Segment Speed (SS)	Traffic speed through current road segment

All VEH signals should be available on all modern vehicle CAN networks while ADAS enabled vehicles will produce a lead vehicle track for safety and Autonomous Cruise Control (ACC) purposes. The information for SPaT and SS comes form the SAE J2735 SPaT/Map message. Thus all signals used in this study are available to a generic ICV while traveling on a connected infrastructure. Most modern vehicles will have access to the VEH and ADAS sourced signals. A total of 13 drive-cycles worth of data were collected along the data drive-cycle by one driver over two days. Details about data collection and availability can be found in the team's previous work [92].

Data Drive-Cycle Selection

In order to gauge the effects of real-world data-based predictions on the performance of POEMS, a real-world dataset was required. It was desired to gather data in conditions which would allow for optimal POEMS performance such that the relative differences between various POEMS methods would be as great as possible. A secondary consideration was that, in order to allow for optimal ML and ANN prediction performance, the data collection should be conducted along a repeating drive-cycle and that this cycle should be short enough that more than 10 cycles could be collected in a single day. The drive cycle which was selected was a 4 mile long drive-cycle along urban arterial roads in downtown Fort Collins, Colorado which is shown in Figure 5.3.

Figure 5.3: Selected data drive-cycle; drive order was purple, yellow, blue, then green, red circles represent traffic signals

In order to assess the characteristics of the data drive-cycle, it was determined that the data drive-cycle and the EPA dynamometer drive cycles should be characterized by their distributions of speeds and accelerations. These basic statistical measures were chosen in order to allow for easy comparison between the drive-cycles. The drive cycle characteristics data is shown in Table 5.2.

Table 5.2: Drive-cycle characteristics for data drive-cycle and EPA drive cycles

Drive-Cycle	**Mean Non-Zero Speed (MNZS)-m/s**	**Standard Deviation of Non-Zero Speeds (SNZS)-m/s**	**Mean Absolute Acceleration (MAA)-m/s^2**	**Standard Deviation of Absolute Accelerations (SAA)-m/s^2**
Data	18.6988	8.5699	1.1557	1.1432
UDDS	10.7923	5.5850	0.4723	0.4859
US06	23.1791	9.5014	0.6538	0.7851
HWFET	21.7191	4.1752	0.1713	0.2443

Based on these characteristics, the similarity of the data drive-cycle and the EPA dynamometer drive-cycles was calculated using the multivariate normal distribution. The relative similarities between the EPA cycles and the data drive-cycle are shown in Table 5.3.

Table 5.3: Relative similarities between EPA dynamometer drive-cycles and the data drive-cycle

UDDS	**US06**	**HWFET**
0.5885	0.2394	0.1721

It must be stressed that the comparison between a data drive-cyle and the EPA dynamometer drive cycles

could only be calculated after data collection was done and the data drive-cycle was known. Of the candidate data drive-cycles tried, the drive-cycle shown in Figure 5.3 resulted in the most favorable comparison to EPA dynamometer drive cycles. The selected data drive-cycle was most similar to the UDDS EPA dynamometer drive-cycle because higher numbers imply that the real-world drive cycle from Figure 5.3 is more similar.

5.2.3 Subsystem 1: Perception

Having collected an extensive real-world ICV dataset, a comprehensive study on prediction methods was conducted. The initial analysis of the prediction study can be found in [25] and is summarized below:

A wide field of potential prediction algorithms including classical ML and ANN methods were considered. The candidate methods are listed in Table 5.4.

Table 5.4: Candidate Prediction Methods.

Method	**Method Type**
Long Short Term Memory (LSTM) Deep Neural Network (DNN)	ANN
Convolutional Neural Network (CNN)	ANN
CNN-LSTM	ANN
Decision Trees	ML
Bagged Trees	ML
Random Forest	ML
Extra Trees	ML
Ridge	ML
K-Nearest-Neighbors (KNN)	ML
Linear Regression without Interactions (LR)	Statistical
Linear Regression with Interactions (LRI)	Statistical

All methods were trained, tested, and validated on a 9/2/2 data-split basis respectively. The training and evaluation metric was Mean Absolute Error (MAE), where X is the predicted velocity value, Y is the actual velocity value, and n is the total number of timesteps, where

$$MAE(X,Y) = \frac{\sum_{i=1}^{n} |X_i - Y_i|}{n}. \tag{5.1}$$

An extensive study was conducted on different combinations of the signals in Table 5.1 as well as different combinations of macro-parameters for the methods. From this general study, the best results for each method for 10, 15, and 30 second time horizon speed predictions in terms of MAE (mph) are listed in Table 5.5.

Table 5.5: The candidate prediction methods results organized from best performing to worst performing.

Method	**MAE - 10s**	**MAE - 15s**	**MAE - 20s**
LSTM	1.78	2.55	3.09
CNN	1.84	2.77	3.50
CNN-LSTM	1.97	2.7	3.26
Decision Trees	2.69	3.60	4.12
Bagged Trees	2.23	3.09	3.67
Random Forest	2.30	3.15	3.72
Extra Trees	1.99	2.73	3.30
Ridge	2.67	3.84	4.67
KNN	2.67	3.84	4.67
LR	2.65	3.82	4.65
LRI	2.57	3.60	4.28

The results of the general study showed that the LSTM had the best performance at 10, 15, and 20 seconds.

Based on this collected evidence, it was concluded that an LSTM should be used withing the POEMS system. For further discussions and details, the reader is referred to the team's previous publications [25, 88].

5.2.4 Subsystem 2: Planning

HEV POEMS planning subsystems generally fall into two groups: (1) those based on Pontryagin's Maximum Principle (PMP) such as ECMS [101], a-ECMS [79], as well as their derivatives, and (2) those based on DP. The advantages of PMP methods is that these are "real-time" strategies since they are relatively computationally cheap. But this method is typically non-optimal and recent research suggests that the equivalence factor prediction is analogous to velocity prediction [102]. The advantages of DP based methods is that they guarantee discovery of the globally optimal solutions assuming that the vehicle velocity prediction is accurate. The research team discovered the critical importance of this aspect through documenting that even if significant and real world velocity mispredictions are present, the solution is still near optimal [52] which has lead to new method of real world practical implementation [80, 86]. Additionally, the rise in the use of AI within the CAV space has led to deployments of vehicles with high-performance GPUs on-board the vehicle which potentially enables real-time computation of DP [103], which has been a common criticism for eventual DP implementation. For these reasons, DP methods were selected for this study.

DP is a numerical method based on Bellman's Principle of Optimality, which solves multistage decision-making problems and finds the global optimal solution by operating recursively backwards through time and storing only the optimal controls at each step [48, 104]. DP and its derivative strategies have been applied to

the problem of FE optimization for HEVs previously [64, 66, 74, 78] for full and partial drive cycles as well as for perfect and real predictions.

DP can be thought of as a recursive equation solver with memory. A recursive solution to a problem is to evaluate all possible paths by evaluating every possible combination of decisions independently. While a recursive solution will find a global optimum it will require an exponentially increasing number of function evaluations for each additional time-step. DP solves this run-time problem by iterating backwards through time and storing the optimal controls for each discrete state value at each time-step then evaluating the same controls from the same discrete state values until the first time-step. The result of the backward iteration is an optimal control matrix which can be used to find optimal controls at each time-step based on the current state values when iterating forwards. The backwards iteration step is referred to as the optimization step while the forward iteration step is referred to as the evaluation step. The DP method is shown schematically in Figure 5.4.

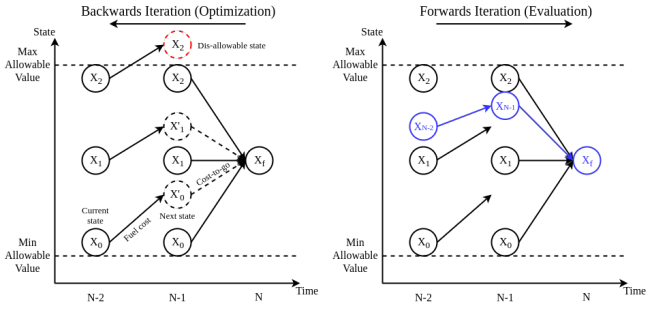

Figure 5.4: Schematic of DP Method

The optimization step of the DP method, as shown in Figure 5.4, creates an optimal matrix which can be used to compute optimal controls at each step by combining current and "remembered" costs. The optimization step iterates backwards from the last time-step (N) to the first which is not shown. The state values (represented by solid-outlined circles) show discrete state values. At time-step $N-1$, the model is evaluated for each of the discrete state values at each discrete control value which results in a series of new "intermediate" state values (represented by dashed-outlined circles) and associated control costs. Following this, the lowest cost (optimal) control is selected for each discrete state value. At time-step $N-2$ the same process is repeated but in addition to the control cost, the cost-to-go is calculated and added. The cost-to-go from a given intermediate state value is calculated by interpolating from the stored optimal control costs from state $N-1$. This process repeats itself until the first time-step is reached. The DP method shown in Figure 5.4 is constrained in two ways: (1) a large penalty is applied for distance from the desired end state value at time-step N which forces the optimal controls for all state values at time-step $N-1$ to produce the same state value at time-step N and (2) controls which lead to intermediate states which are above or below the maximum and minimum value lines (represented by red dashed-outlined circles) respectively are not considered. The output of the optimization step is a optimal control matrix which stores the optimal controls for each discrete starting state value at each time-step.

The evaluation step of the DP method, also shown in Figure 5.4, iterates forward from the first time-step through the last time-step from a given starting state value. At each time-step, interpolation is done using the starting state value (represented by blue solid-outlined circles) and the optimal control matrix values for the current time-step to determine the optimal control for the current time-step. The optimal control is then applied and the starting state value for the subsequent time-step is calculated. This process is repeated until the penultimate time-step is reached.

High-Fidelity DP Solution for the HEV Optimization Problem

The formulation of the DP problem for the 2010 Toyota Prius is as follows:

- The powertrain state x is the battery SOC
- The powertrain control u is the engine power
- The exogenous input for the powertrain w is the vehicle speed
- The time index k denotes the current time-step

The general form of the dynamic equation is shown below. It uses a high-fidelity model of the vehicle to generate the SOC at time-step $k+1$ based on the SOC at time-step k, the engine power at time-step k, and the vehicle speed at time-step k as:

$$x(k+1) = x(k) + f(x(k), u(k), w(k))\Delta(t). \tag{5.2}$$

where $f(x(k), u(k), w(k))$ is the charging/discharging rate for the battery $dSOC/dt$. The charging/discharging rate function $f(x(k), u(k), w(k))$ can be written as:

$$\frac{dSOC}{dt} = \frac{P_{batt}\epsilon_{chg}}{V_{oc}C} = \frac{(P_{batt,mot} + P_{batt,gen})\epsilon_{chg}}{V_{oc}C} \tag{5.3}$$

where V_{oc} and C are the battery open-circuit voltage and charge capacity respectively. The charging/discharging efficiency is defined as:

$$\epsilon_{chg} = \begin{cases} C_{chg} & P_{batt} \geq 0 \\ C_{dchg} & P_{batt} < 0 \end{cases} \tag{5.4}$$

where C_{chg} and C_{dchg} are constants reflecting the battery's efficiency in charging and discharging respectively. The powers $P_{batt,mot}$ and $P_{batt,gen}$ are calculated as:

$$P_{batt,mot} = \frac{T_{mot}\omega_{mot}}{\epsilon_{mot}} \tag{5.5}$$

$$P_{batt,gen} = \frac{T_{gen}\omega_{gen}}{\epsilon_{gen}}. \tag{5.6}$$

The efficiencies ϵ_{mot} and ϵ_{gen} are the efficiencies of the motor and generator respectively. Note that the efficiencies are in the denominator as the terms $P_{batt,mot}$ and $P_{batt,gen}$ are the power that the battery must provide to each to produce the required output powers $P_{mot} = T_{mot}\omega_{mot}$ and $P_{gen} = T_{gen}\omega_{gen}$ The following process is followed:

Starting with the current vehicle speed $w(k)$ and acceleration $\dot{w}(k)$ the vehicle power can be calculated using the road loads power equation.

$$P_{veh} = (m\dot{w}(k) + A + Bw(k) + Cw(k)^2)w(k). \tag{5.7}$$

where m is the vehicle mass and A, B, and C are vehicle specific constants. For a given engine power u_i, the electric power required is:

$$P_{elec} = P_{veh} - u_i. \tag{5.8}$$

For the given u_i, the engine torque and speed can be interpolated from the engine IOL and the combination of engine speed (ω_{eng}) and torque (T_{eng}) along with electric power can be used to determine the torques and speeds of the motor and generator from the planetary gearset dimensions.

The torques are calculated as follows:

$$T_{whl} = \frac{P_{veh}R_{whl}}{w(k)} \tag{5.9}$$

$$T_{pt} = \frac{T_{whl}}{\rho_{fd}} \tag{5.10}$$

$$T_{gen} = \frac{-\rho}{1+\rho}T_{eng} \tag{5.11}$$

$$T_{ring} = -\rho(T_{gen} - T_{eng}) \tag{5.12}$$

$$T_{mot} = T_{pt} - T_{ring} \tag{5.13}$$

where T_{whl} and R_{whl} are the torque applied at and the radius of the driven wheels respectively, T_{pt} is the output torque of the power-train (before the differential) and ρ_{fd} is the final drive ratio, ρ is the gear ratio of the sun gear to the ring gear for the planetary gearset, T_{ring} is the torque of the ring gear, T_{gen} is the torque of the

generator, T_{eng} is the torque of the engine, and T_{mot} is the torque of the motor.
The speeds are calculated as follows:

$$\omega_{whl} = \frac{w(k)}{R_{whl}} \tag{5.14}$$

$$\omega_{mot} = \omega_{ring} = \rho_{fd}\omega_{whl} \tag{5.15}$$

$$\omega_{gen} = \frac{\rho + 1}{\rho}\omega_{eng} - \frac{\omega_{ring}}{\rho} \tag{5.16}$$

where R_{whl}, R_{sun}, and R_{ring} are the radii of the wheel, sun gear, and ring gear respectively, T_{pt} is the torque produced by the powertrain before the differential, and ρ_{fd} is the final drive ratio.

The cost function for the DP problem for control u_i at time-step k can be formulated as either a FE maximization or a fuel consumption minimization. Since fuel consumption minimization is more intuitive and widely used in previous studies and, thus, will be utilized in this study.

$$J_i(k) = J_{im} + \begin{cases} J_{ctg} & k > N \\ J_{pen} = (x_f - x(k+1))^2 C_{pen} & k = N \end{cases} \tag{5.17}$$

where $J_{im,i}$ is the cost of fuel consumed to reach the intermediate state value which is calculated using the engine speed and torque and the engine FC map, J_{ctg} is the cost-to-go to the next state which is calculated through integration, and J_{pen} is the manually assigned penalty function associated with not arriving at the desired final SOC at the final time-step $k = N$.

Model Predictive Control (MPC) Methods

MPC is a framework to implement prediction-based optimal control. It utilizes a model of the system and a fixed time horizon to generate operational decisions. The DP model discussed in the previous section can be directly utilized in a fixed-horizon MPC framework with a few modifications.

The FCDP and a generic MPC method are shown schematically in Figure 5.5.

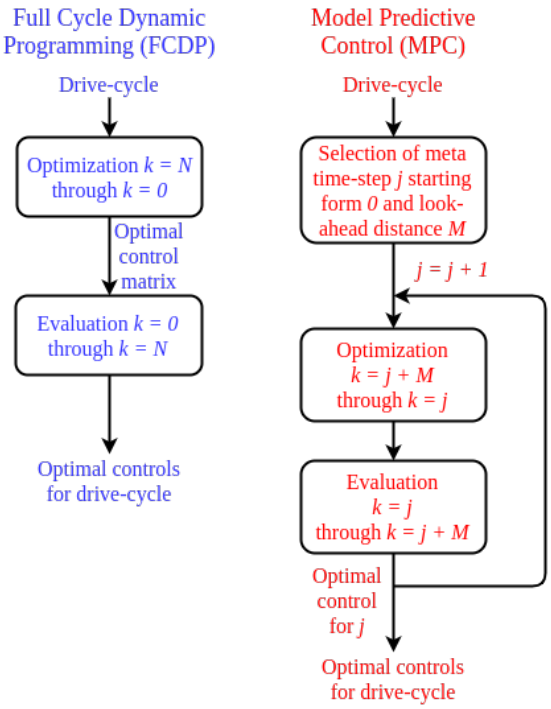

Figure 5.5: Schematic comparison between FCDP and MPC methods

In effect, MPC performs the DP method on a shortened drive-cycle at each step of the actual drive-cycle. Naturally, MPC should take significantly longer to run on a per time-step basis as full drive-cycle DP. A more detailed explanation can be found in [25].

5.2.5 Subsystem 3: Vehicle Plant

This study was conducted using a validated Autonomie model of a 2010 Toyota Prius. The 2010 Prius is equipped with a Toyota e-CVT gearbox which utilizes two electric motors (motor and generator) connected to the engine and the differential through a planetary gearset to create a Continuously Variable Transmission (CVT) [105]. Because of the e-CVT architecture, the Prius driveline is controlled entirely by torque commands without having distinct gear states, thus the only powertrain control for the Prius is torque split and the only powertrain state is battery SOC.

Due to the lack of a publicly available FE model specific to the 2010 Toyota Prius, the model used was a generic Autonomie power-split HEV model which was modified to represent a 2010 Toyota Prius by setting the following parameters to the publicly available values shown in Table 5.6.

Table 5.6: Parameters and values for Autonomie 2010 Toyota Prius Model.

Parameter	**Value**
Overall Vehicle Mass	1530.87 kg
Frontal Area	2.6005 m^2
Coefficient of Drag	0.259
Coefficient of Rolling Resistance	0.008
Wheel Radius	0.317 m
Final Drive Ratio	3.267
Sun Gear Number of Teeth	30
Ring Gear Number of Teeth	78
Battery Open-Circuit Voltage	219.7 V
Battery Internal Resistance	0.373 Ω
Battery Charge Capacity	6.5 Ah

Validation of the Autonomie 2010 Prius model was conducted based on publicly available test results from Argonne National Laboratory (ANL) Downloadable Dynamometer Database (D^3) [106]. The FE results obtained via the model for three EPA dynamometer drive-cycles are compared to those found in D^3 in Table 5.7.

Table 5.7: EPA dynamometer drive-cycle FE (km/L) results from Autonomie 2010 Toyota Prius model and ANL D^3.

Drive-Cycle	**Data**	**Model**	**Percentage Difference**
UDDS	32.14	31.79	1.09 %
US06	29.72	30.30	1.95 %
HWFET	19.26	18.98	1.45 %

With all modeled FE values within 2% of those found in the ANL D^3 database, the Autonomie 2010 Toyota Prius model was considered validated for further research. It should be noted that, in accorance with physical testing procedure, the initial SOC for the vehicle model was set to fully charged for validation purposes but was set to 50% for further research. Thus, FE results for the same EPA dynamometer drive-cycles later in the paper with baseline control will be slightly lower than those listed in table 5.7.

5.2.6 System Outputs

In addition to FCDP and PP-MPC, the CV-MPC method was implemented. The CV-MPC method is functionally identical to PP-MPC except that the prediction vector is replaced with a speed vector where all speeds are the current vehicle speed. The CV-MPC method acts as a "null" predictive method which can serve as

a point of comparison. The value of a given level of prediction fidelity can be gauged by its performance relative to PP-MPC and CV-MPC. A comparison of the DP derived methods for a sample drive cycle is shown in Figure 5.6.

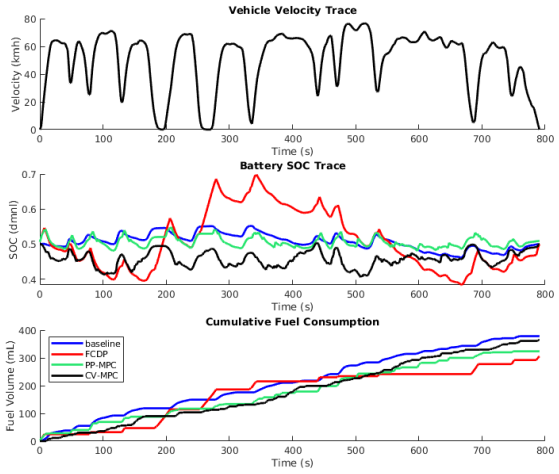

Figure 5.6: Comparison of DP derived methods and Autonomie baseline control on sample drive cycle

For the sample drive cycle in Figure 5.6, the FCDP method outperformed the PP-MPC method which outperformed the CV-MPC method and all outperformed the Autonomie baseline control method. Because of the double-sided charge-sustaining penalty, all SOC traces started and ended at exactly 50% which means that fuel consumption can be compared directly without electrical equivalence. For the sample drive-cycle, FCDP was able to outperform PP-MPC because it has more freedom to deviate from the start and finish SOC constraints. Generally, the longer the time horizon, the more effective PP-MPC should become. A study was conducted on the UDDS, US06, and HWFET EPA dynamometer drive-cycles to demonstrate this. Results for the study are shown in Table 5.8.

Table 5.8: Fuel Economy (km/L) for 2010 Toyota Prius model with DP derived methods and Autonomie baseline on EPA dynamometer drive cycles (Time Horizon only effects the PP-MPC and CV-MPC methods).

Drive-Cycle	**Time Horizon**	**Baseline**	**FCDP**	**PP-MPC**	**CV-MPC**
UDDS	10	28.28	40.32	39.11	35.10
UDDS	15	28.28	40.32	39.45	35.13
UDDS	20	28.28	40.32	39.71	35.00
US06	10	17.57	20.05	18.20	17.50
US06	15	17.57	20.05	18.44	17.20
US06	20	17.57	20.05	18.76	17.21
HWFET	10	28.13	28.59	26.30	24.24
HWFET	15	28.13	28.59	26.56	24.90
HWFET	20	28.13	28.59	26.64	24.37

An immediately noticeable trend is that increases in time horizon resulted in better FE for PP-MPC which allowed the PP-MPC FE to approach but not reach the FE produced by the FCDP method. Another noticeable effect is that the relative efficacy of the methods varied between the drive-cycles with the DP derived methods showing massive improvement over baseline in the stop-and-go UDDS drive-cycle, while the PP-MPC and CV-MPC methods did not result in FE improvements for the relatively static HWFET drive cycle.

That DP derived methods present the greatest potential for FE improvement in low speed stop-and-go conditions is not a surprise. Low speed stop-and-go conditions are where traditional control methods perform worst as they are unable to operate the IC engine in its most efficient areas. DP methods use knowledge of the future speeds of the vehicle to continue to operate the IC engine efficiently in stop-and-go conditions. An interesting result is that, even with inaccurate information about future vehicle velocity, the CV-MPC method significantly outperformed Autonomie baseline by a significant amount on the UDDS drive-cycle.

5.3 Results

5.3.1 Direct Analysis of Velocity Prediction Accuracy using MAE

Based on the results of the general study documented in Section 5.2.3, a second, specific, study was carried out in order to optimize prediction fidelity from LSTM DNNs.

Long Short-Term Memory (LSTM) ANNs are a special case of Recurrent Neural Networks (RNNs) developed by Hochreiter and Schmidhuber [107] which utilize LSTM neurons in hidden layers. While classical recurrent neurons use a single gate to establish the relationship between inputs and outputs, LSTM neurons contain multiple gates which determine how much information should be remembered and forgotten within the neuron as well as the weighting of old and new information. The presence of the remember and forget gates allows LSTM neurons to utilize information from multiple time steps in the past [33, 35]. For this reason, LSTM networks are ideally suited for problems where immediate and relayed reactions to inputs are present [108].

Because of its demonstrated feasibility, the LSTM is the prediction model which will be focused on. The following optimal architecture was arrived at:

Table 5.9: Structure of Optimal LSTM DNN.

Layer	Composition
1	Input layer - n_{inputs} fully connected
2	64 LSTM neurons
3	Dropout - 10%
4	Batch normalization
5	32 LSTM neurons
6	12 LSTM neurons
7	Output layer - $n_{outputs}$ fully connected

The LSTM DNN described in Table 5.9 was selected for its high performance and reasonable training time. Adding more complexity to the network past the optimal network failed to generate significant performance gains. The LSTM DNN was trained on the following groups of signals defined in Table 5.10.

Table 5.10: Data Groups for LSTM DNN.

Group Label	Composition
A	Speed, Acceleration, Engine Speed, Gear, Steered Angle, Throttle Position, Brake Pressure
B	A + HS + LV
C	A + HS + LV + SPaT + SS

The data groups were selected to reflect the data available to different categories of vehicle. A vehicle with neither ADAS nor connectivity only has access to A. Vehicles with ADAS and GPS navigation but no infrastructure connectivity have access to A and B. ICVs have access to all data groups. For groups A, B, and C a cross-validation study was run wherein the LSTM DNN was trained on 9 random laps, validated on 2 random laps, and tested on 2 random laps 30 times. The average MAEs for the cross-validation study are shown in Figure 5.7. The standard deviations of MAEs were all less than 5% of the mean values.

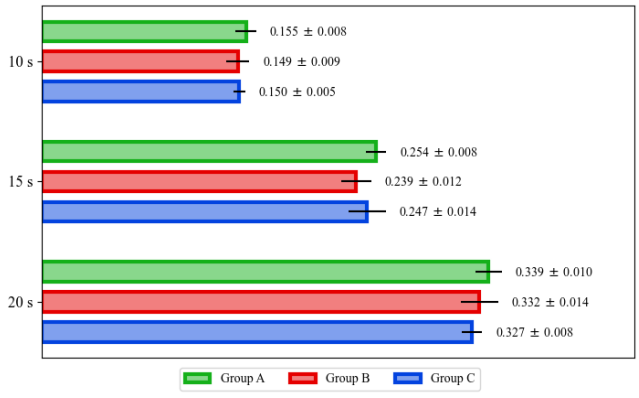

Figure 5.7: MAEs for LSTM DNN trained on data groups A, B, and C for 10, 15, and 20 second horizons

As is evident in Figure 5.7, the difference in prediction performance between LSTM DNNs trained on the different data groups was minimal if slightly favoring group B over A and C. A visual comparison of the predictions for all groups at 10 and 20 seconds is shown in Figure 5.8.

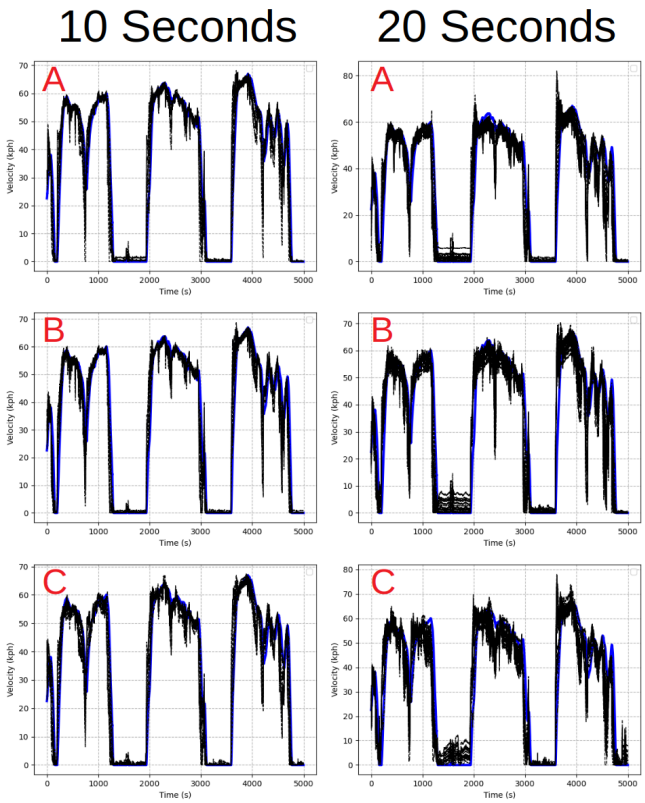

Figure 5.8: Predicted (black) vs. actual vehicle velocity (blue) for LSTM DNN trained on all data groups at 10 and 20 seconds prediction horizon

As the prediction window increases, the LSTM DNN predictions are still able to rougly hold the shape of the velocity trace but produce a greater volume of mis-predictions. The predictions generated using LSTM DNNs trained on the different groups look slightly differently and produce slightly different MAEs but the time horizon length has, by far, the greater impact.

5.3.2 Overall System FE Output

Using the predictions from the cross validation study mentioned in Section 5.3.1, FE simulations were conducted using the DP derived methods and Autonomie baseline controls. The mean FE results for the study are listed in Table 5.11 and percentage improvements over baseline for the DP derived methods with all data groups and at 10, 15, and 20 seconds are shown in Figure 5.9.

Table 5.11: FE (km/L) simulation results based on cross-validation study predictions.

Group Label	Prediction Horizon (s)	Baseline	FCDP	PP-MPC	RP-MPC	CV-MPC
A	10	18.33	24.10	21.78	20.73	20.07
B	10	18.33	24.10	21.78	20.85	20.07
C	10	18.33	24.10	21.78	20.83	20.07
A	15	18.33	24.10	21.87	21.24	20.01
B	15	18.33	24.10	21.87	20.45	20.01
C	15	18.33	24.10	21.87	20.15	20.01
A	20	18.33	24.10	22.22	20.80	20.00
B	20	18.33	24.10	22.22	20.75	20.00
C	20	18.33	24.10	22.22	21.05	20.00

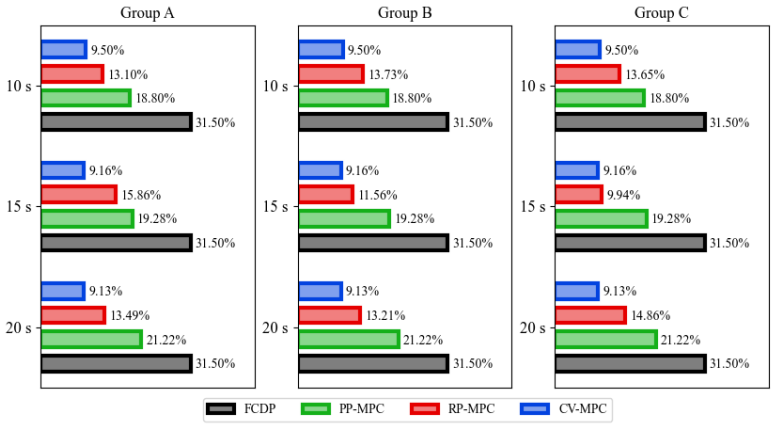

Figure 5.9: Percentage FE improvements for DP derived methods for all data groups and time horizons

5.3.3 Results Summary

The FE results for the DP derived methods, when taken in conjunction with the results of the LSTM prediction illustrate several trends:

1. With perfect predictions MPC methods will produce better FE results for longer prediction horizons.
2. A greater volume of mis-predictions will result in worse FE results for MPC methods
3. The small differences in prediction MAE observed between the data groups at all three time horizons are insufficient to explain the large differences observed in FE percentage improvement over baseline for the RP-MPC method between the data groups for the 15 and 20 second horizons.

It is illustrative that, for all cases, the average performance of the RP-MPC method came in between that of the CV-MPC and PP-MPC methods. The PP-MPC method, by definition, produces no mis-predictions while the CV-MPC method, by definition, produces only mis-predictions when the vehicle is moving. It would be logical

for the RP-MPC method which produces some degree of mis-prediction to produce FE improvements which are somewhere between those produced by the CV-MPC and RP-MPC methods. The differences in vehicle future velocity prediction MAE between the data groups shown in Figure 5.7 were relatively small where the differences in FE improvement performance based on those predictions shown in Figure 5.9 were significant. Furthermore, no consistent trend links the prediction MAE with the percentage FE improvement which leads to the conclusion that MAE is an insufficient metric to describe mis-prediction levels with respect to the RP-MPC method. Further research should be conducted to investigate whether other metrics serve better in this role.

The robustness of DP to velcity prediction error is directly demonstrated in the CV-MPC method which uses a "null" prediction of constant current speed over the entire prediction horizon. It showed significant improvements over baseline while the RP-MPC method showed significant improvements over CV-MPC. An examination of the data trace for all methods using predictions based on group A data for a 10 second prediction horizon are shown in Figure 5.10.

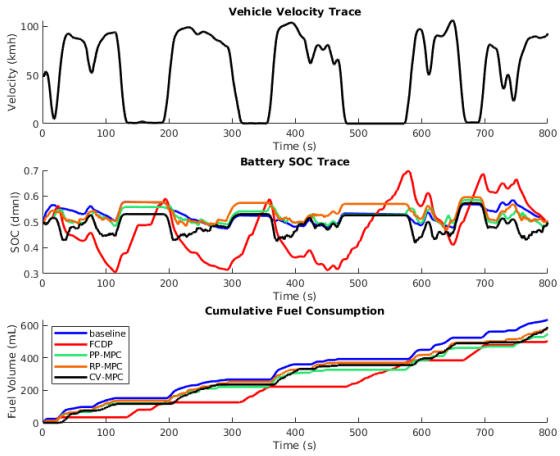

Figure 5.10: FE simulation data trace for all methods

It can be clearly seen that the MPC methods discover similar local optima, and produce similar optimal state trajectories while the FCDP method, with much more freedom to deviate from the final SOC constraint, takes a substantially different path and ends up using less fuel.

5.4 Conclusion

In order to to demonstrate the function of various implementations, the data available to different types of vehicle were classified, an extensive real-world driving dataset was collected which incorporated said data, ML and ANN methods were used to predict the ego vehicle future speed using different groups of data, and the best predictions were used in FE simulation to determine the effectiveness of practically implementable POEMS. The

results of the velocity prediction study showed that when using a LSTM DNN, high-fidelity velocity prediction was possible using only data which is available to conventional vehicles without ADAS or V2X connectivity and that the addition of ADAS and V2X connectivity resulted in modest fidelity gains. The results of the FE study showed the following:

- FE improvement achievable with RP-MPC approaches that achievable with PP-MPC.
- RP-MPC consistently outperformed CV-MPC.
- Predictions made with ADAS and V2X resulted in greater FE improvement in the 20 second window.

An unavoidable conclusion is that the relationship between prediction fidelity and FE improvement using DP-derived methods cannot be explained by differences in prediction MAE.

This study shows that POEMS implementation on HEVs and PHEVs is feasible with causal and implementable prediction and control technologies and would lead to significant improvements in HEV and PHEV fleet efficiency if implemented. The same system architecture as autonomous vehicles (perception, planning, control, plant) can be applied to energy efficiency through the deployment of POEMS enabled vehicles. The FE improvement which would result is significant and the technology can be implemented currently. The results of this study thus serve as a step towards real world implementation and commercialization.

5.5 Chapter Conclusion

This section of the research partially addresses research question 1, task 1.3. Research question 1 is restated here:

Research Question 1: *How effective are actual velocity predictive optimal energy management strategies in improving energy efficiency and reducing emissions in hybrid electric vehicles, and how do they compare to other EMS approaches?*

Hypothesis: Real-time, actual velocity predictive optimal energy management strategies, are implementable

This research effectively addresses the research question by demonstrating the feasibility and effectiveness of actual velocity predictive optimal energy management strategies (POEMS) in improving energy efficiency and reducing emissions in hybrid electric vehicles (HEVs) and plug-in hybrid electric vehicles (PHEVs). By utilizing machine learning methods and artificial neural networks, high-fidelity velocity prediction is achieved using available vehicle data. The study shows that incorporating advanced driver assistance systems (ADAS) and vehicle-to-everything (V2X) connectivity leads to modest improvements in prediction accuracy. Additionally, model predictive control (MPC) approaches, specifically receding horizon (RP-MPC), outperform constant velocity (CV-MPC) strategies in terms of fuel efficiency. The research highlights the significant potential of implementing POEMS in HEVs and PHEVs to achieve substantial fleet efficiency improvements. The findings

provide valuable insights for practical implementation and commercialization, contributing to the advancement of energy management strategies in hybrid vehicles.

Chapter 6

Mobility Energy Productivity Evaluation of Prediction-Based Vehicle Powertrain Control Combined with Optimal Traffic Management

This study builds upon previous research by evaluating the integration of Predictive Optimal Energy Management Strategies (POEMS) and Intelligent Traffic Systems (ITS) to quantify system efficiency improvements. Using the Mobility Energy Productivity (MEP) metric, real traffic patterns in Fort Collins, Colorado are modeled, and data is collected using a probe SUMO vehicle. Results show that combining POEMS and ITS leads to promising synergistic benefits in terms of energy consumption and travel times. This study was published at SAE World Congress and it is considered as Task 2.1 of research question No. 2 [109]. My unique contributions consisted of conceptualization, formal analysis, and investigation. Alongside Aaron Rabinowitz and Kaisen Yao, I actively participated in developing the methodology, conducting the research, and analyzing the data. I was also involved in writing the original draft together with Kaisen Yao, while Dr. Zachary D. Asher, Dr. Thomas Bradley, Dr. Suren Chen, Dr. Christopher Hoehne, Dr. Jacob Holden, and Eric Wood provided valuable input during the review and editing process.

6.1 Introduction

The fuel-based transportation system has a significant impact on human interactions with the environment and our national economy. When compared to other modes of transportation such as aircraft, rail, and marine,

road-based travel is responsible for the greatest share of CO2 emissions, greenhouse gas (GHG) emissions, and energy usage. Vehicles transport 11 billion tons of freight and passengers over 3 trillion vehicle-miles annually. The transportation sector accounts for over 30% of total US energy consumption, and the average US household spends more than 15% of total family expenditures on transportation, making it the costliest expense category after housing [110]. Knowing that transportation emissions surged more than emissions from any other sector over the last thirty years, transportation emissions must be a primary focus of mitigation efforts [111, 112]. Employing emerging techniques to minimize the environmental consequences of road-based transportation can thus go a long way into mitigating the entire environmental implications of the transportation industry. Connected and automated vehicle (CAV) technology and electrification are two examples with significant promise to reduce emissions from road-based transport and facilitate decarbonization of the transportation sector. Aside from improvements in powertrain technology, recent automotive sector developments have resulted in considerable advancements in CAV technology and improved vehicle control strategies. Vehicle connectivity and automation are distinct technologies that can exist separately from one another yet have significant synergistic characteristics. The ability of a vehicle to communicate information with other cars and infrastructure is referred to as connectivity. Vehicle-to-vehicle (V2V), vehicle-to-infrastructure (V2I), and other cooperative communications networks can provide this functionality [9, 43, 45, 76, 77, 84, 113, 114]. Vehicle automation refers to any scenario in which management of a vehicle capacity that would typically be monitored by a human driver is transferred to a computer which is referred to as Advanced Driver Assistance System (ADAS). Examples of ADAS are Cruise control, adaptive cruise control, active lane-keep assist, and automated emergency braking that may be found in today's vehicles. Vehicle electrification is another key component to improve fuel economy and reduce emissions. Hybrid Electric Vehicles (HEV) and Plug-in Hybrid Electric Vehicles (PHEV) have recently received a lot of attention due to their higher potential to improve fuel economy (FE) and emissions compared to traditional Internal Combustion Engine (ICE) vehicles [73]. However, there is still scope for enhancing the performance of the current generation of HEVs [74]. Recent application of CAV technology shows improvement in energy efficiency on HEVs and PHEVs through implementation of Predictive Optimal Energy Management Strategies (POEMSs) [68, 78–82]. POEMS is an application of optimal control where a mathematical optimization problem is formulated by defining the mass of fuel used as a cost to be minimized over a fixed drive cycle [78]. POEMS can be formulated as a real time control using either Pontryagin's Minimum Principle (such as in ECMS [115]) or using Dynamic Programming (DP) over a limited prediction time horizon. The application of DP over a limited prediction time horizon is referred to as Model Predictive Control (MPC). In either case predicted future vehicle velocity is used as an input to the strategy [38, 44]. POEMS performance is, thus, dependent on the quality of future vehicle velocity predictions. In recent years, vehicle connectivity and sensing technologies as well as advances in Machine Learning (ML) and Artificial Neural Network (ANN) technology have made high fidelity predictions feasible [17–20] enabling the implementation of POEMS. Intelligent technology has become a key

solution to traffic control in urban cities to mitigate congestion and reduce vehicle delay. Intelligent traffic signal control efforts primarily focus on applying different algorithms to meet the needs of traffic safety and efficiency with the data from monitoring cameras, road sensors, existence detectors, etc. [116]. Typical modes of operation for traffic signals include pre-timed (fixed time) and actuated operations. Despite being straightforward and easy to coordinate between intersections, pretimed operation is more cost-effective for close intersections with constant traffic volumes but lacks flexibility to adjust with traffic demand and possibly causes excessive vehicle delays. Actuated operation, on the other hand, can adjust phase durations and sequences by detecting real-time traffic conditions, including prolonging or shortening phase durations and skipping a phase based on traffic demand. However, actuated operation does not have a fixed cycle length and is therefore hard to coordinate among intersections. Traffic signal designs are critical to traffic safety and efficiency at intersections during day-to-day service including normal or heavy traffic scenarios [117]. Significant research efforts have been put forth to study signal timing optimization techniques to mitigate recurring traffic congestions during rush hours. An improved automatic traffic volume detection technique using V2I communication was proposed to get the traffic information in time for the following optimizations [118]. Discrete dynamic optimization models for optimal cycle length and green time allocation were evaluated to identify the most appropriate design to deal with congested traffic scenarios [119]. In recent years, there have been some emerging research efforts investigating intersection signal designs for non-recurrent congestion. A cell transmission model for a signalized intersection was developed for different congestion evacuation schemes [120]. GPS data was utilized for a global network modeling to evaluate the traffic condition with matrix factorization and clustering methods during emergency recovery [121]. A signal timing optimization model using queue length as the penalty value has also been developed under traffic incident scenarios, in which a heuristic algorithm (simulated annealing algorithm) was adopted [122]. With the need to minimize energy and time expended during travel also comes the need to quantify the benefits of doing so in a united and holistic way. The Mobility Energy Productivity (MEP) metric developed by researchers at the National Renewable Energy Laboratory (NREL) measures travel accessibility to opportunities with weightings for travel time, travel cost, and energy use at any given location [123, 124]. MEP has been constructed as a theoretically grounded but simplistically presented metric to help cities and transportation planners understand holistic impacts of novel and emerging transportation strategies and technologies on the quality of mobility in their jurisdictions. A high MEP score equates to more productive and energy efficient mobility, or more simply, a greater access to opportunities in the context of cost, time, and energy of modes that provide mobility in a location. MEP is used as an evaluation metric for this study as it is desirable to exemplify potential synergistic travel time and energy benefits that this study explores. Many existing studies use a combination of Energy Management Strategies (EMS) with Intelligent Traffic Systems (ITS). Most of these studies used eco-driving or POEMS with real world traffic data [125–129]. Only a few studies investigated the effect due to synergic application of EMS and optimized Traffic Management Systems (TMS) on fuel economy and traffic efficiency [130, 131]. There

is a significant research gap in addressing the effect of application of POEMS and TMS methods simultaneously on fuel economy and mobility. To address this research gap, this paper investigates the effect of POEMS and traffic signal timing optimization on each other's performance. The main contributions include:

- **Simultaneous implementation of POEMS and adaptive traffic signal strategy:** A validated SUMO model is used along with traffic signal and vehicle optimal controls acting individually and simultaneously.
- **Case studies development:** Four case studies are developed to evaluate the effect of aforementioned energy and traffic optimization on each other's performance at the corridor in Fort Collins, CO.
- **Performance assessment using the MEP metric:** MEP metric which documents the combined benefits of improved energy efficiency from POEMS with reduced travel time and improved energy efficiency from optimal traffic signal timing is utilized as an assessment metric.

6.2 Methodology

In this section, the experimental method of drive cycle development and real-world data collection is explained. Then evaluated FE and TMS optimization methodologies as well as MEP metric/data overview are discussed. At the end an overview of all studied and developed case studies are presented.

6.2.1 Drive Cycle Development

Over the course of two days, one driver gathered a total of 13 drive cycles. The chosen driving cycle was a 4-mile drive cycle through urban arterial highways in downtown Fort Collins, Colorado. Data gathering followed driving from the College Mulberry intersection to Shield Mulberry intersection to Shield Prospect intersection to College Prospect intersection and back to origin point which is shown in Figure 6.1.

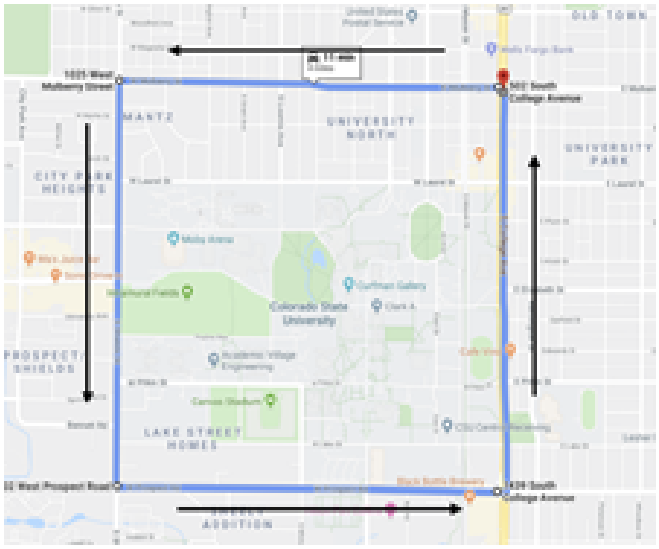

Figure 6.1: Driving map for selected drive cycle.

This drive cycle was selected with the intention that it would be generally representative of urban arterial driving. In order to accomplish this, the drive cycle was selected and tested in order to verify that it was sufficiently similar to the Environmental Protection Agency (EPA) Urban Dynamometer Driving Schedule (UDDS) drive cycle. Figure 6.2 shows velocity vs. time trace of one of the 13 collected laps of the data drive cycle.

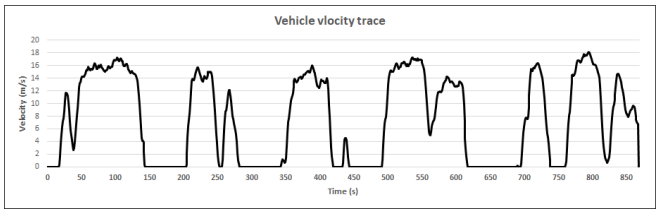

Figure 6.2: Velocity vs. time trace of one drive cycle.

The similarity assessment of characteristics of the data drive cycle and UDDS EPA dynamometer drive cycle was published in a previous study [68].

6.2.2 FE Optimization

Predictive Optimal Energy Management Strategies (POEMS) for HEVs employs forecasts of future vehicle velocity to determine an ideal powertrain control approach, resulting in improved energy economy. A POEMS, as seen in Figure 6.3, is made up of three primary subsystems.

1. The perception system, which anticipates vehicle motion based on historical and present vehicle motion, powertrain conditions, driver inputs, ADAS, and V2X (Vehicle to Everything) data.

2. The planning subsystem, which calculates optimal controls based on anticipated vehicle velocity.

3. The vehicle plant, which may be either the actual car or a high-fidelity simulation model of the vehicle.

The outputs of the system are the fuel consumption and change in State of Charge (SOC) of the HEV battery.

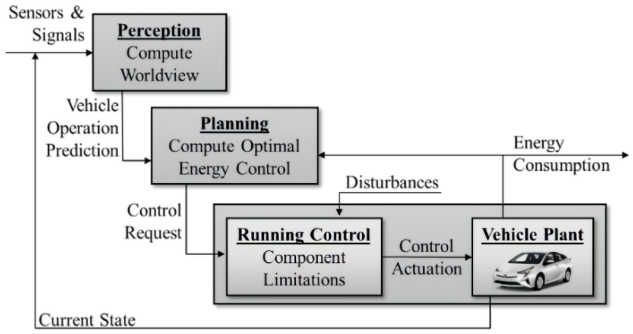

Figure 6.3: POEMS logic system.

Perception Subsystem

In order for POEMS to be implementable in real world conditions, the future vehicle velocity must be derived from actual predictions based on available data rather than from prior knowledge of a vehicle velocity trace. Data used in this prediction must also be data which is generally available to connected vehicles. A practical taxonomy of this data is given in Table 8.1.

Data Source	Signal	Description
VEH	General Vehicle Signals	Signals such as speed, acceleration, throttle position, and steered angle which can be found via CAN on any vehicle
VEH	Historical Speeds (HS)	Historical speed data for the vehicle at the current location
ADAS	Lead Vehicle Track (LV)	Relative location of confirmed lead vehicle from ADAS system
V2I	Signal Phase and Timing (SPaT)	Signal phase and timing of next traffic signal
V2I	Segment Speed (SS)	Traffic speed through current road segment

Table 6.1: Data sources and associated signals

The use of various ML and ANN techniques in the creation of future velocity predictions were considered and a deep Long Short-Term Memory (LSTM) ANN was found to be the most effective. The reader is directed to prior publications for more discussion and information [25, 68, 88].

Planning Subsystem

The planning system for HEV POEMS can be stated as a classical optimal control problem with the battery SOC and powertrain gear as the states, the torque split and gear shift as controls, and the vehicle velocity as an exogenous input. The objective is to minimize fuel consumption while observing battery SOC constraints.

Solutions to the HEV fuel consumption minimization problem follow two forms. The first is a nominally real time control scheme based on Pontryagin's Minimum Principle (PMP) such as ECMS and a-ECMS [79, 101] and derivative methods. Although nominally real time control methods, these still require future knowledge to compute an equivalence factor which is analogous to a prediction [102]. The second form is DP based methods which compute a globally optimal solution based on a future velocity prediction. DP methods explicitly require high-fidelity predictions to function properly but the exact relationship between prediction quality and DP effectiveness is not known [79].

In order for DP POEMS to be implemented in real time the method must be adjusted to use a limited horizon prediction. The limited horizon prediction is used to generate the optimal controls for the given time-step and the process is repeated at each time step. This method is referred to as Model Predictive Control (MPC). The reader is directed to the prior publication [79] for more discussion and information.

Plant Subsystem

In order to maximize the realism of the FE results of the study, the plant subsystem used was a validated Autonomie model of a 2010 Toyota Prius. This model is based on the Autonomie power-split HEV model with the vehicle parameters shown in Table 6.2 derived from publicly available information about the 2010 Toyota Prius. In lieu of a manufacturer provided model, this Autonomie implementation of a Prius model is as accurate as can be attained.

Parameter	Value
Overall Vehicle Mass	1530.87 kg
Frontal Area	2.6005 m^2
Coefficient of Drag	0.259
Coefficient of Rolling Resistance	0.008
Wheel Radius	0.317 m
Final Drive Ratio	3.267
Sun Gear Number of Teeth	30
Ring Gear Number of Teeth	78
Battery Open-Circuit Voltage	219.7 V
Battery Internal Resistance	0.373Ω
Battery Charge Capacity	6.5Ah

Table 6.2: HEV vehicle parameters

With these values the model was run for the UDDS, US06, and HWFET EPA dynamometer drive-cycles and the results Table 6.2 [68] were compared against those found in Argonne National Lab's Downloadable Dynamometer Database (ANL D3) [106]. The results of this comparison are shown in Table 3. Considering all the above listed discrepancies to be within the acceptable range, the Autonomie Toyota Prius model was used for FE evaluation for this study.

Drive-Cycle	Data	Model	Percentage Difference
UDDS	32.14	31.79	1.09%
US06	29.72	30.30	1.95%
HWFET	19.26	18.98	1.45%

Table 6.3: EPA dynamometer drive cycle FE (km/L) comparison results from Toyota Prius model and Argonne National Lab Downloadable Dynamometer Database

6.2.3 Traffic Optimization

Real-life drive cycles and simulated drive cycles are compared to decide which car following models in SUMO (Simulation of Urban MObility) are most realistic. Parameters for SUMO vehicle configuration inputs are calculated based on real drive cycles used for EMS. The parameters include acceleration rate, maximum speed, deceleration rate, and emergency deceleration rate.

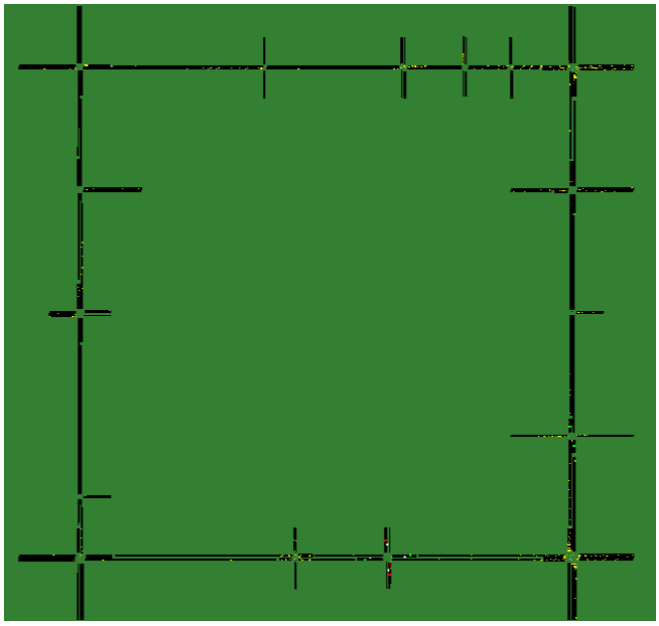

Figure 6.4: SUMO Network.

Dynamic Phase Selection and Queue Length Dissipation Sequence Algorithm

SUMO traffic network according to real-life drive cycles is built to demonstrate TMS optimization results and extract drive cycles for EMS optimization. TMS optimization is Dynamic Phase Selection combined with Queue Length Dissipation algorithm (DPS+QLD), which dynamically changes phase sequences and signal timing based on instant traffic volume change.

- **Dynamic Phase Selection (DPS) - Phase Sequence Selection:** After a traffic congestion has occurred, typically very few or no vehicles from the approach with minor roads use the green light. Therefore, such a period can be allocated to other phases to improve the mobility of the remaining approaches to avoid long queues. DPS can adaptively choose the best phase sequence of a cycle to make the traffic more efficient with the help from monitoring detectors. Starting at the major road movement, the next phase is chosen dynamically based on all candidate phase options with the following algorithm [102]:

  1. Compute the priority for each phase given in the list of indices (the sequence of potential phases that will be used for the next phase when the current one is over) for next possible movements as 'next' attribute. Priority is made according to the number of active detectors for that phase. A detector is deemed "active" when either of the following conditions is met:

     (a) The time gap between consecutive vehicles is shorter than the threshold.

     (b) Vehicle existence is detected after the signal has turned to red from the last cycle.

  2. The current phase is available to continue implicitly if its maximum duration (MaxDur) is not reached. The current phase detector gets a bonus priority.

3. The phase with the highest priority is used for the next cycle over other possible movements.
4. If no traffic is detected, the phases will follow the default cycle defined by the first value in the 'next' attribute.
5. If a particular phase needs to remain active for a no-traffic scenario, it must have a high maximum duration value and its index number is on the 'next' list.
6. If the time that an active detector was not served exceeds the preset time threshold, such a detector will receive bonus priority of the time that was not served. This could prevent those phases serving more traffic from being consistently served.

Based on the algorithm introduced above, DPS can choose the next phase according to the real-time traffic situation. In such a case, a certain amount of time could be saved for better movement of the intersection for other phases.

- **Queue Length Dissipation (QLD) - Optimal Green Light Calculations:** After phase sequences are selected, queued-up vehicles on the approach need longer green light time for congestion mitigation. However, the required green time should be calculated based on the queue lengths of not only the current approach, but also other approaches of the intersection at the same time to avoid causing additional congestion in other directions. Therefore, a maximum green time $g_{\max}$ should be considered to balance the green time allocations among different approaches. Based on the analytical method by Akçelik [132, 133] , the average green time and cycle length of an actuated controller adopt a fixed unit extension setting by assuming the arrival headway follows the bunched exponential distribution [134]. Existing vehicles remaining in front of the green light are defined as bunched vehicles while new arriving vehicles are defined as free vehicles. Different proportions of bunched and free vehicles define minimum and maximum green time, $g_{\min}$ and $g_{\max}$ respectively. The green extension time e_g is set based on the queue length at the red light ending time point, and the phase change does not happen during the saturated portion of the green period.

  The green time g can be estimated by the following equations introduced by Akçelik [132]

$$g = g_s + e_g \tag{6.1}$$

  where g is the green time and g_s is the saturated portion of the green period, and e_g is the extension time if the phase change happens after the queue clearance period. The green time boundary is set as

$$g_{\min} < g < g_{\max} \tag{6.2}$$

The green light distribution for the approach with the incident follows the rules considering the queue lengths of other approaches [132]

$$g = \begin{cases} g_s + e_g, \text{ for } g_s < g_{sj} \\ g_s, \text{ for } g_s > g_{sj} \end{cases} \tag{6.3}$$

where g_{sj} = the saturation portion of the green period of other directions and j = 1, 2, 3.

Traffic signal optimization will be conducted in two phases. During the first phase immediately following the incident, dynamic phase selection (DPS) is used for skipping the unused phase of the blocked approach due to incidents to save the time loss of the intersection operation. The second phase is when the incident is cleared, and the queue length information is collected to calculate the optimal signal timing to dissipate the queue as soon as possible. When $g_{\max}$ is reached, the controller will move to the next phase to avoid redundant green time causing long queue lengths on other approaches. After the first cycle, queue length information at the red end time point is collected again for the following signal timing calculations. The traffic signal control optimization covers both crash and recovery stages. DPS is used to skip unnecessary phases during crash stage, and the queue length dissipation algorithm is used to dissipate the queue length at crash lanes as soon as possible. The whole process for this optimization is called DPS+QLD. Assessment metrics for traffic optimization is segment average speed/travel time and is provided as an input to calculate the MEP metric.

6.2.4 MEP Metric & Data Overview

To evaluate the impacts of these case studies on productive, energy-efficient mobility, the MEP metric is calculated for each case using local land use data, travel data, and vehicle characteristics. The MEP metric quantifies access to six types of opportunities (jobs, education, recreation, shopping, healthcare, and meals). This can be done for any given location by computing travel time isochrones, proportioning opportunities access by engagement frequency, and weighting the resulting opportunity measure by time, cost, and energy of any mode that can be used to access the opportunities. This calculation happens in three steps for each location the MEP metric is being quantified at:

1. Quantify the cumulative number of opportunities that a travel mode (e.g., car) can reach within a certain travel time threshold.

2. Normalize all reachable opportunities by a) their relative magnitude of occurrence (e.g., in a city, there typically are a lower number of healthcare facilities compared to retail stores); and b) their engagement frequencies (e.g., healthcare opportunities are engaged less frequently compared to grocery or shopping opportunities). Engagement frequencies are derived from the National Household Travel Survey in 2017 (NHTS) [135].

3. Weight the cumulative opportunities measure using time, energy, and cost decay functions such that more weight is assigned to modes that provide faster, affordable, and energy-efficient access to opportunities.

The equation to compute MEP can be mathematically described as follows:

$$MEP_i = \sum_k \sum_t \left(o_{ikt} - o_{ik(t-10)}\right) \cdot e^{M_{ikt}} \tag{6.4}$$

where o_{ikt} = the opportunity measure, which represents the number of opportunities that can be reached by mode k in time t from location i; and M_{ikt} is further defined as:

$$M_{ikt} = \alpha e_k + \beta t + \sigma c_k \tag{6.5}$$

where:

M_{ikt} = Composite decay function for time, energy, and cost

e_k = the energy intensity in kWh per passenger-mile of mode k

t = is the travel time in minutes

c_k = the cost in dollars per passenger-mile of using mode k

α, β, and σ = the weighting parameters

The weighting parameters for α (energy), β (time), and σ (cost) are $-0.5, -0.08$, and -0.5 , respectively. For more details on the MEP methodology see [123, 124].

MEP can be applied to multiple modes (e.g., walking, transit, biking, driving), but for this analysis we focus on impacts to light-duty vehicles driving on the specified route in Fort Collins, CO. The drive mode MEP is calculated using a routable road network in Fort Collins with average vehicle speeds for all road links in the region, and activities by type are evaluated using parcel level third-party land use data. We translate fuel economy improvements and travel speed improvements from simulations outlined in above sections to the baseline real-world observed speeds by link and average driving fuel economies to evaluate optimization scenarios on MEP scores in the case study area. The calculation of the MEP metric with a 10-minute time difference involves determining the number of opportunities that can be accessed within a 10-minute travel time for each mode of transportation. First, isochrones are created for each mode of transportation (e.g., walking, biking, driving, public transit) to represent the areas that can be reached within a 10-minute travel time. These isochrones are constructed using geospatial analysis techniques and data on travel speeds and distances. Within each 10-minute isochrone area, the quantity of different types of opportunities, such as jobs, grocery stores, restaurants, and other amenities, is enumerated. This means counting the actual number of these opportunities within the specified area. To calculate the MEP metric, these enumerated opportunities are then standardized and weighted based on time, cost, and energy coefficients. The time weighting factor takes into account the proximity of opportunities to the location of interest. Opportunities that are closer to the location are given higher weightage than those

that are farther away. In other words, having access to opportunities within a shorter travel time is considered more valuable. The cost and energy weighting factors consider the cost in terms of dollars and energy in terms of BTUs per passenger-mile. For example, if accessing a certain number of shopping opportunities within 10 minutes of walking or biking is compared to accessing the same number of shopping opportunities by driving, the driving mode will have a lower weighting due to its higher cost and energy consumption. The actual values of the weighting factors and the specific calculations for the MEP metric are beyond the scope of the provided text, but additional technical literature by Hou et al. may offer more details [124]. By applying these weighting factors to the standardized opportunities within the 10-minute isochrone areas, the MEP metric can provide a quantified assessment of the opportunity potential within the reachable area. This calculation helps evaluate the quality of mobility options and the availability of various opportunities within a 10-minute travel time for each mode of transportation.

6.2.5 Case Studies

In order to evaluate the individual and combined effects of POEMS and TMS on system level MEP, a series of four scenarios was evaluated in the SUMO model of Fort Collins, Colorado. The scenarios were defined as follows:

Case Study 1: EMS (baseline) + TMS (baseline)

Case Study 2: EMS + Optimized TMS

Case Study 3: TMS + Optimized EMS (POEMS)

Case Study 4: Optimized EMS (POEMS) + Optimized TMS

In each case, vehicle trajectories were generated using SUMO and then EMS was applied post-hoc to those trajectories. Because EMS does not affect vehicle trajectories and TMS does not use vehicle fuel economy as an input, EMS does not need to be applied in-loop with TMS.

Case Study 1:

In the first case study the baseline EMS and baseline TMS using validated Autonomie and SUMO, models are developed, and corresponding baseline fuel economy and travel time are calculated.

To calculate the baseline travel time from SUMO, abstracted drive cycles including key parameters are fed along with traffic volume, traffic network, vehicle model, and route information. The key parameters from drive cycle abstraction include acceleration rate, maximum speed, deceleration rate, and emergency deceleration rate.

After calculating these parameters from real-life data, the acceleration rate is 1.9 m/s^2, deceleration rate is 2 m/s^2, and emergency deceleration rate is 6 m/s^2. By comparing different car following models in SUMO, EIDM (Extended Intelligent Driver Model) is selected to represent the human driver behavior because the travel time

and lane change behavior are most close to real-life data. Table 6.4 shows the results comparison from SUMO using EIDM and real-life data driving the same route of the network.

Case Study 2:

The second case study considers the effect of optimized TMS (traffic signal time optimization) along with baseline EMS on travel time and fuel economy values respectively.

Case Study 3:

The third case study considers the effect of baseline TMS along with optimized EMS (POEMS) on travel time and fuel economy values respectively.

Case Study 4:

The fourth and last case study considers the effect of optimized TMS (traffic signal time optimization) along with optimized EMS (POEMS) on travel time and fuel economy values respectively.

Parameters	Real-Life Data	EIDM
Travel time (s)	770	737
Travel distance (m)	6480	6506

Table 6.4: Comparison results from SUMO model (EIDM) and real life data

6.3 Results and Discussion

Figure 6.6 shows a comparison of the optimized results based on running vehicles at each simulation time point (a), average travel time vs simulation time step (b), and average speed vs time step (c) with validated simulation results (case study 1 and 2).

6.3.1 Case Study MEP Impacts

For the four case studies outlined, we evaluate MEP impacts to the area immediately surrounding the driving route (shown in Figure 1), which is defined as a 250 m^2 buffer bounding box around the driving route. Table 5 presents the MEP impacts for all four cases (case 1 being the baseline), and Figure 5 displays the spatial impact of each case to MEP at a 250 m^2 grid resolution. Improvements are observed to be the strongest along the southern part of the case study area along Prospect Rd in all three optimal scenarios. While traffic signal corridor optimization in the optimal TMS only case improves travel speeds and fuel economies along the route (as opposed to only fuel economies and no effective impact on overall speed in optimal EMS only), the optimal

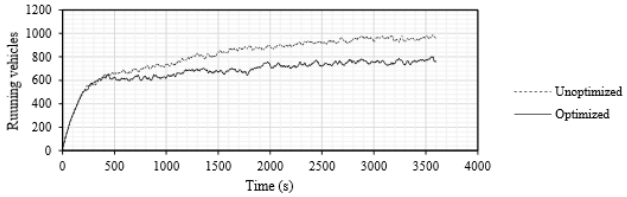

(a) Running vehicles

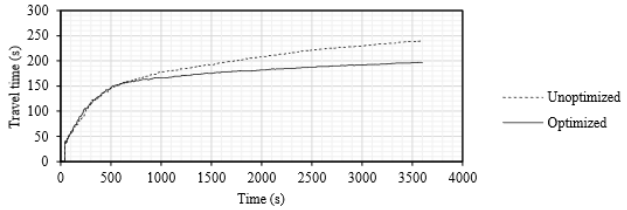

(b) Travel time

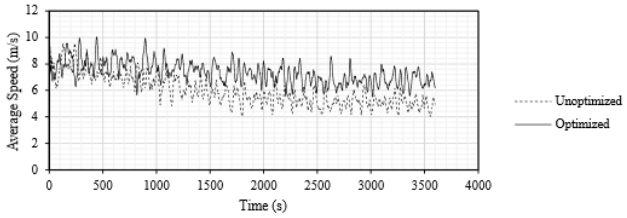

(c) Average speed

Figure 6.5: Comparison of running time (a), Travel time (b) and Average speed (c) vs. time for case studies with baseline TMS (case study 1 and 3) and optimized TMS (case study 2 and 4)

TMS only case shows the smallest improvement. While the TMS optimization generally optimizes travel speeds on most of the links (up to 8 m/s improvement over baseline and a link-length weighted average of 20%), travel speeds on some links are sacrificed for greater corridor improvements (e.g., some link segments on College Ave have slightly decreased speeds around -1 m/s from baseline). This could be construed as a more realistic case (where speeds on some links are improved at the cost of reduced speeds on others) as opposed to the optimal EMS case, where the network efficiency (i.e., travel speeds on the links) is assumed to be practically immune to the efficiencies brought about by improved fuel economy. Further investigation into the tradeoffs in EMS only and TMS only scenarios is warranted.

The cumulative improvement from combined EMS and TMS optimization also results in MEP improvements that surpass the arithmetic summation of MEP impacts EMS only and TMS only optimization. The increase in cumulative gains is derived primarily from the increase in FE for the optimal EMS+TMS case. This shows that the combination of optimal EMS and TMS in concert is best for increasing the quality of driving accessibility in terms of MEP. It is often the case that EMS and TMS optimizations are conducted and implemented in isolation as the stakeholders interested in these improvements are fairly disjoint. While the traffic operations community is primarily responsible for finding and implementing TMS improvements, EMS improvements come from vehicle manufacturers. The result here corroborates that idiom "The whole is greater than the sum of the parts," and

that it would be beneficial for both vehicle and traffic system communities to come together for delivering the greatest (MEP) benefits to the travelers.

Case Study		Mean FE and TT Improvements	Drive MEP	Relative MEP Improvement
1	Baseline	–	29.36	–
2	Optimal TMS only	16.1% FE; 20% TT	29.44	0.28%
3	Optimal EMS only	17.7% FE; 0% TT	29.60	0.82%
4	Optimal EMS+TMS	43.2% FE: 20% TT	29.82	1.57%

Table 6.5: MEP impacts for four case studies evaluated. These impacts consider MEP scores only in a 250 m^2 buffer around the route in Fort Collins, Colorado. For these results, the road-miles impacted was 8.2% of all road-miles in the study area (i.e., most links in the area are not modified with improvements). TT = Travel Time.

It is important to note here that the case studies evaluated show realistic impacts that are achievable for only improvements on a small corridor (roughly 2 km^2 area with only 8.2% of road-miles simulating optimization). We tested a scenario that translates the average improvements by road class across the whole city of Fort Collins, CO, and found that an optimal TMS and EMS case that applies to 7.2% of road-miles across the city improved the city-wide MEP score by 18.5%. This shows that EMS and TMS optimization when applied at scale may result in significant improvement of the mobility and energy efficiency of a city's transportation system. Full network optimizations need to be tested to corroborate this claim.

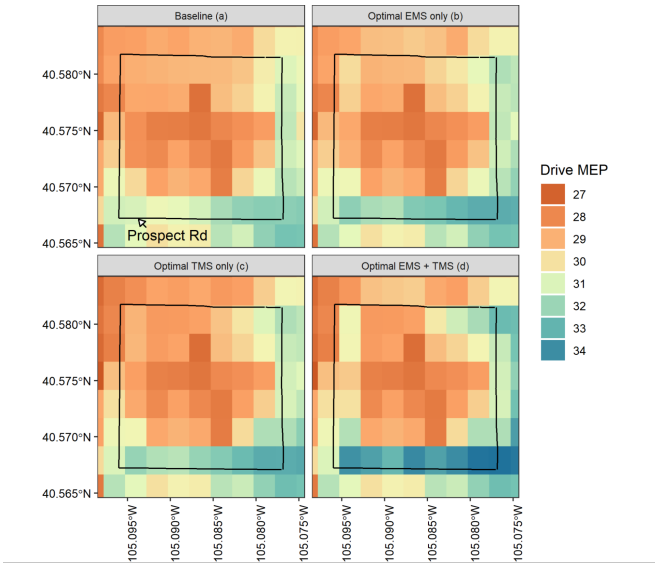

Figure 6.6: MEP scores at 250 m^2 resolution for the four scenarios (a-d) simulated. The driving route which had modified speed and fuel economies is labeled in (a) and shown as a black line overlay.

MEP scores at 250 m2 resolution for the four scenarios (a-d) simulated. The driving route which had modified

speed and fuel economies is labeled in (a) and shown as a black line overlay.

6.4 Summary and Conclusion

In a connected world, vehicles and infrastructure can and must be developed in a synergistic manner in order to enable the greatest efficiency for a given transportation system as a whole. Using previously developed optimal EMS and optimal TMS methods individually and in tandem, this study demonstrates that substantial additional fleet level efficiency benefits may be attained by the application of both simultaneously over the combined effects of each individually. FE improvements of 16.1% and 17.7% over baseline were obtained respectively from the application of optimal TMS and EMS individually where a 43.2% improvement over baseline was obtained from their simultaneous application. These FE improvements, combined with travel time improvements from optimal TMS, resulted in MEP improvements of 0.28% and 0.82% for optimal TMS and optimal EMS respectively and 1.57% for the application of both simultaneously. In both FE and MEP terms the improvements from the application of both optimal EMS and optimal TMS were greater than the sum of the individual improvements. The results of this study illustrate the fundamental interconnectedness of vehicle level and infrastructure level energy optimization and underscore the importance of the benefits which can be attained through connectivity. Overall, by finding evidence of a positive synergistic relationship between vehicle and transportation system level optimal controls this study lays the groundwork for a new direction of research in collaborative development between transportation stakeholders to optimize system level efficiency.

6.5 Chapter Conclusion

This section of the research partially addresses research question 2, task 2.1. Research question 2 is restated here:

Research Question 2: *How can the integration of predictive optimal energy management strategies, intelligent traffic systems, and deep neural networks enhance transportation vehicle energy efficiency, reduce travel time, minimize environmental impact, and develop accurate emission models for individual vehicles?*

Hypothesis: There are promising synergistic benefits to travel time and energy efficiency when POEMS and Optimal TMS are combined.Also, Accurate and simple emission modeling and characterization can be used to inform energy management control developments.

This research effectively addresses the research question by demonstrating that the simultaneous application of predictive optimal energy management strategies (EMS) and Traffic Management systems (TMS) can lead to substantial improvements in energy efficiency and travel time of transportation vehicles while reducing their environmental impact. The study shows that individual application of optimal EMS and optimal TMS results in

significant fuel efficiency (FE) improvements over baseline, with a simultaneous application yielding even greater FE improvements. The combined application also leads to Mobility Energy Productivity (MEP) improvements, demonstrating the interconnectedness between vehicle-level and infrastructure-level energy optimization. The findings highlight the importance of connectivity and collaboration between transportation stakeholders for optimizing system-level efficiency. Overall, this research lays the groundwork for a new direction of research in collaborative development, emphasizing the potential for integration of predictive optimal energy management strategies and intelligent traffic systems to achieve improved energy efficiency, reduced travel time, and minimized environmental impact in transportation systems.

Chapter 7

High-Fidelity Modeling of Light-Duty Vehicle Emission and Fuel Economy Using Deep Neural Networks

This study aims to expand upon previous research by utilizing deep neural networks (DNN), including recurrent neural networks (RNN) and convolutional neural networks (CNN), for vehicle-out emissions prediction. The study comprehensively assesses the performance of these DNN architectures and conducts sensitivity analysis for input predictor selection. Training and testing datasets are used, and a random route is selected for validation. The study also evaluates the impact of different groups of input data on prediction accuracy. Results demonstrate that deep recurrent and convolutional neural networks outperform other prediction models, indicating their potential for improved usability compared to shallow and basic neural networks. The findings serve as a constructive resource for scholars and users of vehicle emissions models, with implications for real-time technology implementation and control. This study was published at SAE World Congress and it is considered as Task 2.2 of research question No. 2 [136]. I collaborated with Shantanu Jathar and Aaron Rabinowitz. Our contributions encompassed conceptualization and formal analysis. I took the lead in the writing of the original draft, with subsequent review and editing assistance from Dr. Thomas Bradley, Dr. Zachary D. Asher, and Dr. Alvis Fong.

7.1 Introduction

Air pollution control has become a major global concern in recent decades. Large cities have become the main consumers of energy and produce locally and globally relevant quantities of air pollutant emissions [137] .

Most of this energy is produced from fossil fuel combustion that decreases air quality, causing climate change and human health issues [70,138]. Regulators, including the United States Environmental Protection Agency (EPA), National Highway Traffic Safety Administration (NHTSA), and the California Air Resources Board (CARB), have been successively creating new greenhouse gas emission standards and fuel economy standards to reduce the negative effects of transport [139].

Previously, various methods have been proposed to estimate emissions of vehicles which can be used to calculate fuel economy and emission rates. These methods have attempted to produce high fidelity models which could enable control and management of pollutant rates for different types of vehicles or fleets. High fidelity models for emissions are necessary for effective emissions control because chassis dynamometer tests often fail to capture the effects of real-world driving such as driver behavior, weather, traffic and road conditions, and can often under-predict on-road emissions [140]. The Motor Vehicle Emission Simulator (MOVES) developed by the EPA is currently the most widely used emission modeling system that accounts for vehicle operating modes [141]. Modified versions of the MOVES model have also been applied in both US and global contexts [142]. Aziz and Ukkusuri [143] combined the MOVES model with hierarchical clustering based link driving schedules using dynamic time warping measures to estimate fleet emissions. Combined with automotive system simulators such as FASTSim and Autonomie, emission models have been used to simulate instantaneous emissions in virtual driving conditions [144]. Recently, Artificial Neural Networks (ANNs) have been successfully used by automotive and transportation researchers in applications including engine management systems and fuel economy enhancement [44, 145–147], autonomous vehicles [148, 149], and mobility and drivability improvements [150, 151]. Besides, ANNs have been applied to predict and, in some cases, control tailpipe emissions from gasoline and diesel engines [152–154]. However, only in a few instances have deep neural networks (DNN) been used to model the in-use tailpipe emissions from on-road vehicles [142, 155]. One of the major advantages of ANNs is their ability to generalize. Considering that MOVES is specifically designed to model the emission in the United States, to use MOVES for other nations, very precise information about the emission performance and activity of vehicles is required. Emission predictions are challenging because there are several powertrain components that their operations affect the emissions volumes. That is why ANNs are the solution in problems with more complexity because of their ability to learn and mimic the behavior of emissions rate and providing much better accuracy as a result.

Advances in computing technology have enabled the practical training and implementation of increasingly complex ANNs [156]. This has enabled the use of time-delayed ANNs and history-sensitive (recurrent) ANNs. The Long Short-Term Memory (LSTM) ANN, developed by Hochreiter and Schmidhuber in 1997 [107], is a network that can account for both delayed effects and recurrent effects. The main potential advantage of LSTM is that it can openly select the previous vehicle status data to predict emissions whereas traditional time-dependent emission neural networks (such as conventional recurrent neural networks (RNN)) select data as the model input

in a fixed previous timespan. While the conventional RNNs have just one activation function, LSTMs have three interacting gates with corresponding activation functions. A standard LSTM unit generally called a memory block consists of a cell, three gates which play an important role in remembering, updating, forgetting, and regulating the flow of the data into and out of the cell. The increase in computing power has also allowed for the practical use of pattern recognition networks such as the convolutional ANN (CNN) [2]. These complex ANNs, when used in sequence prediction, can use current inputs to predict long term and delayed behaviors without much front-end processing.

Based on previous work at Colorado State University [3] and using DNN architectures, high-fidelity emissions and fuel consumption models were developed to predict in-use tailpipe emissions and fuel consumption of a light-duty diesel vehicle (LDDV). The LSTM and CNN architectures were tested relative to each other and other methods such as a Feed Forward Neural Network (FFNN), statistical linear regression and the EPA MOVES model. Simultaneously, various combinations of available data were used as predictors and the effectiveness of using each set was discovered. This work is focused on the study of the applicability and accuracy of ANNs on emission predictions versus previously used emission and fuel consumption simulators (e.g., MOVES, MLR) and effects of different predictor sets on the model performance. This work shows that deep ANNs can be used with more sample test vehicles and more route types to extrapolate its promising prediction accuracy for implementation and industrialization.

7.2 Methodology

In this section, the experimental method of drive cycle development and real-world data collection is explained. Then all studied and developed models are introduced.

7.2.1 Drive Cycle Development and Emission Data Collection using PEMS

Data used in this study was collected on five total drive cycles conducted in Fort Collins Colorado in 2018 using an LDDV. Data collected consisted of vehicle position data collected via GPS, vehicle operation data collected via Controller Area Network (CAN) using the J1939 protocol, and emissions data collected via an Axion R/S Portable Emissions Measurement System (PEMS) [157]. Four of the routes driven were a 10-mile urban drive cycle; this route is shown in Figure 7.1. The fifth route was a different, shorter, drive cycle used for testing the results.

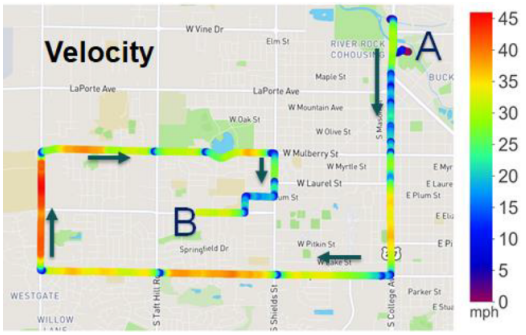

Figure 7.1: Driving map for one of the experiments on the fixed route, Source: [2,3]

7.2.2 Development of models

The datasets from the experiments include tailpipe emissions, CAN-derived vehicle parameters, and geographic coordinates (latitude, longitude, and elevation). Intake fuel rate (g/s) and exhaust fuel rate (g/s) were measured to track if the combustion is complete and how much fuel rate difference can be calculated throughout the experiments, which out data indicates it has a negligible difference between these. In-use tailpipe emissions of CO_2, CO, NO_X, HC (Hydrocarbons), and $PM10$ (Particulate Matter) at $1Hz$ were measured using PEMS. Descriptions of the vehicle used and data collected are provided in Table 7.1 and Table 7.2.

Table 7.1: Vehicle specifications

Attribute	Diesel Vehicle
EPA Tier Standard	Tier 1
Model Year	2003
Make and model	Volkswagen Jetta
Engine displacement	1.9 L
Gross vehicle weight	4023 lbs.
Vehicle miles	120,000
Emissions control	Exhaust gas recirculation

This study seeks to develop a high-fidelity model of emissions and fuel consumption for an LDDV using ANN methods. The effectiveness of these ANN methods were assessed through comparison to linear regression models and the EPA MOVES model. Details of all methods are provided in Table 7.3.

Table 7.2: Details of measured parameters

CAN-derived vehicle parameters
Velocity (mph), Engine speed (RPM), Manifold air pressure (kPa)
Intake air temperature (F), Exhaust fuel rate (g/s)
Intake fuel rate (g/s), Fuel consumption (g/s)
PEMS-derived emission parameters
CO_2 (%, g/s), NO_X (ppmv, g/s)
HC (ppmv, g/s) ,CO (%, g/s), $PM10$ (mg/m^3, g/s)
GPS-derived parameters
Latitude (deg), Longitude (deg), Altitude (deg)

Table 7.3: ANN and other methods

Models	**Type**	**Prediction Target**
Deep FFNN	A three hidden layer feed-forward neural network	Emissions/ Fuel consumption
Deep LSTM	A three hidden layer recurrent neural network with LSTM neurons	Emissions/ Fuel consumption
Deep CNN	A two convolutional neural network with two convolutional layers and two pooling layers	Emissions/ Fuel consumption
Linear Regression	Statistical regression method	Emissions/ Fuel consumption
MOVES	Lookup table software	Emissions

To assess the impact of individual predictors on the performance of the Artificial Neural Network (ANN), we initially considered various combinations of predictors. Since the existing literature on the correlation between real-time emissions and vehicle measurements is limited, we employed a method inspired by [158] to divide the predictors into different combinations.

The predictors were classified into two main categories: Externally Observable Variables (EOV) and Internally Observable Variables (IOV). EOV variables, also known as vehicle variables, are not specific to a particular vehicle and can be used as inputs for the ANN to predict emissions and fuel consumption. These predictors, such as speed and altitude, do not rely on CAN (Controller Area Network) data and can be implemented on non-vehicle hardware platforms like cloud-based systems.

On the other hand, IOVs, or engine variables, such as engine speed and fuel consumption, require access to

the CAN bus, typically through an OBD-2 (On-Board Diagnostics) connector. In Table 7.4, we indicate whether the data used are IOVs or EOVs. The selected combination sets are presented in Table 7.5.

Table 7.4: EOVs and IOVs

Predictor Name	**Predictor Symbol**	**Variable Type**
Vehicle Velocity	V	EOV
Vehicle Acceleration	ACC	EOV
Time since recording	time	EOV
Vehicle Altitude	Alt	EOV
Vehicle Specific Power	VSP	EOV
Engine Velocity	RPM	IOV
Intake Air Temperature	IAT	IOV
Manifold Air Pressure	MAP	IOV
Fuel Consumption	FC	IOV

VSP was calculated using

$$VSP = v * [acc * (1 + \epsilon) + g * r + g * C_r] + 0.5 * \rho * v^3[(C_D * A)/m] \tag{7.1}$$

where v is the velocity in m/s , acc is the acceleration in m/s^2, ϵ is the mass factor for the rotational masses (0.1), g is the acceleration of gravity ($9.8m/s^2$), C_r is the coefficient of rolling resistance 0.014), is the density of air ($1.02 - 1.07kg.m/\rho^3 kgm$), C_D is the drag coefficient, A is the vehicle frontal area (2.56 m^2), and m is the vehicle mass in kg. VSP is the instantaneous power demand of the vehicle divided by its mass (here kW/tonne), which is an estimation of the power demand on the engine in driving mode. It is an important parameter in estimation of the emissions as well as fuel consumption because it has most of the defining dependent parameters of vehicle emissions and it can also be used for the experiments that the powertrain specifications are unknown.

Table 7.5: Selected combination sets of predictors

Class	**Input combination sets**		**IOV**
	Emission Prediction	Fuel Consumption	**needed**
C1	V, ACC, time	V, ACC, time	no
C2	V, ACC, time, VSP	V, ACC, time, VSP	no
C3	V, ACC, time, Alt	V, ACC, time, Alt	no
C4	V, ACC, time, VSP, Alt	V, ACC, time, VSP, Alt	no
C5	V, ACC, time, VSP, Alt, RPM	V, ACC, time, VSP, Alt, RPM	yes
C6	V, ACC, time, VSP, Alt, RPM, IAT	V, ACC, time, VSP, Alt, RPM, IAT	yes
C7	V, ACC, time, VSP, Alt, RPM, MAP	V, ACC, time, VSP, Alt, RPM, MAP	yes
C8	V, ACC, time, VSP, Alt, MAP, IAT	V, ACC, time, VSP, Alt, MAP, IAT	yes
C9	V, ACC, time, VSP, Alt, RPM, IAT, MAP	V, ACC, time, VSP, Alt, RPM, IAT, MAP	yes
C10	V, ACC, time, VSP, Alt, RPM, IAT, MAP, FC	– – –	yes

7.2.3 Artificial Neural Network (ANN)

ANNs are classified as one of the branches of machine learning techniques. ANNs are composed of artificial neurons that are intended to imitate the structure of the human neurons. The basic structure of an ANN consists of three layers: one layer of input neurons, a hidden layer of connected neurons, and a layer of output neurons. ANNs can be trained from a dataset using a set of calculations starting from the input layer through the output layer, and then by setting the cost function the outputs are modified to increase the accuracy of the predictions. The results from the cost function are then used to tune the biases and weights. In most cases, the more data that can be fed to a neural network, the more accurate it will become but predictive accuracy is dependent on the architecture of the network and the choice of input predictor variables. ANNs can model the nonlinear features of the input dataset so they have the advantage to produce outputs that are not limited to linear combinations of the inputs provided to them. However, ANNs are generally black box models that make it harder to interpret their results. There are many types of ANNs, which among them Feed-Forward Neural Network (FFNN), Recurrent Neural Network (RNN), and Convolutional Neural Network (CNN), are studied in this research.

7.2.4 Feed-Forward Neural Network

Feed-forward neural networks are the most basic type of artificial neural networks that are also used in this study. The information passes through the nodes only in the forward direction and there are no feedbacks in the cell of this type of neural network. Generally, they can solve many nonlinear problems by learning the features of the input dataset. The process of training FFNN involves changing the weights and biases to optimize the performance of the network. A deep FFNN is used due to its natural simple structure which makes the training process faster than the following explained complex neural networks. Figure 7.2 illustrates the general structure of the FFNN. The detailed calculation procedure of the FFNN can be found in [159].

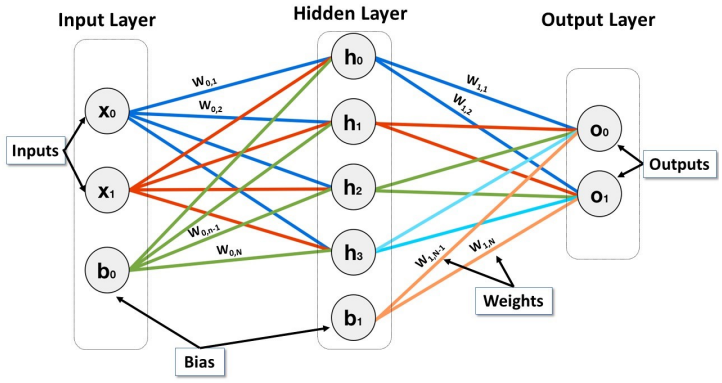

Figure 7.2: The general structure of a single layer FFNN model [4]

In this research a deep FFNN model is applied to the dataset with three hidden layers. The final structure

has 200, 150, 100 neurons in the first to third hidden layers, with the total number of five layers including input and output layers. The activation function is chosen as sigmoid.

7.2.5 LSTM

Generally, RNNs are able to process sequential data when the state of the hidden layers at the current time-step becomes an input to the hidden layers at the next time-step, thus allowing the network to continue to learn after training. However basic RNNs struggle to keep long term dependencies, Long Short-Term Memory is a memorable type of RNN which was designed by Hochreiter & Schmidhuber [107]. A standard LSTM block is formed of a cell, and three internal gates of an input gate, an output gate, and a forget gate. The cell remembers values over arbitrary time intervals, and the three gates regulate the flow of information into and out of the cell. LSTM networks are well-suited to classifying, processing, and making predictions based on time series data since there can be lags of unknown duration between essential events in a time series. Simply, LSTM networks have some internal contextual state cells that act as long-term or short-term memory cells. The state of these cells modulates the output of the LSTM network. LSTM offers significant benefits when it comes to addressing long-term dependencies, making it particularly valuable for predicting vehicle emissions. This is crucial because a vehicle's emissions can be influenced by factors that occurred several seconds or even minutes ago. For instance, a vehicle's emissions can be affected by its speed from a few seconds prior or the gear it was in a few minutes ago. In contrast, FFNNs struggle to handle such long-term dependencies, resulting in less accurate predictions. Additionally, LSTM exhibits superior resilience to noise, which further enhances its effectiveness in predicting vehicle emissions. This attribute proves valuable since the data used for training the model can often be noisy due to factors like sensor errors or varying weather conditions. In contrast, FFNNs are more susceptible to the adverse effects of noise, leading to less accurate predictions. Figure 7.3 shows the internal structure of the LSTM model. The details of the computation are available in [107, 160, 161].

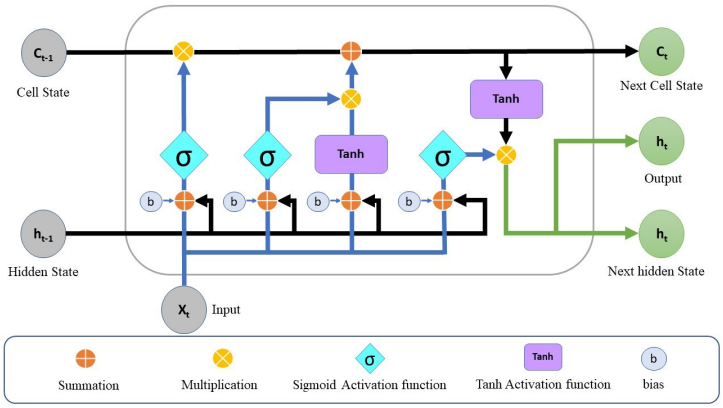

Figure 7.3: The general structure of the LSTM model

The LSTM is developed based on Keras in Python. The structure of LSTM is chosen systematically by

analyzing the effects of NN parameters (number of neurons, epochs, number of hidden layers, etc.). Finally, a three hidden layer structure is chosen in which the layers have 50, 30, 30 neurons. 300 epochs are selected for training and the activation function is chosen as "ReLu". Relu runs much faster and also prevents gradient vanishing. Callbacks are also considered to avoid overfitting.

7.2.6 CNN

A CNN is a robust ANN technique used for both regression and classification. The fundamental working principle of CNN is to split an input domain into a series of small divisions and then, in order to extract the features, the input is passed through the series of convolution and pooling layers. Each convolution layer applies a filter to each input channel in order to extract specific characteristics, for example edges and corners in image recognition. The pooling layers reduces the input dimensionality to reduce the computation cost and redundancy in input samples. Finally, input is flattened and fed to fully connected layers to produce the network output. CNN is especially useful for purposes where large amounts of input data are to be processed for the presence of features or sequences [107, 162]. A typical CNN structure is shown in Figure 7.4.

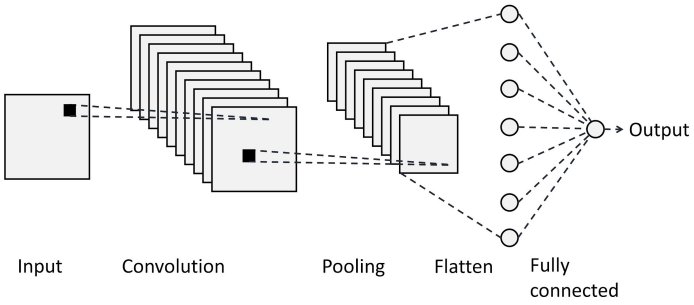

Figure 7.4: The general structure of the CNN model.

CNN model is developed with the same procedure as LSTM. The final structure has two hidden layers with 100, 100 neurons in the first and second layers. ReLu activation function is chosen and the length of 1D convolution window is selected as 2 and filter number, kernel size, and maximum pooling size are selected as 100, 3, 2.

7.2.7 Linear Regression

Apart from discussed neural network methods, we have developed a linear regression model. This helps us to demonstrate an in-depth comparison between the prediction accuracy of developed ANN and the most used traditional machine learning technique for both emission and fuel consumption.

In this study, a multivariable linear regression (MLR) model is applied to the input predictors for emission and fuel consumption regression. The following equation is the general formulation of the multivariable linear regression method.

$$Y = \beta_0 + \beta_1 X_1 + \beta_2 X_2 + \beta_3 X_3 + ... + \beta_n X_n \tag{7.2}$$

where Y is the predicted variable, $X_1, X_2, \ldots, X_n$ are the dependent input predictors, β_0 is the bias term, and $\beta_0, \beta_1, \ldots, \beta_n$ are the coefficients (weights) that are estimated fitting the model to the measured variable. Initially, the coefficients (weights) are chosen randomly by the built-in MLR model in the sklearn package in Python. This model changes the coefficients in the fitting process to reduce the error indicated in the assessment metrics section.

7.2.8 MOVES

Motor Vehicle Emission Simulator (MOVES) is the EPA developed tool that is able to estimate emissions in different user-defined situations [162]. MOVES is a simple model that has a physical basis for estimation of the emissions based on speed, time, fuel type, vehicle type, meteorological data and road conditions. The model can be used for different geographic scales such as national, county, and project scale emission estimations [163]. MOVES can estimate emissions by the distribution of time spent in operation modal bins that are defined based on VSP bins and speeds [164]. In modeling process of MOVES by using the measured velocity dataset during the actual on-road experiments, and defining vehicle type (diesel), geographical areas (project scale), pollutants (CO_2, CO, NO_X, HC and $PM10$), vehicle operating characteristics, and road types, emissions of the test vehicle were estimated. When a drive cycle for the experiment is added into MOVES along with other input parameters such as vehicle type and model year, fuel type, and meteorology data, MOVES calculates emission rates for operating mode bins associated with the input parameters and VSP which is calculated on a second-by-second basis for a vehicle operating over the drive cycles. Then, MOVES calculates total emissions over the test by using the emission rates and operating mode distribution. MOVES calculation results for emission rate can be different for each combination of source type (fuel type, vehicle type), model year and operating mode (speed, acceleration and VSP). The estimated emissions were compared to the measured emissions. The current version of MOVES (MOVES2014b) was used in this study.

MOVES is a simple model that has a physical basis for estimation of the emissions based on speed, time, fuel type, vehicle type, meteorological data and road conditions. When a drive cycle for the experiment is added into MOVES along with other input parameters such as vehicle type and model year, fuel type, and meteorology data, MOVES calculates emission rates for operating mode bins associated with the input parameters and VSP which is calculated on a second-by-second basis for a vehicle operating over the drive cycles. Then, MOVES calculates total emissions over the test by using the emission rates and operating mode distribution. MOVES calculation

results for emission rate can be different for each combination of source type (fuel, type, vehicle type), model year and operating mode (speed, acceleration and VSP).

Assessment metric

For evaluation of model accuracy, we used Mean Absolute Error (MAE) criteria parameter which is formulated in Equation 7.3. Where P_i and M_i are the predicted value and the actual value of the target parameters respectively and N is the total number of data points in the dataset, MAE is defined as follows:

$$MAE(P, M) = \frac{\sum_{i=1}^{n} \mid P_t - M_t \mid}{N} \tag{7.3}$$

7.3 Results

7.3.1 Input Predictors Classes Comparison

All ANN's (FFNN, LSTM, CNN) and MLR were trained over three fixed route experiments out of the four, and validation was performed on the last fixed route experiment. Then the random route experiment was used for performance testing. The result of these tests are to downselect a set of prediction inputs (C1-C10) that will be used for emissions prediction evaluation, and a set of prediction inputs (C1-C9) that will be used for fuel consumption prediction evaluation.

Figure 7.5 and 7.6 show the comparison of emission prediction accuracy for the selected classes based on MAE over the validation dataset and test dataset using a three hidden-layer LSTM respectively.

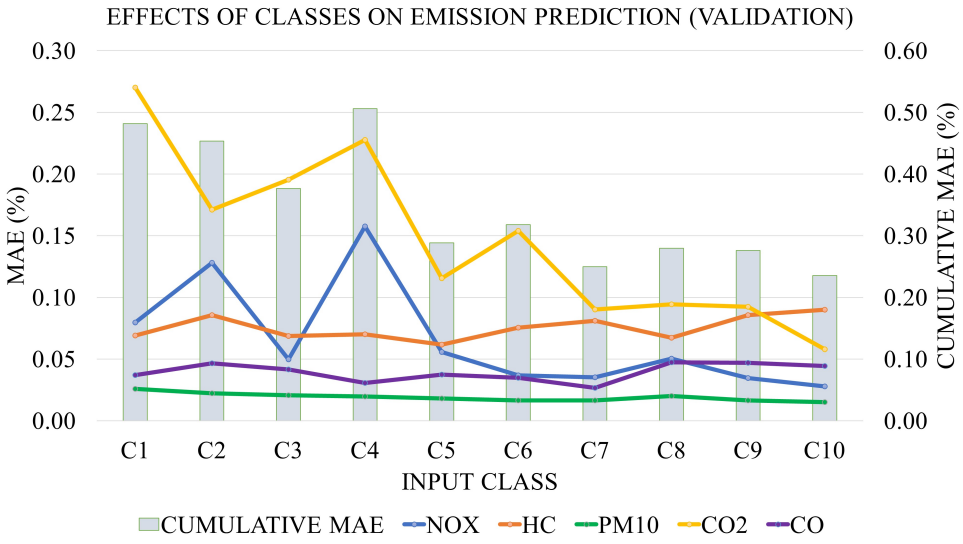

Figure 7.5: Effect of input classes on emission prediction MAE (validation)

Table 7.6: Emission prediction MAE (%) for different input classes (validation)

Input Classes	NO_X	HC	$PM10$	CO_2	CO	**Cumulative MAE**
C1	0.08	0.07	0.03	0.27	0.04	0.48
C2	0.13	0.09	0.02	0.17	0.05	0.45
C3	0.05	0.07	0.02	0.20	0.04	0.38
C4	0.16	0.07	0.02	0.23	0.03	0.51
C5	0.06	0.06	0.02	0.12	0.04	0.29
C6	0.04	0.08	0.02	0.15	0.03	0.32
C7	0.04	0.08	0.02	0.09	0.03	0.25
C8	0.05	0.07	0.02	0.09	0.05	0.28
C9	0.03	0.09	0.02	0.09	0.05	0.28
C9	0.03	0.09	0.02	0.06	0.04	0.24

The values of the MAE are also shown in Table 7.6 and 7.7. Comparing the values it can be inferred that adding more predictors in input classes decreased the error. Also, it can be observed that MAP among the inputs contributed to better predictions. Using fuel consumption as a predictor also made the prediction more accurate. Overall, the choice of input classes in terms of IOV versus EOV categorization was found to be crucial. The trends seen in the LSTM results were also present in the results for the other algorithms evaluated. Thus, class 10 (C10) was selected as the primary input class (set of inputs) for emissions prediction.

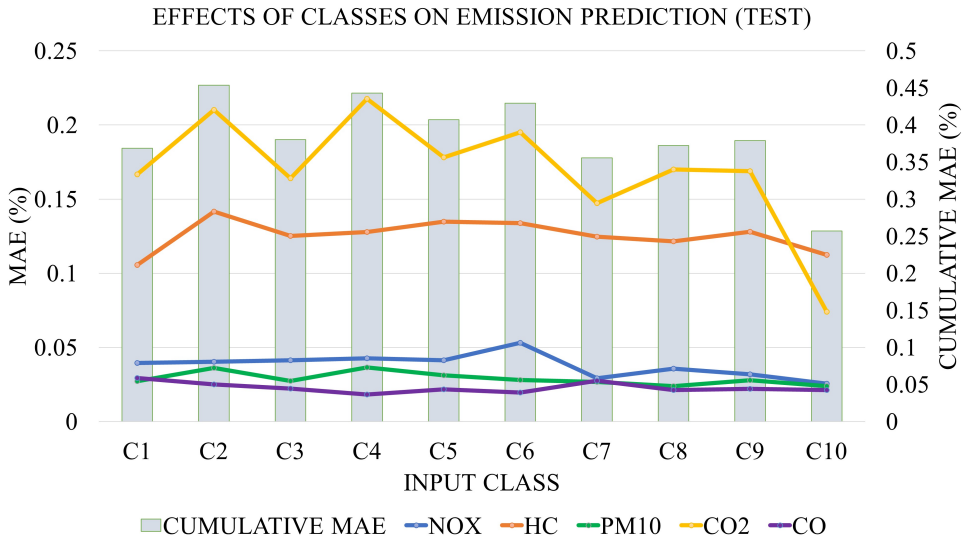

Figure 7.6: Effect of input classes on emission prediction MAE (test)

Table 7.7: Emission prediction MAE (%) for different input classes (test)

Input Classes	NO_X	HC	$PM10$	CO_2	CO	**Cumulative MAE**
C1	0.04	0.11	0.03	0.17	0.03	0.37
C2	0.04	0.14	0.04	0.17	0.03	0.45
C3	0.04	0.13	0.03	0.16	0.02	0.38
C4	0.04	0.13	0.04	0.22	0.02	0.44
C5	0.04	0.13	0.03	0.18	0.02	0.41
C6	0.05	0.12	0.03	0.20	0.02	0.43
C7	0.03	0.12	0.03	0.15	0.03	0.36
C8	0.04	0.12	0.02	0.17	0.02	0.37
C9	0.03	0.13	0.03	0.17	0.02	0.38
C9	0.03	0.11	0.02	0.07	0.02	0.26

Figure 7.7 shows the emission prediction results for class 10 (C10) using the test dataset applied by the LSTM method. The model shows very promising prediction results.

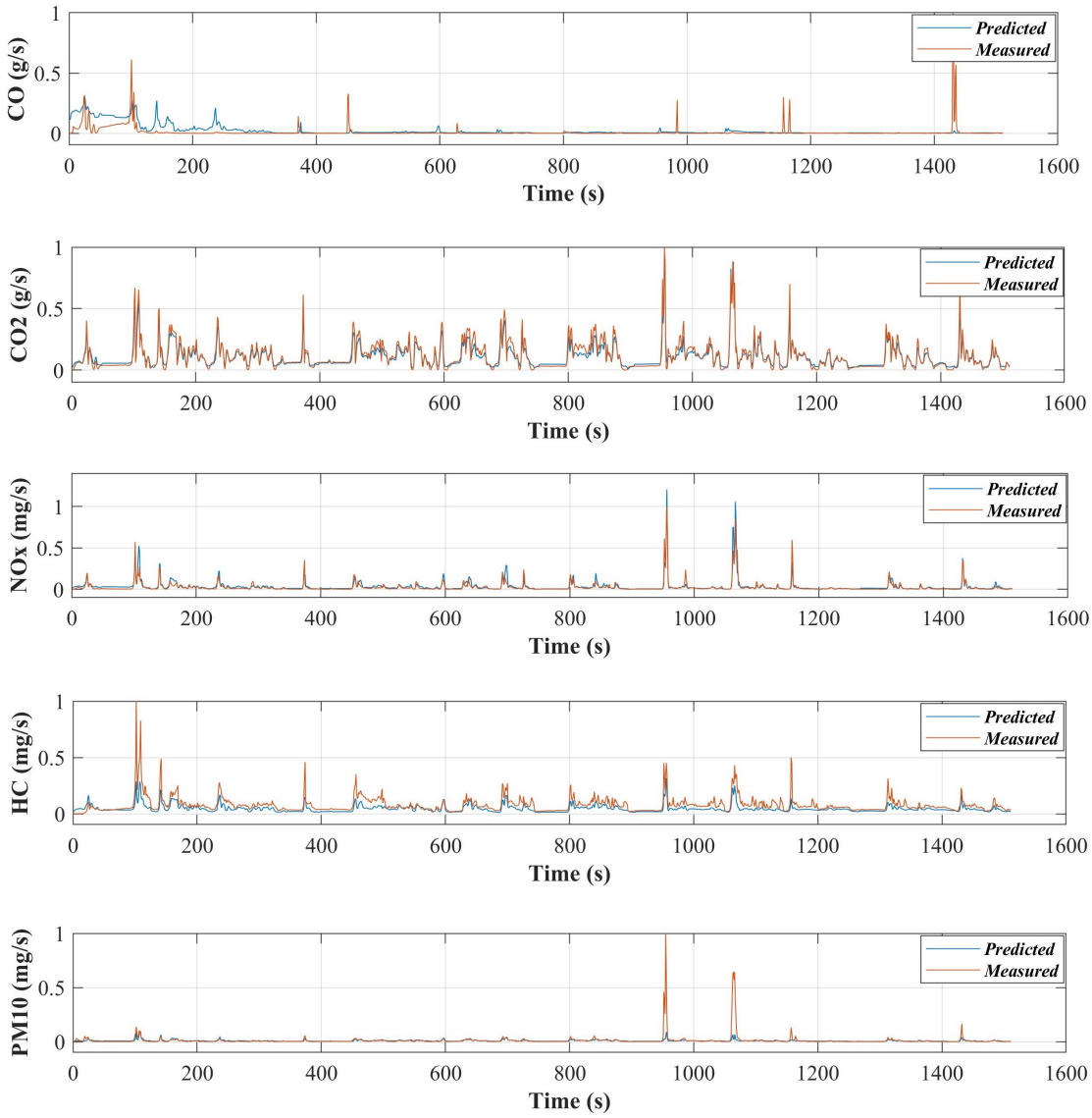

Figure 7.7: Emission prediction by LSTM (test)

Similar to the methods used to select a set of inputs for emission prediction, the validation and test route experiments were fed to the ANN and MLR models to compare the predicted fuel consumption based on different input classes. Figure 7.8 and Table 7.8 show the comparisons and values of the logarithmic MAE over the validation dataset using LSTM, FFNN, CNN, and MLR. Likewise to emission prediction results, we can observe that fuel consumption predictions follow the same pattern for most of the input classes for ANN methods hence, for MLR it is not the same.

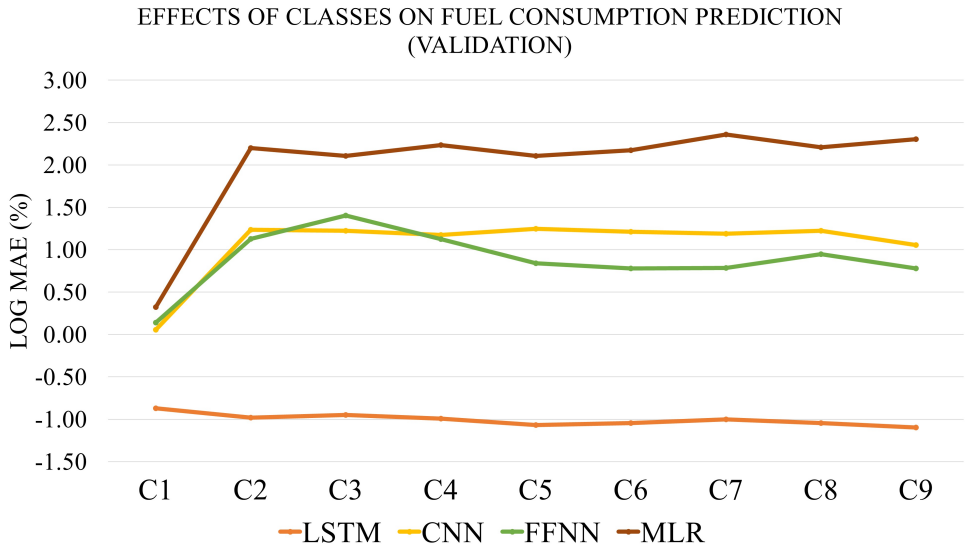

Figure 7.8: Effect of input classes on fuel consumption prediction MAE (validation)

Table 7.8: Fuel consumption prediction logarithmic MAE (%) for different input classes (validation) using LSTM, CNN,FNN and MLR

Input Classes	LSTM	CNN	FFNN	MLR
C1	-0.86	0.13	0.22	0.46
C2	-0.94	1.24	1.13	2.20
C3	-0.91	1.23	1.41	2.11
C4	-0.94	1.18	1.13	2.23
C5	-1.04	1.25	0.84	2.11
C6	-1.01	1.21	0.78	2.17
C7	-0.98	1.19	0.79	2.36
C8	-1.02	1.22	0.95	2.21
C9	-1.1	1.05	0.78	2.30

Also, the effect of adding IOV parameters can be seen the most in class 7 and class 9. Thus, class 9 (C9) was selected as the primary input class for fuel consumption prediction.

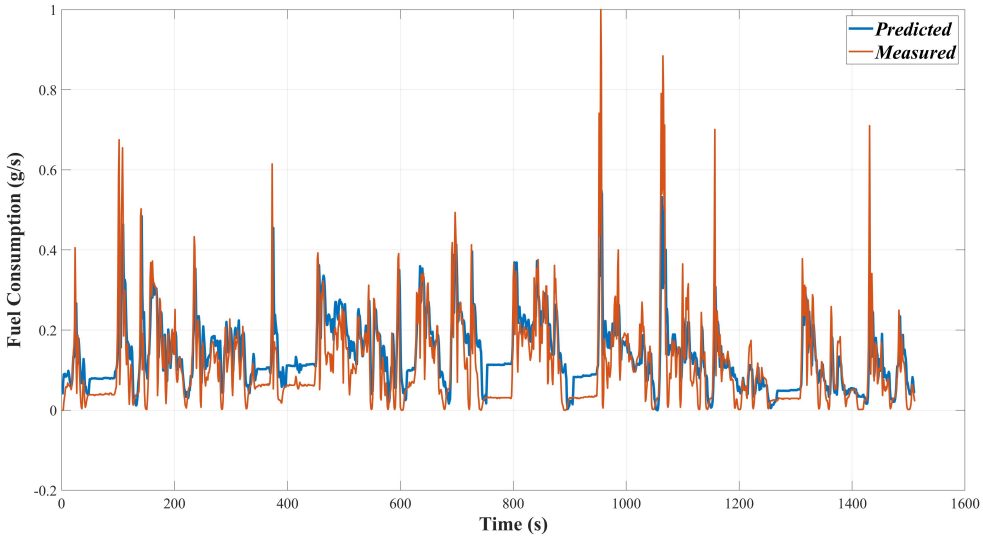

Figure 7.9: Fuel consumption prediction by LSTM (test)

Figure 7.9 shows the fuel consumption prediction results for class 9 (C9) using the test dataset applied by the LSTM method. The model shows relatively good fit with some mispredictions, which has much lower MAE than other models prediction results.

Effectiveness of Models

As can be seen from Figures 7.5 and 7.6, the sets of experimental measurands that were used as inputs to the ANNs effect on the error in prediction for the emissions of NO_x, CO, and $PM10$. These emissions are very difficult to predict as a function of time because they are very nonlinear, consisting mostly of long stretches with zero-value, with occasional spikes. Because the ANNs were trained using summative regression error metrics [165], they struggle to predict data which is mostly flat but shows a few spikes as the difference in error between a good fit and a bad fit will be minimal. Thus, in order to gauge the effectiveness of the ANN model for predicting emissions, the error from the best ANN model was compared to a "null" prediction which was a vector of zero values. The results for the best ANN and the "null" prediction are shown in Figure 7.10.

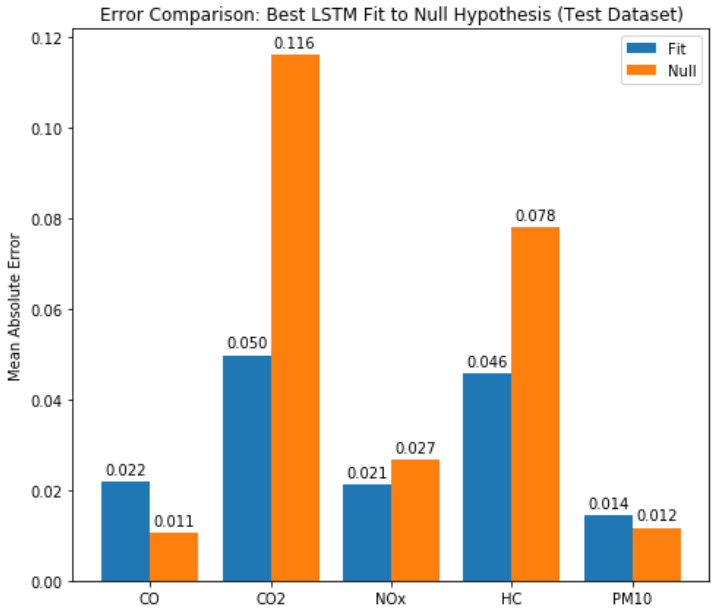

Figure 7.10: Comparison of error between best ANN prediction and "null" prediction

The results of the comparison to "null" suggested that the ANN models were capable of predicting CO_2,HC and NO_X emissions traces but did not predict CO or $PM10$ better than a very simple model. Given the dynamics of the input data for these emissions data, it was not surprising that the ANNs struggled to predict over the course of the test and validation drive cycles, many machine learning methods would face similar difficulties, and the development of methods that can model these dynamics is a topic of continuing research.

Effect of Individual Predictors

The contributions of individual predictors to reducing MAE for the deep LSTM were determined using a designed experiment and linear regression. The experimental design was a 2^4 full factorial on the IOVs MAP, IAT, FC, and RPM. Based on the results of the previous section the output variable for the regression was prediction error for CO_2. The residual of the fit was 0.922 with an overall F-statistic of 32.66. The results of the regression are presented in Table 7.9.

Table 7.9: Statistical results of individual predictors effects on emission model accuracy

Regressor	**coef**	**std.err**	**t**	**P(>|t|)**
Intercept	0.1019	0.004	27.482	0.000
MAP	-0.0152	0.003	-4.581	0.001
IAT	-0.0060	0.003	-1.819	0.096
FC	-0.0341	0.003	-10.284	0.000
RPM	0.0025	0.003	0.757	0.456

Defining statistical significance as a $P(>|t|)$ of 0.05, the regression showed that the presence of MAP and FC decreases the fit MAE for CO_2, HC, and NO_x. Moreover, further emission comparison is made with MOVES modeling tool. Details of the emission rates are provided in Table 7.10.

Table 7.10: Comparison of measured emission rates to MOVES emission rate estimations

Emission	**Average emission rate (g/mile)**				
Comparison	CO_2	NO_x	HC	CO	$PM10$
Test Dataset	626	1.82	0.34	0.49	0.041
MOVES	532	3.27	0.79	5.23	0.017
LSTM	625.72	1.82	0.34	0.49	0.04
CNN	619.99	1.79	0.33	0.48	0.04
FFNN	555.58	0.91	0.26	0.33	0.03
MLR	1297.39	2.8	0.55	0.10	0.05
Relative Error (RE) rate (%)					
MOVES	15	26.7	132.3	967	58.5
LSTM	0.05	0.02	0.09	0.05	0.03
CNN	0.96	1.83	1.57	1.06	0.99
FFNN	11.25	50.24	23.15	32.11	30.20
MLR	307.25	254.1	262.2	120.14	217.15

Finally, the total comparison has been made for emission and fuel consumption prediction. All developed ANN models and MLR (tested with C10 for emission and with C9 for fuel consumption) are compared in Tables 7.11 and Table 7.12.

Table 7.11: Comparison of measured emission rates to all models emission rate estimations (test)

Emission	**MAE(%)**				
Comparison	CO_2	NO_x	HC	CO	$PM10$
LSTM	0.06	0.03	0.09	0.04	0.02
CNN	0.89	1.57	1.23	1.05	0.87
FFNN	12.52	52.60	25.78	34.12	33.54
MLR	380.01	236.4	267.88	122.15	201.01

Table 7.12: Comparison of fuel consumption prediction accuracy for all models (test)

Developed models	**MAE(%)**
LSTM	0.08
CNN	1.05
FFNN	6
MLR	201

7.4 Conclusion

In this research, several deep neural network approaches have been considered for light-duty diesel vehicle emission and fuel consumption prediction. Five different methods including deep recurrent neural network (RNN), deep convolutional neural network (CNN), deep feed-forward neural network (FFNN), and deep long short-term memory network (LSTM) have been developed. Also, a multivariable linear regression (MLR) method has been developed for a more extensive comparison within machine learning-derived methods. We used the collected data from a portable emission measurement system (PEMS) which was a total number of four experiments along a fixed route that were performed by the same driver using an LDDV in spring 2018 in Fort Collins, Colorado. Additionally, one experiment was conducted on a random route for testing the performance of the models. Several input classes of dataset variables were defined and sensitivity analysis for finding the best combination was done. The results show that the deep neural network performance consistently improves when given datasets with more variables (EOV and IOV). It is also found that manifold absolute pressure (MAP), engine speed (RPM), and fuel consumption are the most beneficial parameters categorized as IOV for emission prediction. For fuel consumption, the same pattern is observed given more variables for all ANN methods. Selecting the best-fitted classes for emission and fuel consumption, all the models were simulated. Also, a simulation is done for emission prediction using MOVES. The results show that DNNs has high accuracy compared to other neural network models. Specifically LSTM had the best performances for both emission and fuel consumption prediction. We recommend using LSTM and other deep RNN that are history-sensitive that can account for both delayed effects and recurrent effects for more accurate emissions and fuel consumption predictions. This model, if developed for a vehicle and integrated within the vehicle controller, may have value for real time vehicle/engine controls optimization thereby producing real-time reductions in fuel consumption and emissions. Our work does not reflect changes in emissions from variations in fuel, engine operation over time, driver behavior, and ambient conditions. In addition, the models can be improved to better predict CO and $PM10$ in their extreme fluctuations which needs to be investigated in future work.

7.5 Chapter Conclusion

This chapter of the research partially addresses research question 2, task 2.2. Research question 2 is restated here:

Research Question 2: *How can the integration of predictive optimal energy management strategies, intelligent traffic systems, and deep neural networks enhance transportation vehicle energy efficiency, reduce travel time, minimize environmental impact, and develop accurate emission models for individual vehicles?*

Hypothesis: There are promising synergistic benefits to travel time and energy efficiency when POEMS and Optimal TMS are combined.Also, Accurate and simple emission modeling and characterization can be used to inform energy management control developments.

This research effectively addresses the research question by employing deep neural networks to develop sophisticated emission models for individual light-duty diesel vehicles (LDDVs). The study compares various neural network approaches and a linear regression model, utilizing data obtained from portable emission measurement systems. The findings reveal that deep neural networks, particularly LSTM, exhibit remarkable precision in predicting emissions and fuel consumption. The study proposes the integration of these models into vehicle controllers to optimize real-time performance, leading to substantial reductions in fuel consumption and emissions. Nonetheless, it acknowledges the necessity for further investigations concerning fuel variations, engine operation dynamics, driver behavior, and ambient conditions. In essence, this study showcases the promising potential of deep neural networks in advancing emission modeling and enhancing overall vehicle efficiency.

Chapter 8

Identifying and Assessing Research Gaps for Energy Efficient Control of Electrified Autonomous Vehicle Eco-Driving

This study provides an overview of energy-efficient control strategies in automotive vehicles and highlights the importance of future research on Autonomous Eco Driving (AED) for Battery Electric Vehicles (BEVs). It proposes a system-level diagram of AED and identifies three research gaps: real-world perception of Autonomous Vehicles (AVs) for AED, sparse sensor data for global AED estimation, and performance evaluation of a planning subsystem integrated with AED in a physical vehicle. This study was published as a book chapter in the Springer editorial and it is considered as Task 3.1 of research question No. 3 [166]. This chapter benefited from my contributions in conceptualization and formal analysis. Additionally, I participated in the investigation process alongside Aaron Rabinowitz, Chon Chia Ang, Sachin Sharma, and Parth Kadav. I played a key role in developing the methodology section and collaborated with Aaron Rabinowitz, Chon Chia Ang, Parth Kadav, and Sachin Sharma in writing the original draft. The chapter was further refined through the review and editing contributions of Dr. Zachary D. Asher, Dr. Thomas Bradley, and Dr. Richard T. Meyer.

8.1 Introduction

Transportation's reliance on nonrenewable hydrocarbon fuels creates serious concerns about energy supply, cost, and environmental safety. In the pursuit for green, sustainable transportation systems, consideration of

vehicle energy consumption is crucial [167]. Efficient alternative energy vehicles and advanced vehicle control technologies are two areas of research that might provide solutions to the need for increasing Fuel Economy (FE) and complying with current and upcoming environmental regulations [109, 168].

The need for energy efficient vehicles has facilitated the development of new vehicle technologies such as Hybrid Electric Vehicles (HEVs) and Plug-in Hybrid Electric Vehicles (PHEVs) and Battery Electric Vehicles(BEVs) [169]. Compared to vehicles powered with only an Internal Combustion Engine (ICE), HEVs provide significantly improved fuel efficiency [169]. The reason is due to their ability to recover braking energy and the fact that an extra powertrain degree of freedom is available to more cost-effectively meet the driver-required power. PHEVs exhibits even longer range and even further reduced need for hydrocarbon fuels [170]. This is owed to their enhanced battery capacity and their ability to be charged from wall power. BEVs are projected to further improve automotive transportation sustainability with a commercially viable and a readily accessible product [171].

The other major development facilitated by the need for energy efficient vehicles is advanced vehicle control technologies which is the focus of this research. Collectively these advanced control strategies are typically referred to as energy management strategies. These technologies are also becoming more implementable thanks to developments in AVs such as advanced perception subsystems, planning subsystems, and more. As AV technology continues to evolve commercially, it is crucial to ensure synergistic development with energy efficient controls to ensure transportation sustainability as well.

Further details regarding energy efficient vehicles and energy efficient control technologies are presented in the following subsections.

8.1.1 The Evolution of BEVs: The Modern Era

Since 2000, battery electric vehicles (BEVs) have made significant progress and achieved several commercial milestones [172]. The first highway-legal BEV with a lithium-ion battery that could travel more than 200 miles on a single charge was the Tesla Roadster, which was shipped in 2008 [173]. The Mitsubishi i-MiEV, which went into serial production in 2009, was the first modern highway-legal BEV [174]. In 2010, the first Nissan Leaf was delivered to customers. Until 2011, the Mitsubishi i-MiEV was the world's most popular BEV, with 2,450 units sold in 30 countries between 2008 and 2012 [175]. By 2016, more than one million BEVs had been sold worldwide. The introduction of the Tesla Model 3 in 2017 helped push BEV sales beyond the one million mark, and annual worldwide market share surpassed 1%. In 2018, annual worldwide sales surpassed 2 million units, with the Tesla Model 3 selling over 100,000 units in a single year, becoming the first BEV to achieve this milestone. In 2019, BEVs accounted for one out of every two new vehicles registered in Norway. By 2020, the Tesla Model 3 had overtaken the Nissan Leaf as the best-selling BEV in history, with over 500,000 units sold worldwide since its launch in 2013. Tesla also became the first automaker to produce more than one million BEVs. In Norway, BEVs account for 10% of the vehicles on the road. In 2020, global BEV sales crossed the 10 million unit mark for the

first time, and the Nissan Leaf achieved the milestone of 500,000 units sold worldwide. By 2021, the worldwide sales of the Tesla Model 3 had surpassed one million units, and BEVs came in 27 distinct configurations, with 11 different manufacturers producing them. Table 8.1 shows the top five BEVs with the greatest ranges in the 2020 model year [176]. The literature on BEVs is extensive and constantly evolving. Although BEVs were once seen as a niche sector with an uncertain future, they have now become a commercially mature and desirable technology with the potential to establish sustainable transportation [177,178]. As we focus on the real-world implementation of energy-efficient control technologies, it is important to consider the applicability of these technologies to BEVs, which are growing and becoming an increasingly important part of the transportation sector.

Table 8.1: Model year 2020 BEV examples

Make and Model	Vehicle Type	Electric Motor/Battery-pack	City (mpge)	Electric Range (miles)
Tesla Model 3 Long Range	Sedan/Wagon	211 kW / 230 Ah	136	373
Chevrolet Bolt BEV	Sedan/Wagon	150 kW / 188 Ah	127	259
Hyundai Kona Electric	SUV	150 kW / 180 Ah	132	258
Kia Soul	Sedan/Wagon	201 kW / 180 Ah	127	243
Jaguar I-PACE	SUV	294 kW / 90 kWh	80	234

As a vehicle, a BEV is quiet, simple to drive, and free of gasoline expenditures when compared to conventional vehicles [179]. Additionally, as a form of urban transportation, it has many benefits. It does not produce any emissions along urban corridors (reducing urban air pollution due to transportation), it easily handles frequent start-stop driving, it gives full torque from a stop, and eliminates the need for gas station stops provided that charging is available at in public or at home [180]. Additionally, the utility industry is evolving, with renewable energy sources gaining traction and the "smart grid" which is the next generation of the electricity grid, is now in the process of being built. BEVs are seen as a key component of this new power system, which includes renewable energy sources and high-tech grid technologies [181,182]. All of this has resulted in increased interest and growth in this method of transportation.

As a system, BEVs can be modeled as a combination of several subsystems. Each of these subsystems interacts with the others to make the BEV function, and a variety of technologies may be used to run them. Figure 8.1 depicts major subsystem components and their contribution to the overall system. Some of these components must communicate significantly with others, while others have little or no interaction. Regardless of the situation, the operation of an BEV is dependant on such interaction of all these subsystems [183]. These subsystems are important to understand and utilize to develop energy efficient control strategies.

8.1.2 Energy management and energy efficient strategies for electrified vehicles

Energy management strategies (EMS) in HEVs and PHEVs control the power/torque split selection between the combustion engine and the electric motor, in which the amount of power/torque provided by each power source is combined to satisfy driver demand while reducing the amount of non-renewable fuel use and increasing

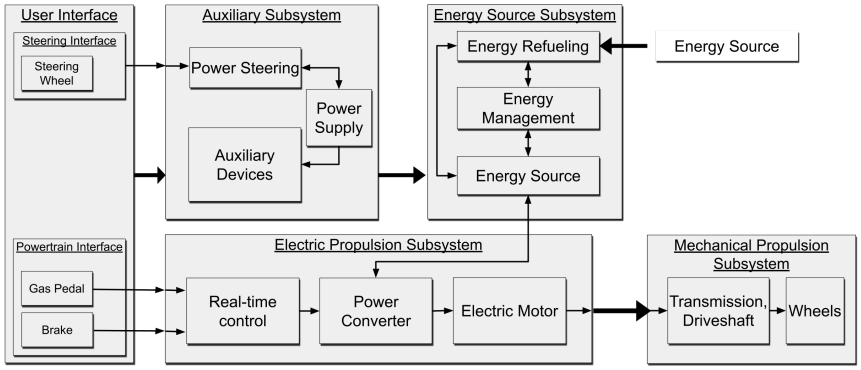

Figure 8.1: A general systems-level viewpoint of BEV, adapted from [5]

powertrain utilization efficiency [184, 185]. Energy efficiency strategies seek to directly decrease the energy required to drive from one point to another by either modifying the second-by-second vehicle velocity or by choosing an alternative route. This is particularly important for BEVs since energy efficiency strategies result in a direct increase in range thus enabling higher utility [186]. Overall, it has been shown that intelligent energy management and energy-efficient use of electrified vehicles increase vehicle FE and reduce global energy consumption, greenhouse gas emissions, and air pollution emissions.

Generally there are three types of vehicle control that reduce fuel consumption for a drive cycle with a fixed starting point and a fixed ending point: (1) powertrain EMS (P-EMS), (2) Eco-Routing (ER), and (3) Eco-driving (ED) [187,188]. P-EMS decreases fuel consumption by increasing the efficiency of the vehicle powertrain operation without modification of the drive cycle [189]. However, ED and ER decrease fuel consumption by decreasing the energy output of the vehicle through modification of the drive cycle and route [190, 191].

Powertrain EMS (P-EMS)

As previously mentioned, electrified vehicles will benefit greatly from the development of P-EMSs. To meet driving demands, the primary goal of a P-EMS is to distribute the power request into multiple propulsion sources (specifically for HEVs and PHEVs) [192, 193]. If we take into account battery performance (i.e. the current rate and lifespan) and tailpipe emissions levels, an efficient P-EMS can improve fuel efficiency. However, it is challenging to devise P-EMSs due to the uncertainty of future driving conditions [194–197]. Furthermore, the P-EMS should have a sufficiently simple and fast real-time controller with a desired computational speed for the implementation of a global optimisation algorithm. The performance of P-EMSs strongly depends on future vehicle velocity and power request which is influenced by external factors (e.g., traffic information and surrounding vehicles) [198]. Research groups all over the world have proposed various solutions which are briefly summarized:

1. **Rule-based P-EMS**: Here a P-EMS is implemented with either deterministic rules or with fuzzy rules.

(a) **Deterministic**: The first application of deterministic rule-based techniques to the energy management of HEVs was in [199]. In place of the original electric assistance technique, Banvait et al. [200] described a charge depletion–charge sustaining (CD–CS) strategy. Following the cooperative control approach for the auxiliary power unit, the speed-switching power is compelled to acquire a proper curve together with the ideal brake specific fuel consumption [201, 202].

(b) **Fuzzy Logic**: Fuzzy logic belongs to intelligent control strategies, but it dispenses with precise mathematical models of controlled systems. However, it contains self-learning capability, high flexibility, and resilience, and is thus commonly used to solve complicated nonlinear issues [203–205]. Denis et al. [206] developed a Sugeno-type fuzzy logic controller by using the moving average of the previous speed and the present global discharge rate as inputs in order to take use of the trip data. Li et al. has presented an adaptive-equivalent consumption reduction technique that combines a fuzzy inference system to increase self-adaptation. [207].

2. **Optimization-based P-EMS**: In most cases, an optimization-based P-EMS is generated by formulating an optimal control problem.An Optimization-based P-EMS delivers FE improvements by explicitly or implicitly simulating vehicle operation and managing the vehicle powertrain components to reduce fuel consumption. An optimization-based P-EMS can accomplish FE improvements for conventional cars with ICE and BEVs, but the highest FE benefits are gained from vehicles with additional powertrain operating degrees of freedom such as HEVs and PHEVs [188, 208, 209]. The actual FE improvement from an Optimization-based P-EMS is significantly dependent on the chosen driving cycle and propulsion systems [210]. One of the first optimization-based P-EMS studies, for example, showed a 28% FE increase in a HEV by optimizing gear changing and battery charging/ discharging [211].

   (a) **Globally Optimal P-EMS**: Dynamic programming (DP) [210, 212], Portryagin's minimum principle (PMP) [213–215], Stochastic Dynamic Programming (SDP) [56, 216–218], Genetic Algorithm (GA) [219, 220], and Particle Swarm Optimization (PSO) [221, 222] are among the key optimization techniques.

   (b) **Real-time Optimal P-EMS**: Real-time optimization-based P-EMS is primarily composed of equivalent consumption-minimization strategies (ECMSs) and its variations such as adaptive ECMS [192, 223–225]. But predictive rules-based strategies can also be implemented in real time and DP methods can be implemented in real time through the use of a look-up table [226].

   (c) **Prediction-based Optimal P-EMS**: The goal of a Prediction-based Optimal P-EMS is to discover the best control strategy for minimizing fuel consumption within the time frame when prediction data exists [9, 60, 168, 197, 227–230].

Eco-routing (ER)

Classical vehicle routing algorithms seek the quickest or shortest routes [231, 232], while ER algorithms seek routes with the lowest energy consumption costs. When given a starting point and a destination, ER generates a route that minimizes the amount of energy required to complete the journey. Routing is often performed on a graph where intersections represent different junctions, connected by edges roads, and costs indicate the estimated energy required to go between two junctions that the road links. The route with the lowest overall energy for the journey may then be found using minimal path routing. The complicated time-variant functions that explain the expenses are often derived by researchers. For example, Dijkstra's routing method is a popular option among academics [233]. Users route preferences, such as favoring highways or avoiding toll roads, might be considered while planning a path. Furthermore, it may utilize the number of passengers as an input to determine if the car is eligible to use high-occupancy vehicle lanes. Similar to other shortest route routing applications, a green routing service needs a server to handle diverse routing requests. However, operating and managing a routing server is costly and needs precise and thorough real-world traffic and network data which is difficult to access and analyze [234–237]. It should be noted that the ER navigation system may produce up to three routes for each journey depending on multiple minimization criteria, such as distance, travel time, and energy usage. For conventional ICE vehicles, there are currently various ER algorithms capable of generating energy-optimal routes based on historical and real-time traffic data [238–240], but there has been minimal study on PHEVs to date [241]. As shown in [242], the performance of ER algorithms is very sensitive to the energy model used to estimate the energy cost on each network connection. The most difficult component of solving the ER algorithm for PHEVs is locating an energy model capable of calculating both the electrical energy consumption and the gasoline consumption. Jurik et al. [243] addressed the ER challenge for HEVs using longitudinal dynamics. The eco-route for PHEVs was investigated using a charge-depleting first approach in [244] and [245]. To address the ER of HEVs, De Nunzio et al. [246] recently developed a semi-analytical solution to the powertrain energy management based on Pontryagin's minimal principle. Houshmand et al. [247] conceived a combined routing and powertrain control algorithm that simultaneously identifies the energy-optimal route and the ideal energy management approach in terms of battery state of charge and fuel consumption. In [247], however, the option to recharge the battery on some portions of the trip was omitted, and either charge-sustaining or discharge-only operation was permitted.

Eco-Driving (ED)

ED decreases fuel consumption for all vehicle types by applying fuel-efficient driving behaviors along a predetermined route, which may affect travel duration [113]. Due to this increase in travel time, it is difficult to persuade drivers to adopt ED practices [248]. If the driving conditions along the route can be anticipated, ED may be treated as an optimum control question if the driver input is eliminated or disregarded. Current practical

use of ED is realized through a set of heuristic goals, such as eliminating stops, traveling at a fuel-efficient speed (generally, this could be a higher or lower overall speed), and reducing acceleration and deceleration magnitudes, which can achieve FE improvements of approximately 10% for modern vehicles and 30% for fully AVs [249]. FE improvements realized through ED are the focus of this literature review because the energy savings is sufficiently large, and because ED can be directly implemented through AV technology.

Historically, ED implementation research has focused on the FE impact of a single intelligent vehicle technology, such as camera systems, radar systems, LiDAR, Vehicle to Vehicle (V2V), Vehicle to Infrastructure (V2I), or Vehicle to Everything (V2X). As an example of a typical ED study, researchers used projections of the traffic light Signal Phase and Timing (SPaT), a sort of V2I, to influence driving behavior and shown a FE improvement of 12-14% [250]. ED is difficult to adopt in reality since most drivers dislike giving up control [251]. Many studies of ED for AVs conclude that vehicle perception, sensor fusion, and planning must all be achieved for successful implementation. On the other hand, a comprehensive grasp of how each of these components should fit together at the system level is not as clearly defined.

Summary

To summarize, FE improvements realized using a fixed drive cycle are realized through an P-EMS which is a very active area of research but is most effective for HEVs and PHEVs [47,252]. FE improvements from modifying the route is realized through ER which is highly applicable to BEVs but is a relatively mature technology. If FE is improved by modifying the drive cycle but keeping the route the same, then the technique is considered ED which is highly applicable to BEVs and has tremendous potential for further improvements once AV technology is also included [249].

8.1.3 Automated Cyber-physical Vehicles

In addition to improvements in powertrain technology, embedded and cyber-physical systems have had a profound effect on the modern world [251,253]. Embedded computer systems have been integrated with a variety of technological artifacts, such as the power grid, medical devices, automotive and transportation systems, and industrial control and production lines [254–256]. Modern engineering topics are often multidisciplinary and require significant interdisciplinary problem-solving capabilities. AVs are a kind of vehicular cyber-physical system that has experienced tremendous recent innovation and has garnered considerable interest from both industry and academia [257–259]. The strategy for establishing AVs as the primary mode of transportation on the road may have several advantages such as improvements of safety on the roads (e.g., collision avoidance); better mobility for young, elderly, and disabled; and individual improvements of energy efficiency [260]. But at the same time AV technology may increase travel demand and overall mileage due to new user groups, the reduced cost of driver's time, and potential for mode switching (walk, low speed shuttles, transit, regional air,

etc.) [1,114,261]. While the full impact of AV technology remains unknown, it is certain that AV technology will begin to experience commercial adoption in the near future [262].

According to the projections shown in Table8.2, in 2050, the reference case (all fleet vehicles will be Autonomous ICE) will have the lowest transportation energy consumption. At first glance, this may appear counter-intuitive; how could AVs with ICE consume less than BEVs? The reason for this according to Energy Information Administration (EAI) independent statistics and analysis projections data is that more people would prefer to use fleet services rather than their personal vehicles. Case 2, which assumes that all Autonomous Light-duty Vehicles (LDVs) will be BEVs. Another assumption is that AVs will enter both household and fleets, which means that more people will have access to AVs, making transportation easier for people who own vehicles. This, in turn, would have an impact on reliance on public transportation. As a result, an additional research focus is warranted to improve energy efficiency of Autonomous BEVs.In the next subsection, a derivation of the research gap for this type of technology based on its systematic readiness level is given.

Table 8.2: Reference and AV case description, adopted from [1]

Case Name	Assumptions	Description
Reference	AVs enter fleet light-duty vehicles	1% of new light-duty passenger vehicles sales by 2050 and 100% are fleet sales
	AVs are used more intensively	Driven 65,000 miles per year and scrapped more quickly
	Autonomous LDV fuel type	100% conventional gasoline ICE
	Autonomous LDVs affect mass transit modes	Decreases use of transit bus by 12%, transit rail % by 2050
Autonomous BEV	AVs enter household and fleet LDVs	16% are new fleet sales and 84% are new household sales by 2050
	AVs are used more intensively	Driven 65,000 miles per year and scrapped more quickly (fleet) and +10% more annual vehicle miles (household)
	Autonomous LDV fuel type	Increasing share of BEVs with 96% of fleet and 82% household by 2050
	Autonomous LDVs affect mass transit modes	Decreases use of transit bus by 17% by 2033, transit rail 35% by 2050 use of commuter rail 48% by 2050
Autonomous HEV	AVs enter household and fleet LDVs	16% are new fleet sales and 84% are new household sales by 2050
	AVs are used more intensively	Driven 65,000 miles per year and scrapped more quickly (fleet) and +10% more annual vehicle miles (household)
	Autonomous LDV fuel type	Increasing share of HEVs with 96% of fleet and 71% household by 2050
	Autonomous LDVs affect mass transit modes	Decreases use of transit bus by 17% by 2033, transit rail 35% by 2050 use of commuter rail 48% by 2050

Based on the uncertainty of the field there are four new contributions to the field in this article on the topic of ED in autonomous electrified vehicles (BEV and P/HEV), which builds on previous concepts and literature:

1. A holistic and systems-level understanding of the subsystems and integrations needed to implement ED in AVs allowing for comparison between all studies in the field.

2. Application of technology, integration, and system readiness analysis to ED realization in AVs.

3. A definition of the research gaps existing between the current state of the art and realization of ED usage in AVs.

4. A review of initial studies that have started to explore the identified research gaps.

8.2 Research Gap Derivation

One of the most important aspects of scientific advancement is the systematic identification and review of existing research gaps [263]. In order to identify research gaps, a systematic approach is applied to understand components of a general electric AV with ED implementation and the logical flow of operation. In this section, overall system architecture is introduced and a holistic evaluation of system maturity based on the Department of Defense (DoD) approach is conducted.

8.2.1 AED System Architecture

A systems-level perspective of ED implementation for autonomous BEVs, represented in Figure 8.2, is recommended to clarify communication between academic researchers, automotive sector manufacturers and suppliers, government officials, and other organizations.

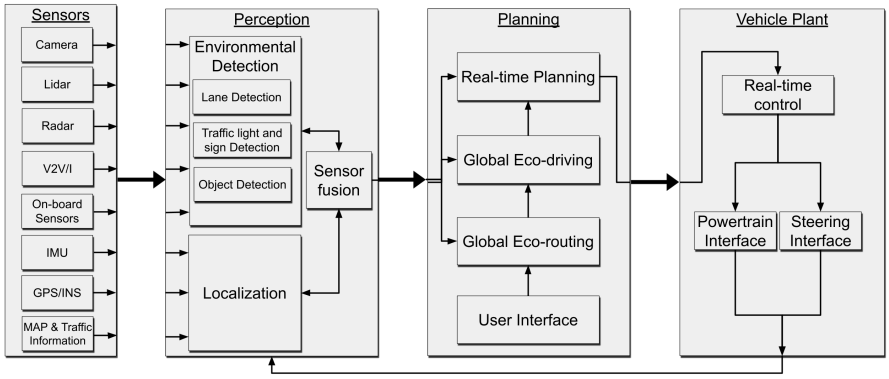

Figure 8.2: A proposed systems-level viewpoint of ED implementation for an AV.

The systems-level viewpoint is composed of four subsystems: a suite of sensors, a vehicle perception subsystem, a vehicle planning subsystem, and a vehicle plant subsystem which include a vehicle running controller. It is the goal of this systems-level perspective to remain closely aligned with the widely acknowledged systems-level perspective on autonomous BEV operation that use energy management strategies. This system receives input from a set of sensors that detect environmental information and also can be used to localize, therefore defining the vehicle's surroundings.An AV learns about its surroundings in two phases. The first step is to look down the road ahead to see if anything has changed, such as traffic lights and signs, a pedestrian crossing, or a barrier. The second phase is concerned with the perception of surrounding traffic. Camera, LiDAR, Radar, V2V and V2I, Inertial Measurement Unit (IMU), GPS and Inertial Navigation System (INS), and map and traffic information are the most typical sensors and data that comprise the sense and perception subsystems of AVs [264]. The real-time planning subsystem employs inputs from the perception subsystem to develop and solve both the long-range (such as Global ER and Global ED) and short-term planning strategies (such as maneuver planning and trajectory planning). It is worth noting that these subsystems also depend on the driving context,

and their boundaries are quite blurred [265]. The real-time control subsystem tracks the longitudinal and lateral trajectories, and interfaces with the vehicle actuators. A control architecture is interfaced to the vehicle powertrain (e.g. controlling propulsion torque, braking torque and gear shifting) and to its steering system. The real-time planning subsystem require feedback from the vehicle, its position relative to the surrounding environment, and predictions of moving obstacles [266], and finally, the powertrain operation from the running controller is actuated in the vehicle plant.

8.2.2 Holistic Evaluation of System Maturity

The National Aeronautics and Space Administration (NASA) developed a seven-level Technology Readiness Level (TRL) rating (shown in Table 8.3) in the 1980s to quantify the risk associated with technology development [267]. NASA now uses this measure to assess the maturity of a specific technology and to compare the maturity of several technologies. Given its practical value, the DoD adopted a TRL model in 1999. While TRL is used similarly by NASA and the DoD, the understanding of TRL varies. For example, NASA requires TRL 6 technologies before a mission can be responsible for them [268], and the DoD requires TRL 7 technologies before they can be included in a weapons system program [8].

Table 8.3: Technology Readiness Levels definition

Technology Readiness Level (TRL)	Definition
9	Actual System Proven Through Successful Mission Operations
8	Actual System Completed and Qualified Through Test and Demonstration
7	System Prototype Demonstration in Relevant Environment
6	System/Subsystem Model or Prototype Demonstration in Relevant Environment
5	Component and/or Breadboard Validation in Relevant Environment
4	Component and/or Breadboard Validation in Laboratory Environment
3	Analytical and Experimental Critical Function and/or Characteristic Proof-of-Concept
2	Technology Concept and/or Application Formulated
1	Basic Principles Observed and Reported

Further, the concept of a System Readiness Levels (SRL) was previously introduced by systems engineering researchers to address the problems applicable at the operating system level. This approach leverages the traditional TRL scale while also including the concept of Integration Readiness Levels (IRL) to produce an SRL index dynamically [8]. The definition of TRL, IRL and SRL and their corresponding levels are tabulated in Tables 8.3, 8.5 and 8.7 respectively.

TRLs

Table 8.4 provides a summary of the TRL for each of the subsystems shown in Figure 8.2, as determined by the authors. These subsystems consist of (1) Sensors and (2) Vehicle Perception for Worldview Creation (3) vehicle planning and (4) application of a physical vehicle plant. These technologies are tabulated in the first column of Table 8.4. The perception subsystem takes in sensor and other pertinent inputs, defines the vehicle's environment, and computes future vehicle operation as an output. The vehicle perception is sent into the planning

Table 8.4: TRL Analysis of Technologies for ED Implementation in AVs

Technology and TRL	Technology Description	TRL Definition	TRL Justification
Sensors subsystem TRL:9	Detects environmental information using cameras, radar, and lidar	Actual System Proven Through Successful Mission Operations	Many commercial products available
Perception subsystem TRL:6	Receives sensor/signal data, fuses data, and works in challenging weather conditions	System/Subsystem Model or Prototype Demonstration in Relevant Environment	Mobileye exists but doesn't provide all functionality; sensor fusion is not well developed
Planning subsystem TRL:7	Solves maneuver planning, path planning, and trajectory planning problems	System Prototype Demonstration in Relevant Environment	Emergency response and derivation of ED are mature
Vehicle plant subsystem TRL:9	Receives driver requests and component statuses, and actuates vehicle operation	Actual System Proven Through Successful Mission Operations	Vehicles by themselves are completely mature

subsystem, which then computes the best control. The planning subsystem is simply responsible for computing the optimum control and issuing a control request; it is not responsible for attaining the goal.

IRLs

Table 8.6 summarizes the IRL for the three alternative integration sites in Figure 8.2 as viewed by the authors. Table 8.6's column 1 contains descriptions of each integration scope. While the TRL is used to assess individual subsystems, the IRL assesses the readiness of each subsystem to integrate with others [8]. A more comprehensive assessment of each subsystem's integration is required than that of the individual subsystem, which normally consists of a basic input/output architecture. If the vehicle operating controller and the vehicle plant are viewed as one high IRL subsystem, there are three theoretically distinct integration points: (1) , (2), and (3) and execution. Due to the little quantity of research that employs these integration scopes, each of these integration points was determined to have a poor technical maturity.

Table 8.5: Integration Readiness Levels definition

IRL	Definition
7	The integration of technologies has been **verified and validated** with sufficient detail to be actionable.
6	The integrating technologies can **accept, translate, and structure information** for its intended application.
5	There is sufficient **control** between technologies necessary to establish, manage, and terminate the integration.
4	There is sufficient detail in the **quality and assurance** of the integration between technologies.
3	There is **compatibility** (i.e. common language) between technologies to orderly and efficiently integrate and interact.
2	There is some level of specificity to characterize the **interaction** (i.e. ability to influence) between technologies through their interface.
1	An **interface** (i.e. physical connection) between technologies has been identified with sufficient detail to allow characterization of the relationship.

SRL

The SRL analysis is the more appropriate method of assessment for the overall system of AED implementation, where the TRL analysis has been performed to individual subsystems and the IRL analysis has been used to subsystem integration. Table 5 shows that, despite the relatively high TRLs of each subsystem, the low IRLs result in a low total SRL. According to the SRL study, if the IRLs are improved, the total SRL will be improved,

Table 8.6: The IRL analysis demonstrates that the technology integrations involved in ED in AVs implementation require significant research.

Integration and IRL	Integration description	IRL definition	IRL justification
Perception and planning integration: IRL 3	detect environmental information	"There is compatibility (i.e. common language) between technologies to orderly and efficiently integrate and interact."	In some cases, the interface between vehicles and SPaT is converted to ED derivation constraints. Sensor fusion specifically has no commonality for ED
Planning when subjected to faulty inputs: IRL 2	Receives sensor/signal data and fuse data	"There is some level of specificity to characterize the interaction (i.e. ability to influence) between technologies through their interface."	Very limited literature.
Planning and use of a vehicle plant: IRL 3	solves several planning problems (maneuver planning, path planning, and trajectory planning)	"There is compatibility (i.e. common language) between technologies to orderly and efficiently integrate and interact."	Some researchers are starting to implement ED on a physical vehicle but progress is slow and there is a lot of work to be done.

and optimal ED for AVs will be applicable to commercial production.

Table 8.7: System Readiness Levels definition

SRL	Name	Definition
5	Operations and Support	Execute a support program that meets operational support performance requirements and sustains the system in the most cost-effective manner over its total life cycle.
4	Production and Development	Achieve operational capability that satisfies mission needs.
3	System Development and Demonstration	Develop a system or increment of capability; reduce integration and manufacturing risk; ensure operational supportability; reduce logistics footprint; implement human systems integration; design for producibility; ensure affordability and protection of critical program information; and demonstrate system integration, interoperability, safety, and utility.
2	Technology Development	Reduce technology risks and determine appropriate sets of technologies to integrate into a full system.
1	Concept Refinement	Refine initial concept. Develop system/technology development strategy.

Table 8.8: The SRL analysis demonstrates that the technology integrations involved in ED in AVs implementation require significant research.

System and SRL	System description	SRL definition	SRL justification
Optimal ED implementation: SRL 1	Perception and planning subjected to errors and implemented in a vehicle plant	"Refine initial concept. Develop system/technology development strategy."	The sets of technologies are not defined and risks basically unknown so this does not meet SRL 2

Research gap analysis summery

The SRL analysis has clearly indicated three research gaps that are inhibiting the implementation of AED, all of which are caused by subsystem integration. These gaps show that research should focus on advancing the following integrations:

1. Performance of integrated sensors and perception subsystems: The effect of Real-world AV perception on identifying the parameters associated with an ED problem.

2. Planning subsystem and noisy inputs: Effect of sparse or missing sensor data on global derivation of AED.
3. Planning and use of a vehicle plant: Performance of a planning subsystem integrated with a physical vehicle plant

8.3 Literature Review

There are a few important studies that have already begun to address these identified research gaps. While there are hundreds of articles that include ED, these integration-based research gaps must be addressed before an ED application of AVs can be commercialized. Each integration research requirement is addressed in the following subsections. Each subsection describes the scope of the research gap and critical studies that are beginning to bridge this research gap are identified and summarized. Studies that lack adequate integration to match the scope of the research gap are excluded.

8.3.1 Research Gap 1: Real-world AV perception with application to the AED problem

The first research gap focuses on real-world AV perception using data from any real-world AV sensors to determine parameters for an ED problem; the scope is illustrated in Figure 8.3. Many published ED studies exist that artificially create constraints for a mathematical optimization problem but real world constraints derived from real world sensors are needed.

Researchers from University of Utah and San Diego State University proposed an ED algorithm for CAVs to improve fuel and operational efficiency of vehicles on the freeways [269]. The proposed algorithm optimizes CAV trajectories with three main objectives - travel time minimization, fuel time minimization, and traffic safety improvement.The first stage of two-state control logic proposed, provides optimal CAV trajectories that can simultaneously minimize freeway travel time and fuel consumption with traffic sensor data and trajectory information as inputs. The second stage of the control logic is focused on ensuring operational safety of CAVs by real time adaptive actions to adjust speeds in response to local driving conditions.

To achieve improved mobility and energy efficiency in mixed traffic conditions, researchers from University of California at Riverside proposed a combination of vision-perceptive technologies and V2I communications [270]. With a neural network extracting vision and V2I information; and a deep Reinforcement Learning (RL) based policy network generates both longitudinal and lateral ED actions with a rule-based driving manager working to regulate the collaboration between rule-based policies and RL policies.

Fleming et al. [271] from Loughborough University outlined a system that uses real-time data from Global Positioning System (GPS) and automotive radar to predictably optimize a vehicle's speed profile and train a

driver toward fuel-saving and CO_2-reducing behavior. Driving data was generated using STISIM Drive simulation software and validated on an instrumented vehicle equipped with radar and GPS sensor.

Table 8.9 summarizes the work in research gap 1. These papers are greatly advancing the commercial implementation of ED in AVs because real world sensors are being used to derive ED constraints. More research is needed in this area especially considering the possibility to utilize traditional AV sensors such as cameras, radar, and lidar.

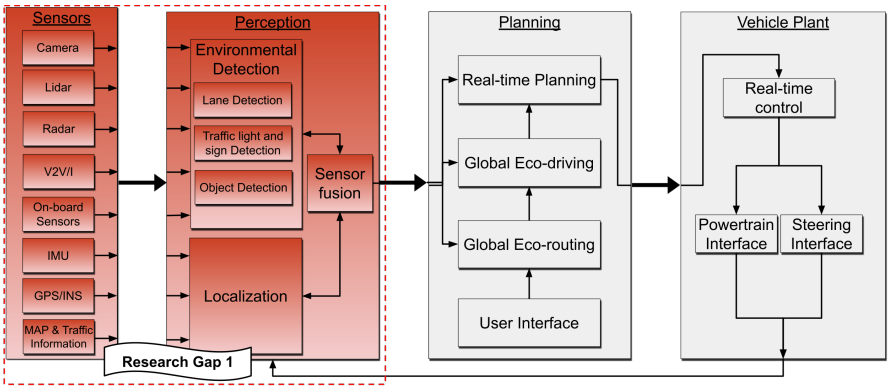

Figure 8.3: The integration scope defined in research gap 1: Real-world AV perception with application to the AED problem

Table 8.9: Summary of existing research that includes the integration scope of Real-world AV perception with application to the AED problem, thus addressing research gap 1.

Research Group	Sensors/signals	Data collection technique	Planning techniques	Vehicle plant
University of Utah and San Diego State University [269]	V2V and V2I	Macroscopic traffic flow model by dividing vehicles into different classes	Travel Time Minimization, Fuel Consumption Minimization, and Safety Improvement	Custom Mathematical Model
University of California at Riverside [270]	Front camera, radar, on-board diagnostics (OBD) and V2V-based SPaT (Signal Phase and Timing) information	Intelligent Driver Model for Traffic Environment and	Hybrid Reinforcement Learning (HRL)	Unity-based Simulator
Loughborough University and University of Southampton [271]	GPS-based localization and Long-range radar	STIMSIM Drive simulation software which simulated 21 km route around Southampton, UK	Fuel consumption and driver preference, and predictive optimization of vehicle speed	2004 Fiat Stilo

8.3.2 Research Gap 2: Sparse or missing sensor data on global derivation of AED

The second research gap focuses on the effect of sparse, missing, or incorrect sensor data which informs the ED problem constraints. Figure 8.4 shows the integration scope associated with this research gap. This gap can include the failure of sensors and infrastructure signals in providing the necessary information for AVs to perform ED as well as studies investigating how an AV can execute an ED function without all necessary information being available to it. Despite this being a common occurrence in real-world applications, there are not many ED papers that address this issue.

On the vehicle side, researchers in University of California Berkeley have developed a stochastic approach with DP optimization to address scenarios in which limited SPaT data is available for AED vehicles [272]. Additionally, a two-layer receding horizon control framework has been proposed to address vehicle speed in scenarios where limited SPaT data is available with the control framework putting emphasis on safety control over velocity planning [273].

SZTAKI also proposed a similar framework to prioritize drive safety over vehicle cruise velocity but with a three layer control framework as opposed to University of California's two-layer control framework [274].

On the infrastructure side, VEDECOM proposed a Road Side Infrastructure (RSI) system that provides environmental information for incoming AV at intersections through the use of camera and lidar [275]. From VEDECOM's research consideration needs to be given for the height positioning and environment of RSI sensors as such factors can affect the robustness of information provided by RSI.

In reviewing the sources related to research gap 2, summarized in Table 8.10, few sources were available in directly addressing how AVs would perform autonomous driving features in faulty sensor and external infrastructure scenarios. While there are sources outlining the benefits and disadvantage of various sensors used in AV perception, such sources lack sufficient coverage on appropriate protocols in events where limited sensor and signal data are available [276, 277]. This suggests future research into research gap could focus on development of such protocols.

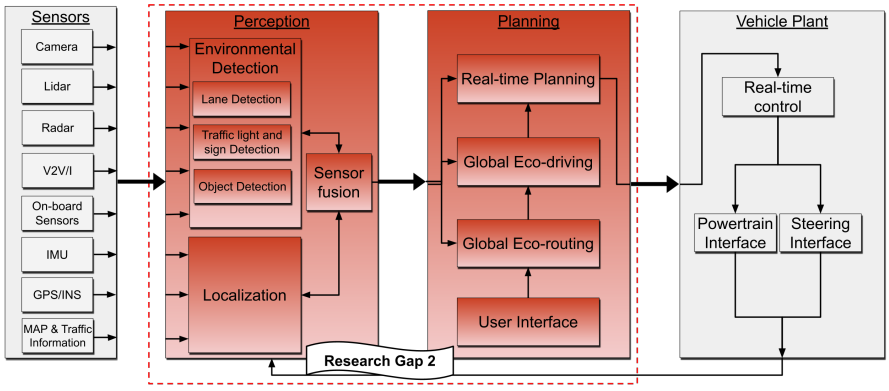

Figure 8.4: The integration scope defined in research gap 2: Sparse or missing sensor data on global derivation of AED

Table 8.10: Summary of existing research that includes the integration scope of sparse or missing sensor data on global derivation of AED problem, thus addressing research gap 2.

Research Group	Sensors/signals	Perception model	Planning techniques	Faulty/Noisy data
University of California, Berkeley [272]	DSRC, Camera, Radar, LIDAR, GPS/INS	V2V/I perception and localization	Stochastic approach with DP optimization	Limited SPaT
VEDECOM [275]	Camera, LIDAR	Road Side Infrastructure (RSI) Central Perception Unit	None. This paper is more focused on external parties providing data for incoming AV	Object distance registered by camera and Synchronization Time for message transmission
University of California, Berkeley [273]	SPaT	ED and Adaptive Cruise Control model	Two-Layer receding horizon control framework (Velocity planning and safety control)	limited SPaT
SZTAKI [274]	Vehicle reference speed and following distance	Vehicle reference speed and following distance	Three layer control framework with driver safety having priority over vehicle cruise speed	Vehicle speed and acceleration

8.3.3 Research Gap 3: Performance of a planning subsystem equipped with AED integrated with a physical vehicle plant

Research outlining the work done on physical AED implementation can be broken down into 4 distinct sections namely: i) what Drive Cycle was used to test AED control algorithm, ii) what planning model was used to enable AV to generate a solution, iii) what type of vehicle plant is used to validate performance of control algorithm and iv) what physical vehicle is used to evaluate control algorithm in real time. Figure 8.5 provides the context of the research gap scope within the AV architecture.

Using a Rollout Algorithm (approximation of DP algorithm) with a multi-layer hierarchical Model Predictive Control (MPC) framework, researchers at Ohio State University evaluated the performance of AED through simulations and physical vehicle implementation [278]. Physical vehicle testing shows the vehicle consumed 22% less fuel compared to baseline scenario with 2.9% savings in trip time while maintaining State of Charge (SOC) at 50%. Results of physical testing were in line with findings from simulation.

University of Wisconsin-Madison developed a control system called Eco-Drive, used to optimize fuel efficiency for purely gasoline vehicles. Eco-Drive uses data available from ODB II port of gasoline vehicles to calculate an optimal vehicle speed to maximize fuel efficiency and implementation was done by automating accelerator pedal position via outputs from Eco-Drive [279]. Testing of Eco-Drive under 100 miles of driven road outline a fuel efficiency improvement of 10-40% depending on urban environments.

Leveraging the NREL Transportation Secure Data Center (TSDC) dataset, a joint effort between General Motors LLC, Carnegie Mellon University, and NREL was carried out to develop an AED vehicle that uses InfoRich Eco-Autonomous Driving (iREAD) to generates optimal travel trajectories [280]. Evaluating iREAD's performance in large-scale, in-depth simulations along with physical evaluations in Vehicle-In-Loop, the research

found fuel savings of 10-20 % depending on road conditions. Although plans were made to test iREAD in road testing, such testing was not done by the time of publication.

On a similar note, Argonne National Labs (ANL) developed a set up to automate evaluation of ED algorithm in a Vehicle-In-Loop (VIL) setting for BEV and ICE vehicles [281]. Testing has shown ANL was successfully in creating a functional and repeatable VIL system with VIL test out-ling a 22% and 16% energy savings for BEV when driven in lead and following position respectively.

For heavy/medium duty trucks, Southwest Research Institute evaluated the performance of SwRI's ED control algorithm in class 8 trucks in accordance to J1321 test procedures [282]. Physical testing of class 8 trucks found SwRI's control algorithm resulted in 7% decrease in fuel consumption and 6% decrease in trip time.

Applying AED in a fleet-based setting, University of California and University of Cincinnati deployed a CAV fleet to evaluate the performance of AED in real time [283, 284]. Evaluating AED performance over 7 road segments and driven over 47 miles, University of Cincinnati's Relaxed Pontryagin's Minimum Principle (RPMP) based AED algorithm yielded fuel savings of 3.3 to 21.2 % with variation depending on hill length and slope grade. Testing their control algorithm over 8 signalized intersections of Southern California, results of University of California's control algorithm outline a fueling savings of 30.98 % for CAV fleet AED in exchange for an 8.51% increase in trip time compare to baseline.

Researchers at Colorado State University also applied predictive acceleration events control to the actual vehicle using customized 2019 Toyota Tacoma parallel-3 (P3)HEV. Their methodology combats long run time issues dynamic programming has for physical implementation by pre-computing the optimal solution for acceleration events. According to the findings of track-based testing using predictive acceleration event control in the real world 7% improvement in FE can be achieved. According to the author, this is the first time this sort of testing has ever been conducted on a real-world vehicle.

The parameters of interest are summarized in Table 8.11. In researching physical implementation of AED, we found that a majority of physical ED research was done on gasoline vehicles. This indicates that ED for physical BEV or Hybrids may be a potential avenue for future research.

8.4 Conclusion

This literature review provides an overview of automotive energy efficient control strategies and discusses that AED for BEVs should be a focus of future research efforts. A systems-level diagram of AED is proposed and an expansion of NASA's TRL analysis (SRL analysis) is performed which identifies three existing research gaps: real-world AV perception with application to the AED problem, sparse or missing sensor data on global derivation of AED, and performance of a planning subsystem equipped with AED integrated with a physical vehicle plant. In other words, there are gaps in knowledge concerning

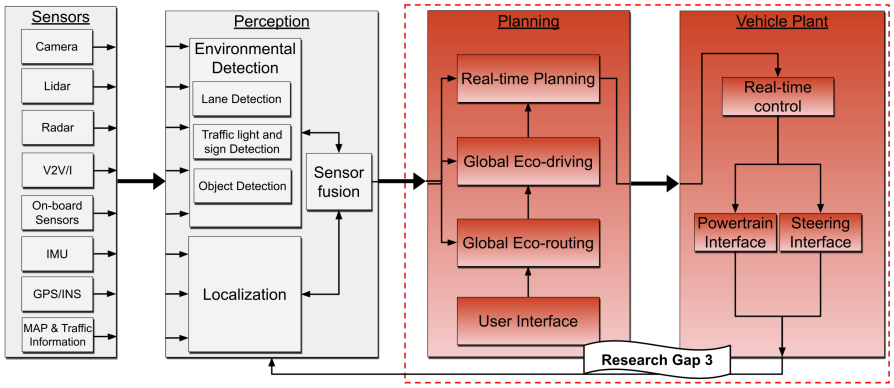

Figure 8.5: The integration scope defined in research gap 3: Performance of a planning subsystem equipped with AED integrated with a physical vehicle plant

Table 8.11: Summary of existing research that includes the integration scope of Performance of a planning subsystem equipped with AED integrated with a physical vehicle plant, thus addressing research gap 3.

Research Group	Drive Cycle	Planning Model	Vehicle plant	Vehicle Realization Type
Ohio State University [278]	Custom Route, Columbus, Ohio	Rollout Algorithm (Approximate DP) and Model Predictive Control	P0 mild-HEV	2016 VW Passat, retrofitted with 48V mild hybrid system
University of Winconsin Madison [279]	Custom mid-size US city drive data	Eco-Drive (DP)	Gasoline Vehicle plant	Unknown Gasoline Vehicle
National Renewable Energy Laboratory [280]	NREL's Transportation Secure Data Center (TSDC) Drive Cycle Data	InfoRich Eco-Autonomous Driving (iREAD)	GM internal model	Cadilac CT6 (BEV)
Argonne National Labs [281]	Multiple Custom Drive Cycle of varying speed limit and HWFET	Analytical Closed Form solutions	Chevrolet Bolt (BEV)	Actual Vehicle
Southwest Research Institute (SwRI) [282]	Modified NREL Port Drayage cycles	Control algorithm with objective of minimizing jerk and acceleration events	2017 Volvo VNL64T300	Actual Vehicle
University of Cincinnati [283]	Rolling segements in Virginia and Maryland	Relaxed Pontryagin's Minimum Principle (RPMP)	2013 ICE Cadillac SRX	Actual Vehicle
University of California, Berkeley [284]	Custom Route Model built using July 2019 Sensys Network data	ECO-ACC (Eco Driving Controller-Adaptive Cruise Controller)	Unknown, PHEV is only stated to have 8.89kWh Battery Capacity	Actual Vehicle
University of California, Riverside [285]	...	...	2015 Volvo VNL	Actual Vehicle
University of Michigan [286]	Custom route, Ann Arbor, MI	Prediction of queuing profile using shock-wave profile model [287]	2017 Toyota Prius Four Turing HEV	Actual Vehicle
Colorado State University [288]	Custom route, Fort Collins, Co	Predictive acceleration event model [287]	2019 Toyota Tacoma	Actual Vehicle

1. An understanding of critical sensors and signals for perception and sensor fusion that enable effective FE vehicle control through AED.

2. An in-depth comprehension of the sorts of fault or missing data from perception that might impact effective FE vehicle control.

3. The operational and real-world problems of effective AED control implementation.

Investigation of the AED literature revealed that, despite the availability of hundreds of papers addressing the idea of ED, there are few papers that provide insights into the AED research gaps which are currently slowing commercial realization. A summary of relevant papers that are beginning to address these gaps are provided and a summary of missing knowledge is given.

The overall conclusion of this research is that focused studies addressing AED research gaps are needed before AV technology and its associated infrastructure is rolled out and fully commercialized. ED considerations need to be a part of AV R&D efforts to ensure that transportation sustainability is improved at the same rate as transportation safety. There are many inconclusive studies about the effect of widespread AV adoption on transportation energy use but some of these worst case scenarios could be alleviated with ED implementation. Focused studies are needed that utilize real-world AV sensors, that investigate the effects of sensor errors, and that include real world BEV implementation.

8.5 Chapter Conclusion

This chapter of the research partially addresses research question 3, task 3.1. Research question 3 is restated here:

Research Question 3: *How can the performance of autonomous eco-driving control differ from simulations when it is operated with a real vehicle?*

Hypothesis: Autonomous Eco-driving control can be implemented in CAVs.

The research gap derivation in this study provides valuable insights for improving the energy efficiency of autonomous eco-driving controls. By identifying the gaps, such as the influence of real-world sensors and handling sparse data, researchers can develop more accurate models and algorithms. Investigating the implications of implementing eco-driving with physical vehicles bridges the gap between simulations and real-world scenarios. Addressing these gaps enables the development of control strategies that optimize energy consumption in actual driving conditions. Overall, this research helps guide future efforts to enhance the energy efficiency of autonomous eco-driving controls.

Chapter 9

Autonomous Eco-Driving Evaluation of an Electric Vehicle on a Chassis Dynamometer

This study explores autonomous eco-driving (ED) control for connected and automated vehicles, with a focus on improving energy efficiency. The research leverages the benefits of Vehicle-to-Everything (V2X) communication to optimize trajectory enhance energy-efficient driving. Various optimization methods, including Dynamic Programming (DP), Genetic Algorithms (GA), and Particle Swarm Optimization (PSO), are utilized and evaluated using a control-enabled electric Kia Soul on a chassis dynamometer. The study emphasizes the potential energy-saving advantages of autonomous eco-driving control in practical and more realistic driving situations, highlighting the importance of optimizing speed planning for enhanced energy efficiency.In the following sections, the design process for the ED system is described, along with the test setup, which includes information about the test vehicle and dynamometer calibration. The findings of the tests are displayed and explained in the results section, which is followed by a summary and conclusion. This study was published at SAE World Congress and is considered as Task 3.2 of research question No. 3 [289]. My contributions encompassed conceptualization and formal analysis. I collaborated with Aaron Rabinowitz, Johan Fanas Rojas, and Parth Kadav in the investigation process. I also played a significant role in shaping the methodology section, and together with Johan Fanas Rojas, I wrote the original draft of the chapter. The work was further enhanced through the review and editing efforts of Dr. Zachary D. Asher and Dr. Richard T. Meyer.

9.1 Introduction

In the past decades, in response to growing environmental and economic concerns, policymakers have begun investing in clean vehicle technology, R&D, demonstrations, and deployment efforts. In the United States, the Environmental Protection Agency (EPA) has been concentrating on improving fuel efficiency, decreasing regulated criteria emissions like Nitrogen oxides (NO_x) and particulate matter (PM), and decreasing greenhouse gas emissions by developing cutting-edge vehicle engine and drivetrain technologies[1-4]. Since electric motors (EMs) are more energy efficient and produce no exhaust emissions, they have been the focus of recent R&D as a

Page 1 of 11 potential solution to the aforementioned problems[5-8]. Hybrid Electric Vehicles (HEVs), Plug-in Hybrid Electric Vehicles (PHEVs), and Battery Electric Vehicles (BEVs) are the three main types of electric vehicle (EV) technologies that have been the subject of the research in the past years [9-11]. The U.S. Department of Energy (DOE) has also been supporting research and development on vehicular electrification by recently announcing a $96 million funding opportunity to assist with the decarbonization of the domestic transportation sector [12].

While the use of alternative fuels, electrified vehicles, and the transition to renewable energy sources are promising, long-term solutions to the aforementioned environmental issues, reducing the emissions of the current vehicle fleet as much as possible is a promising short- and medium-term alternative [13]. Eco-driving (ED) is the control technology of energy-saving driving (such as an energy management strategy), which is accomplished by optimizing the operating point of the engine and/or electric motors at the level of vehicle control algorithms, as defined by extensive research into autonomous driving technology. This study focuses on the integration of automated ED rather than eco-driving which focuses on the driver. Manual ED is susceptible to incorrect acceleration and deceleration events, such as accelerating too quickly or hitting the brakes too violently. This can be caused by a number of factors, including the behavior of vehicles in the immediate area, the stress associated with trying to get somewhere quickly, and the amount of power and torque that is available to the vehicle [14−16].

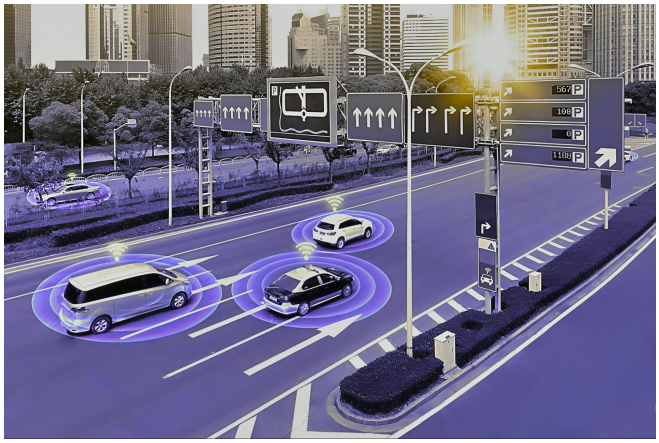

Figure 9.1: An image showing how multiple sensors and V2X technology could be used in CAVs

The combination of connectivity, automation, and electrification results in a more efficient transportation system and a cleaner environment. Connected and automated vehicles (CAVs) are more accurate than human drivers when it comes to following optimal trajectories and considering information outside their line of sight. Therefore, it is preferable to use technologies to improve the performance of BEVs via ED characteristics. This will increase the energy efficiency, range, and market penetration of electric vehicles. There has been a great deal of research on ED applications, particularly those that improve vehicle safety and energy efficiency [17-21]. Figure 9.1 visualizes conceptual CAVs employing multiple sensors and V2X technology [290].

When designing and implementing an autonomous ED system, the method by which an ED algorithm generates the vehicle path will have a significant impact on algorithm performance. In recent years, a lot of research has been conducted on autonomous ED controls, and several approaches for generating an optimal ED trace have been presented and reviewed separately. The advantage of this study is its consideration of real-time implementable strategies. Rules-Based Eco-Driving, Uniformly Discrete Trajectory Optimization, and Spline Trajectory Optimization are the three primary classifications available in the literature: Rules-Based Eco-Driving (RBED), Uniformly Discretized Trajectory Optimization (UDTO), and Spline Trajectory Optimization (STO). A common RBED algorithm is the Intelligent Driver Model (IDM) [23], with several works presenting modified versions of the method in ED simulations. IDM and its derivatives dominate the RBED literature and are often used as a baseline to compare against in the optimal ED literature. Another common technique is the rule-set method. In the surveyed studies, rule-set ED mainly consists of an operation mode control strategy and a fuzzy logic control strategy. Uniformly discretized Trajectory Optimization (UDTO) and Spline Trajectory Optimization methods(STO) are among the most commonly used optimization algorithms for ED. The overall framework of ED is visualized in Figure 9.2.

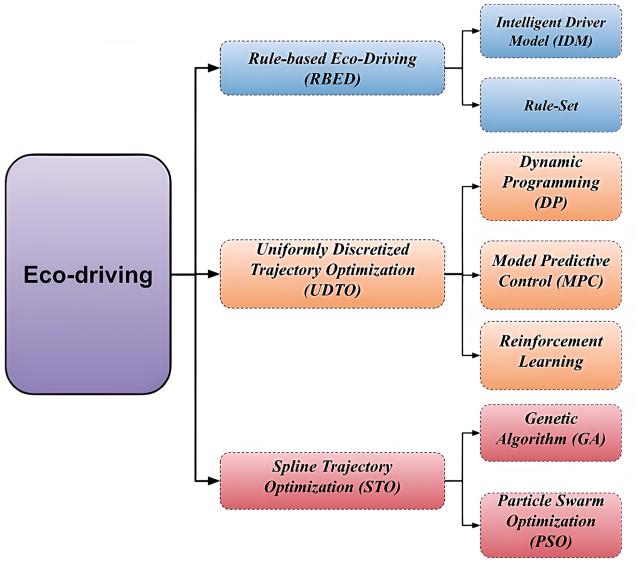

Figure 9.2: The overall framework of eco-driving.

According to what was surveyed, there has been a significant amount of study with simulation. However, there is only a limited amount of test data accessible from the relevant literature to evaluate the ED capabilities of autonomous BEVs in Vehicle Hardware-In-the-Loop (VHIL) circumstances. It is unknown how effective autonomous ED for BEVs will be in decreasing fuel consumption when integrated in a vehicle or under what conditions it will function at its best because the technology is still in its infancy and not yet available for commercial use. In order to effectively build, integrate, and calibrate the ED control system, automobile manufacturers need to have a Page 2 of 11 solid understanding of the repercussions and limitations of automated ED in VHIL driving scenarios. This may help raise customer tolerance for ED automation in BEVs, which in turn may help increase market penetration and wider adoption of the technology.

This study attempts to fill the previously mentioned gap by implementing a selection of common methods in physical electric vehicle plants and evaluating them in terms of energy efficiency and feasibility using VHIL test data. GA, PSO, and DP were tested using physical vehicle dynamometer test data with a control-enabled electric Kia Soul utilizing a 2-wheel-drive chassis dynamometer VHIL test performance of these methods is evaluated relative to each other as well as a baseline scenario. In the following sections, the design process for the ED system is described, along with the test setup, which includes information about the test vehicle and dynamometer calibration. The findings of the tests are displayed and explained in the results section, which is followed by a summary and conclusion.

9.2 Methodology

9.2.1 Eco-driving System Design

Taking a systems-level view on the implementation of ED for autonomous BEVs, as seen in Figure 9.3, is proposed to facilitate more precise communication between universities, automakers, suppliers, governments, and other organizations.

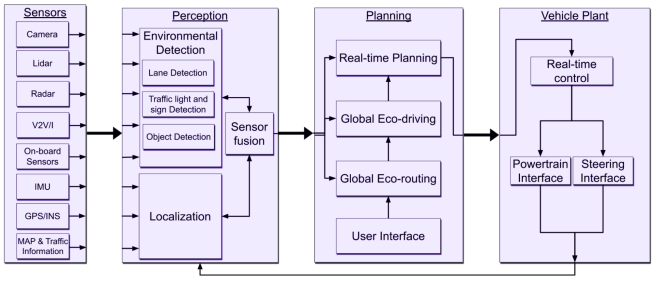

Figure 9.3: System-level viewpoint of ED implementation for autonomous vehicles.

A suite of sensors, a vehicle perception subsystem, a vehicle planning subsystem, and a vehicle plant subsystem, which includes a vehicle running controller, comprise the systems-level viewpoint. This systems model seeks to

remain closely associated with the widely recognized systems-level perspective on autonomous BEV operation that employs energy management tactics.

Perception

This system gets input from a collection of sensors that detect ambient information and can also be used to locate the vehicle's surroundings. An Autonomous Vehicle (AV) acquires environmental knowledge in two phases. The initial step is to examine the road ahead to determine if anything has changed, such as traffic signals and signs, a pedestrian crossing, or a barrier. The perception of nearby traffic is the focus of the second phase. Camera, LiDAR, Radar, Vehicle to Vehicle (V2V) and Vehicle to Infrastructure (V2I), Inertial Measurement Unit (IMU), Global Positioning System (GPS), and Inertial Navigation System (INS), as well as map and traffic data, are the most common sensors and data that comprise the sense and perception subsystems of autonomous vehicles (Figure 9.4) [23].

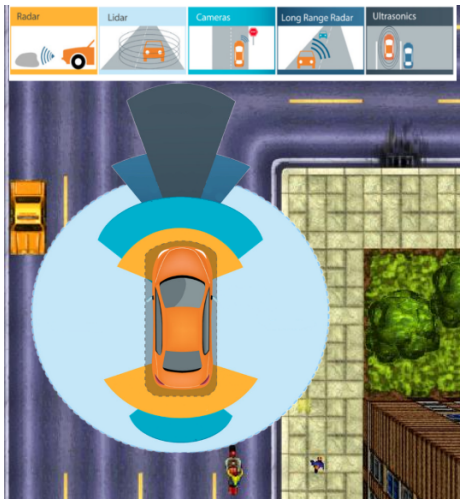

Figure 9.4: An illustration of the type and placement of sensors in an autonomous vehicle that enable the vehicle to perceive its surroundings.

To evaluate EDC (Define) in the real world, the algorithms that generate the optimal ED trace must use only CAV-available information. The CAV's Advanced Driver Assistance System (ADAS) and V2I communication provide information. A CAV can generate ED path constraints with this data. Path constraints include allowable locations (distances along the vehicle path) and speeds at specific locations. Limitations on when and how fast the vehicle can travel at different points along its planned route make up what are called "path constraints" in this analysis.

Path Constraints

In autonomous vehicular control, the ego vehicle should not be designed to break traffic regulations, even if doing so increases efficiency and/or trip time [25]. This indicates that the car should not exceed the speed

limit, disregard traffic signals, or crash. Signal Phase and Timing (SPaT) can produce an inequality at the upper border if the ego vehicle is first in a queue.

Figure 9.5 depicts one such passageway. By restricting travel within the boundary corridor, the ego vehicle is more likely to behave in a way that is consistent with existing traffic patterns. The Intelligent Driver Model (IDM) discussed in [28] is used to choose stop phases to define the limits. For a specified duration of time, the IDM simulation is run, with the upper bound determined by the phases of the traffic lights through which the model vehicle passes, and the lower bound set by the phases of the same signals afterward. Given that the IDM model stands in for a typical motorist, the resulting corridor will accurately reflect typical traffic conditions. Using real-world SPaT [26] data to generate path boundaries adds a more realistic dimension to this research.

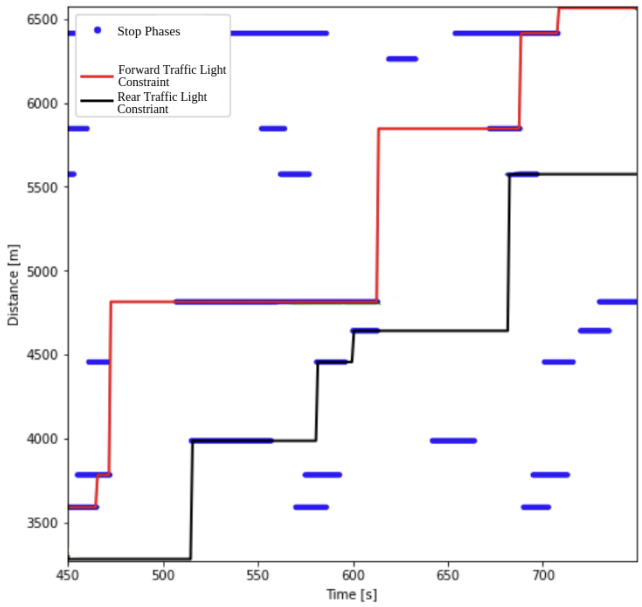

Figure 9.5: Example upper and lower boundaries "corridor".

Phase and timing information for 19 traffic lights over a 4 mile path in downtown Fort Collins, CO was gathered in 2019. The authors gathered these statistics, and their methods are detailed in [28]. Working with the Fort Collins Traffic Operations facility, SPaT data covering many hours at each signal was gathered. A phase map was made using this information and the locations of the traffic lights along the route. The ego vehicle speed must meet the inequality if it is to comply with traffic standards.

Planning (Eco-Driving)

An optimal ED trace is computed by the planning subsystem, which takes into account the limits set by the perception subsystem. As described in the ED system design section, the planning system is assumed to contain an eco-routing, ED, and real-time planning controller, which is the lower level controller that implements eco-routing and ED in real-time. This study is only concerned with the high-level controller and is specifically

focused on the ED controller.

- **Rules-Based Eco-Driving (RBED):** This ED control method minimizes a vehicle's energy use using predetermined rules and historical and present data [29-31]. RBED strategies are easy to apply and are capable of enhancing fuel economy [32]. RBED has also been expanded from controlling a single vehicle to controlling eco-fleets using either cooperative or centralized methods [33, 34].

- **Uniformly Discretized Trajectory Optimization (UDTO):** A specified horizon (position or time) is discretized into a unique collection of points, and an optimization algorithm generates an ideal control action for each point. Dynamic Programming (DP) is a popular UDTO approach. Bellman [20] devised DP to create optimal control solutions for discretization. DP is a computationally intensive ED control approach, and it needs a huge amount of run-time. Much research has been done to solve this issue of DP as an ED control [35-38]. Many works have suggested solver approaches with DP in a Model Predictive Control (MPC) formulation, which permits real-time DP-based solvers [39-43]. These studies used several methodologies to evaluate control costs. [36] came up with a Model Based Reinforcement Learning (MBRL) method for enhancing motor power control in electric vehicles, taking into account road slope but not traffic. Results-wise, MBRL was not noticeably different from DP for this situation. When it comes to ED control, DP and DP-derived methods are more common than reinforcement learning. Like DP, reinforcement learning has difficulty running in real time.

- **Spline Trajectory Optimization (STO):** STO approach was the most often used in the literature for generating ED trajectories [16, 44, 45]. By adjusting the position, velocity, and acceleration of spline knots, ideal ED trajectories are produced. Genetic Algorithm (GA) and Particle Swarm Optimization (PSO) are two optimization techniques that are frequently used in combination with STO. GA simulates natural selection to find an ideal solution. GA simulates natural selection by storing discretized issue choice factors as phenotypes, assessing their fitness, and mating the best phenotypes until a solution converges. Alan Turing introduced the approach in 1950, and Alex Fraser and Jack Crosby codified it in the 1970s [46-48]. GA can be implemented onboard for real-time control using pure serial processing, while parallel computing can significantly reduce run-time for GA-based STO [49-51]. PSO is the second often utilized heuristic method in ED literature. Russell C. Eberhart and James Kennedy developed the PSO model in 1995 in order to examine group member experiences [52]. It generates a field of candidate solutions (particles) and moves them in n-dimensional space according to their optimal solutions and the optimal global solution. Solutions are not necessarily optimal due to the search nature of PSO. The initial position of particles can influence optimality. The addition of mutation to PSO increases optimal solution convergence [53]. PSO was implemented in ED to optimize vehicle energy usage [50,53-55] and platoon behavior at junctions [56]. In a comparison between PSO and DP STO [55], PSO underperformed in energy efficiency

but had a shorter run-time. PSO and GA were utilized to construct the best BEV trajectory [50]. Utilizing a PSO-GA hybrid algorithm yielded better results than using only one. Likewise, [54] investigated the use of PSO and GA to minimize the energy consumption of electric trains.

The methods selected for implementation were DP enabled UDTO, GA enabled STO, and PSO enabled STO with IDM serving as the baseline control to compare against. These methods are extensively defined in the author's previous paper [27]. Also In the team's previous study for optimal control solver methods, three different cost functions were evaluated. Acceleration I^2 Norm (Al2 N) cost function, Road Power Cost (RPC) cost function, and Battery Power Cost (BPC) cost function. In this study, we just used the Battery Power Cost (BPC) cost function, which is an extension of the RPC cost function that takes the motor/inverter's efficiency into consideration, depending on the power needs. For further details, please see the authors' previous paper [27]. Figure 9.6 depicts an example trace generated by ED controllers in the planning subsystem.

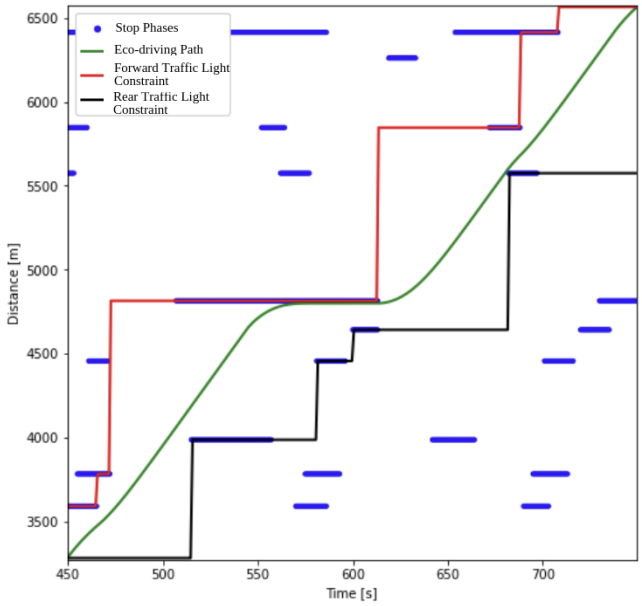

Figure 9.6: Example upper and lower boundaries "corridor" and trace generated by ED controller.

Vehicle Plant

For this study, a 2015 Kia Soul EV was selected as the vehicle of interest (Figure 9.7). This particular BEV was selected because the chassis dynamometer data for it is available from Argonne National Lab (ANL) Downloadable Dynamometer Database (D^3) [57] and because the research team owns a drive-by-wire capable physical vehicle. Table 9.1 shows general specifications for the 2015 Kia Soul EV used for this study.

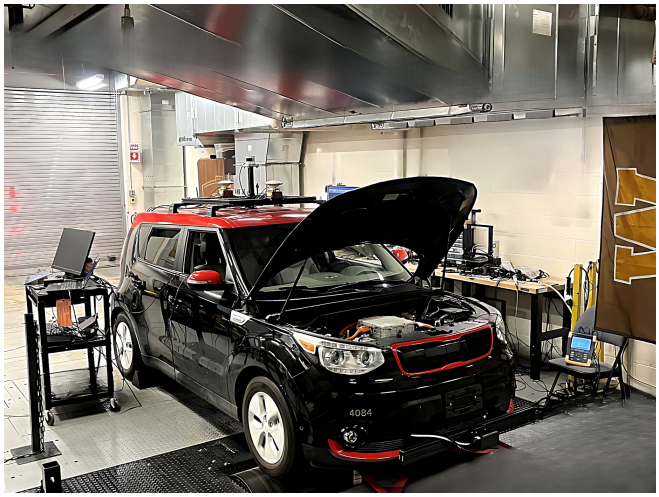

Figure 9.7: 2015 Kia Soul on chassis dynamometer when being tested for this study.

Table 9.1: Kia Soul 2015 EV specifications

Parameter		Value	Units
Weights	Curb mass	1491.8	kg
	Delivered Curb mass	1664	kg
Dimensions	Wheelbase	2.6	m
	Length/Width	4.14/1.8	m
	Frontal Area	2.87	m
Electric Motor	Maximum Power	81	kW
	Maximum Torque	285	Nm
Battery	Useable Pack Energy	27	kWh
	Nominal Pack Voltage	360	V
EPA	Range	93	mile
	Fuel Economy	120 (City) 92 (Highway) 105 (Combined)	MPGe

9.2.2 Development of Eco-driving Test Mode

From pre-defined boundary cases in the author's previous study, four random representative drive cycle cases were selected to evaluate on the chassis dynamometer. Speed vs. time and SOC vs. time comparisons between simulation traces for all methods on drive cycle number 0 (DC_0) are shown in Figure 9.8.

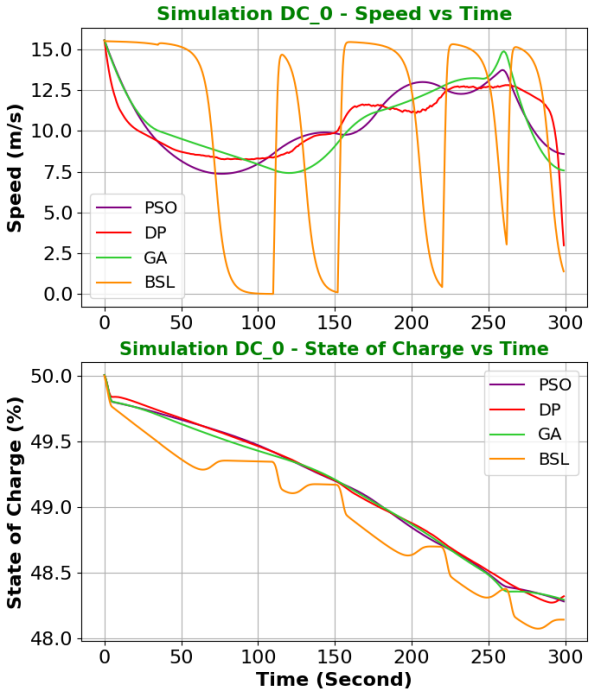

Figure 9.8: Example speed vs. time and SOC vs. time comparison between simulation traces for all methods on drive cycle number 0.

9.2.3 Experimental Design and Data Collection

The experiments were designed to measure the SOC of the vehicle (Kia Soul 2015 EV) running selected trajectory optimized ED traces as well as IDM as a baseline drive cycle on the chassis dynamometer. In our previous study, the authors evaluated the performance of the methods in generating optimal ED traces for 5-minute driving trajectories. To set up the experiments on the chassis dynamometer, first a driver had to specifically run the selected drive-cycles.

Driver setup

The driver's goal is to match the current speed of the vehicle on the chassis dynamometer to the targeted drive cycle speed during the test. This was done by developing a PID speed controller that tries to minimize the error between the vehicle speed and a target speed (from the drive cycle). This is achieved by sending throttle and brake commands to the vehicle using the Robotic Operating System (ROS) [60, 61]. Our team's research vehicle, the 2015 Kia Soul EV, is equipped with Polysync's drive-by-wire solution that allows the user to control the vehicle by sending brake, steering, and throttle commands through ROS. This system interacts with the vehicle through the corresponding actuators by sending controller area network (CAN) signals to the onboard computer. With the drive-by-wire system, we can also collect information from the CAN such as wheel speed,

brake pressure, and steering wheel angle. Figure 9.9 depicts a pipeline for integrating PID controllers with ROS and the drive-kit in a vehicle.

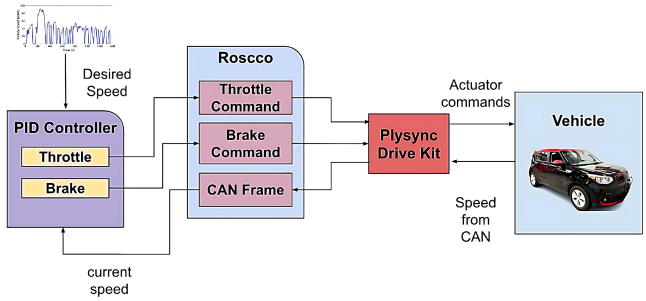

Figure 9.9: PID controller to vehicle integration pipeline using ROS and drive-kit.

- **Drive-kit:** Drive-kit is a drive-by-wire solution that can be installed in the Kia Niro HEV/ PHEV/ EV as well as the Kia Soul EV. When installed, the system provides an Application Programming Interface (API) that allows direct programming or use of middleware line ROS to command the vehicle directly, indirectly, or fully autonomously. The Drive-kit uses sensor imposition to control critical components such as braking, steering, and acceleration, while additional messages from the vehicle's OBD-II CAN provide additional information on the current vehicle states (e.g., steering angle and wheel speeds). Our research team owns The Polysync Drive-kit which is integrated in our research vehicle.

- **Speed Tracking Controller:** A PID controller was developed to perform speed tracking and follow a given drive cycle. The drive cycle possesses time series data representing the speed of the vehicle (which we will call V_k) versus time (which we will call T_k). The speed tracking controller consists of finding the target speed (V_k) associated with its corresponding time (T_k) by matching the elapsed time T_j of our experiment with T_k. The error between the V_k and the vehicle's current speed (V_j) and fed to the PID controller. The PID controller tries to minimize the error between the target speed and the vehicle's current speed. The output of the PID controller is sent to the drive-by-wire system as a throttle command in order to match the drive cycle. Finally, since there is resistance from the chassis and other components, the PID controller was tuned to obtain better tracking performance. Figure 9.9 depicts the overall flow of our speed tracking controller for drive cycle matching.

Chassis dynamometer Calibration

The final step of test preparation was to calibrate chassis dynamometer parameters for accurate road load of the research vehicle during tests. Our research team owns a chassis dynamometer from DynoJet. Team's chassis dynamometer is capable of simulating road-load. By using the offered load control module integrated in the team's chassis dynamometer, we could calibrate the test setup. Figure 9.10 shows the environment of the dynojet software and load control module. The chassis dynamometer is calibrated based on the D^3 from ANL. Road

load calibration is done for constant speed and the Urban Dynamometer Driving Schedule (UDDS) with respect to ANL data. The two tuned parameters, drag coefficient and vehicle mass, were tuned from assumed values in order to best match the battery SOC and battery power traces from the D^3 data. After tuning mentioned parameters, the 2015 Kia Soul EV on our research chassis dynamometer was able to match the D^3 data to within 0.4% with respect to the terms of SOC with Mean Absolute Percentage Error (MAPE) values of 0.82% and 1.552% respectively, for the constant speed test and UDDS. Figure 9.11 shows a comparison between ANL D^3 data and chassis dynamometer for UDDS on the 2015 Kia Soul EV.

Figure 9.10: Road load control module configuration from chassis dynamometer manufacturer (dynojet-224xLC).

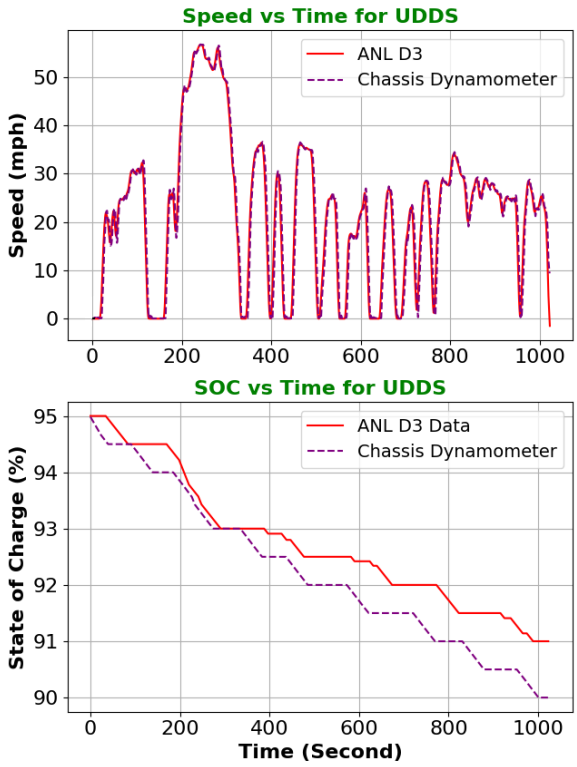

Figure 9.11: Comparison between ANL D3 data and the calibrated chassis dynamometer for UDDS.

9.3 Results

Each optimal ED controller method was evaluated in terms of its ability to produce energy efficient solution traces. The purpose of this study was, specifically, to compare the relative fuel economy improvements of several optimal ED controller methods using the chassis dynamometer. Figure 9.12 shows speed vs. time and SOC vs. time comparisons between physical vehicle dynamometer test traces for all methods on drive cycle number 0.

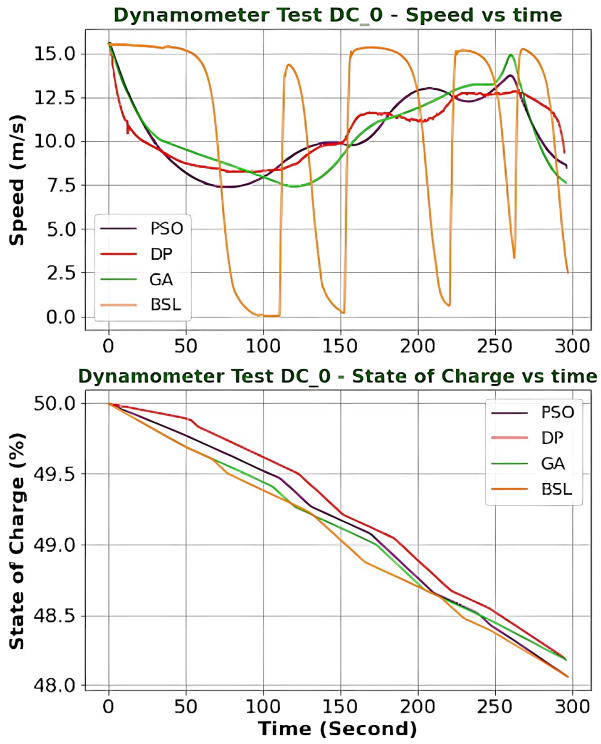

Figure 9.12: Example Speed vs. time and SOC vs. time comparisons between Dynamometer traces for all methods on drive cycle number 0.

A representative example (drive cycle DC_0) is shown in Figure 13 which illustrates Speed vs. time and SOC vs. time comparison between physical vehicle dynamometer test and simulation traces for all methods on drive cycle number 0 . As it can be seen, the physical vehicle dynamometer test traces are smoother compared to the simulation results because SOC can be measured only with a precision of 0.5% which is the output SOC accuracy from CAN. Figure 9.13 shows speed vs. time and SOC vs. time comparisons between physical vehicle dynamometer test traces for all methods on drive cycle number 0.

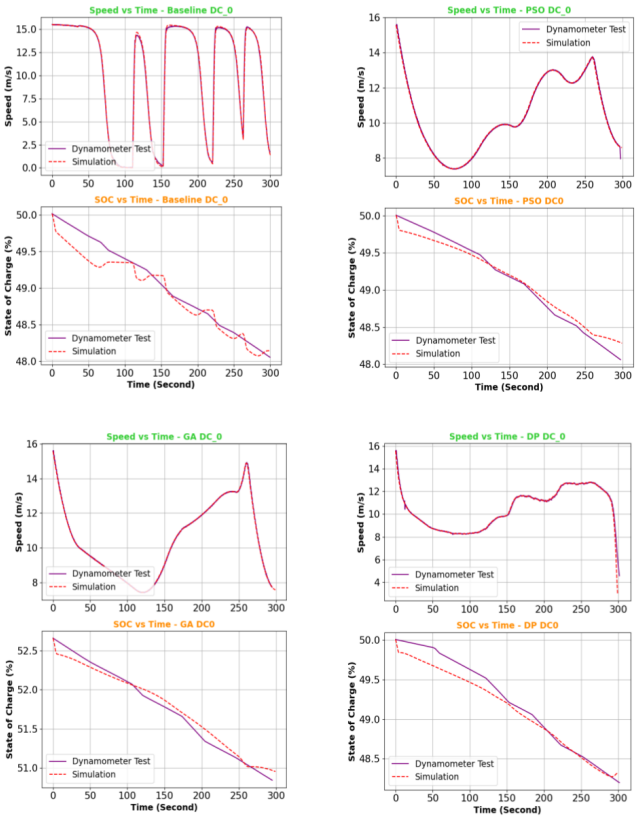

Figure 9.13: Example Speed vs. time and SOC vs. time comparisons between Dynamometer traces for all methods on drive cycle number 0.

The results of the experiment in terms of fuel economy (FE) improvement over baseline are shown in Figure 9.14. physical vehicle dynamometer test results shown in Figures 9.14 verify the previous claim with FE improvement of 5.15%. physical vehicle dynamometer test FE improvements were 33.5% lower than the simulation. Also PSO test results show the same pattern for FE improvement comparison between physical vehicle dynamometer test test results and simulation. PSO was able to improve FE less than other methods, 2.2%. This improvement was 62% lower than the simulation results. These errors could be rooted from many factors such as sensor errors, instrumentation errors and losses, and slower response time of the vehicle vs the vehicle model in simulations. Overall, this can be concluded that DP has the best potential to improve FE. GA also ,due to the relatively great FE improvements both in simulation and physical vehicle dynamometer tests and its lower computational cost, can be a great candidate for implementation.

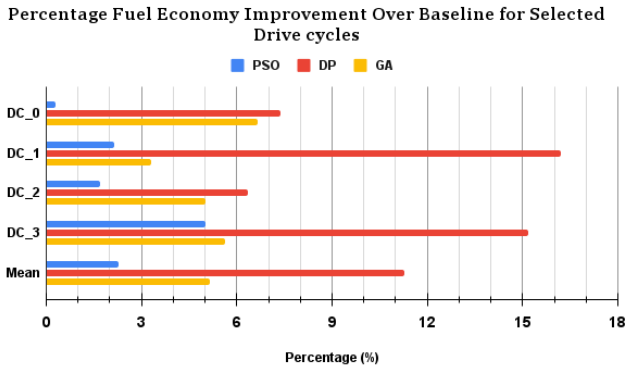

Figure 9.14: FE improvement in terms of percentage over baseline for the studied methods.

The significance of the observed differences in effectiveness could not be assumed due to the considerable uncertainty regarding the FE improvement values. As a result, T-tests were conducted between all possible combinations of techniques, and the results are displayed in Table 9.2.

Table 9.2: Correlation matrix for three optimization methods.

Method	DP	PSO	GA
DP	1.0000	0.0018	0.0139
PSO	0.0018	1.0000	0.0123
GA	0.0139	0.0123	1.0000

9.4 Conclusion

Synergistic benefits of connectivity, automation, and electrification contribute to a more efficient transportation system and a greener environment. In this study, first a systems-level view of autonomous ED was proposed, and subsystems including perception, planning, and vehicle plant were introduced. A great deal of research has been conducted on ED applications. Rules-Based Eco-Driving (RBED), Uniformly Discrete Trajectory Optimization (UDTO), and Spline Trajectory Optimization (STO) are the three primary classifications available in the literature. In our previous study, DP enabled UDTO, GA enabled STO, and PSO enabled STO were selected to be compared in terms of energy efficiency improvement capability in simulation. Not many studies evaluated these methods using physical vehicle dynamometer tests. This study attempts to fill the mentioned gap by testing these methods in a physical electric vehicle plant and evaluating these methods in terms of energy efficiency and practicality. Experiments were developed to assess the SOC of the vehicle (kia Soul 2015EV) using optimized ED traces and IDM as a baseline driving cycle on the chassis dynamometer. A PID controller was utilized to build a link between the research vehicle's planned speed using Python, ROS, and drive-kit. The speed tracking ROS node sends and receives throttle, brake, and CAN frame messages. The PID controller was fine-tuned for tracking precision. The chassis dynamometer is calibrated using Argone's D^3 database (ANL). Constant speed

and UDDS are calibrated for ANL data. The drag coefficient and vehicle mass were modified from anticipated values to match ANL D^3 battery SOC and power traces. Load road module provided by chassis dynamometer manufacturer (dynojet), was used to calibrate based on instantaneous loads. After calibration, the 2015 Kia Soul EV on our research chassis dynamometer matched the D^3 data to within 0.4% in terms of SOC with MAPE values of 0.82 and 1.552 for constant speed test and UDDS. Selected controller methods using real-world data were tested with a control-enabled electric Kia Soul EV utilizing a 2-wheel-drive chassis dynamometer. The physical vehicle dynamometer test performance of these methods is evaluated relative to each other as well as a baseline scenario. physical vehicle dynamometer test FE improvements were compared and evaluated with simulation results. In both simulation and physical vehicle dynamometer tests, DP improves FE by 11% followed by GA with 5.15% improvement in physical vehicle dynamometer test tests.

It can be concluded that DP has the greatest potential for real-world implementation because of its higher FE improvements compared to other studied methods. The fact that FastSim operates efficiently, in addition to being easily implementable in vehicles, suggests that Page 8 of 11 original equipment manufacturers (OEMs) in the automotive industry and companies that develop autonomous vehicles may opt to implement DP in their own vehicles. This study is innovative since it demonstrates that drive-by-wire vehicle-hardware-in-loop may be used as an innovative method, making it easier to test and certify eco-driving systems for applications involving autonomous vehicles. Based on a chassis dynamometer, an integrated drive-by-wire physical vehicle, and simulation results, this system might be utilized early in the design phase to test and evaluate the integration of eco-driving control algorithms for autonomous and intelligent vehicles. This technology enables the testing and evaluation of complex eco-driving operations in a range of simulated environmental conditions and scenarios. This removes the need for test drives, which include their own dangers, expenses, and complications. Also, It is worth noting that incorporating such verified powertrain simulators (e.g. FastSim) into autonomous driving simulators such as CARLA could help researchers and autonomous vehicle developers to compare powertrains' energy efficiency and performance and estimate the impact of technology improvements for autonomous ED. In the future, it can be suggested to evaluate the real run-time and computation power comparison when these methods are configured and tested within the implemented planning subsystem. In the near future, this development will enable the implementation of optimal ED control for CAVs. With the widespread use of fully autonomous CAVs and vehicles, route planning will become entirely predictable, significantly boosting DP's efficiency. Therefore, the authors strongly advise that efforts to develop and execute in this direction should begin immediately.

9.5 Chapter Conclusion

This chapter of the research partially addresses research question 3, task 3.2. Research question 3 is restated here:

Research Question 3: *How can the performance of autonomous eco-driving control differ from simulations when it is operated with a real vehicle?*

Hypothesis: Autonomous Eco-driving control can be implemented in CAVs.

This research adeptly addresses the inquiry regarding the disparity between the performance of autonomous eco-driving control in simulations versus real-world vehicle operations. Through meticulous comparisons conducted via simulation and physical vehicle dynamometer tests, diverse control methodologies are evaluated, leading to the identification of Dynamic Programming (DP) as the preeminent approach, exhibiting superior energy efficiency enhancements. Notably, this study pioneers the innovative utilization of drive-by-wire vehicle-hardware-in-loop for the purpose of validating and certifying eco-driving systems tailored for autonomous vehicles. The outcomes underscore the pressing necessity to expedite the development and implementation of optimal eco-driving control mechanisms for connected and autonomous vehicles, taking into account the imminent proliferation of fully autonomous vehicles alongside the advent of predictable route planning

Chapter 10

Conclusion

This dissertation presents a cohesive sequence of studies that explore the integration of advanced technologies in vehicles to optimize performance, fuel economy, and emissions reduction. The findings offer valuable insights into the potential benefits and challenges of implementing these technologies in real-world scenarios. The initial study focuses on predicting vehicle velocity using Long Short-Term Memory (LSTM) neural networks and Vehicle-to-Infrastructure (V2I) data. This sets the foundation for subsequent research. Building upon velocity prediction, the second study investigates optimal energy management strategies (EMS) for hybrid and plug-in hybrid vehicles. Model Predictive Control (MPC) is identified as a promising approach for significant fuel economy improvements. The third study explores predictive systems, emphasizing the potential of Predictive Optimal Energy Management Systems (POEMS) to improve fleet efficiency. The integration of Advanced Driver Assistance Systems (ADAS) and Vehicle-to-Everything (V2X) connectivity is highlighted. Continuing the research, the fourth study reveals the synergistic benefits of vehicle-level and infrastructure-level energy optimization. Concurrent implementation of optimal Traffic Management Systems (TMS) and EMS leads to substantial fleet-level efficiency improvements. Shifting focus to emissions and fuel consumption prediction, the fifth study employs deep neural network approaches. Long Short-Term Memory (LSTM) networks demonstrate superior accuracy in predicting emissions and fuel consumption in light-duty diesel vehicles. Expanding on the concept of eco-driving, the sixth study explores its application in autonomous vehicles (AVs). The viability of eco-driving capabilities in current vehicles is emphasized, contributing to transportation sustainability. Lastly, the seventh study examines energy efficiency improvements through eco-driving in autonomous electric vehicles. Dynamic Programming (DP) is identified as an effective method for enhancing energy efficiency. Collectively, these studies provide comprehensive insights into the integration of advanced technologies in vehicles. They offer valuable knowledge for optimizing performance, fuel economy, and emissions reduction in future transportation systems. In conclusion, this dissertation showed that the LSTM model has emerged as a powerful tool in automotive research, demonstrating its effectiveness in various applications. Through its ability to capture and learn from

sequential data, LSTM has shown promise in addressing complex challenges within the automotive domain, such as velocity prediction with POEMS, autonomous driving, and vehicular tailpipe emission and fuel consumption prediction. The model's ability to capture temporal dependencies in sensor data and effectively model long-term patterns has contributed to improved reliability and cost-efficiency. LSTM's ability to learn from past experiences and make accurate predictions based on the current context makes it a valuable tool for perception, planning, and control tasks in autonomous driving research. Given the successful applications of LSTM in various automotive research topics, it is reasonable to suggest that this model will continue to be a valuable asset in future studies. However, it is important to note that the effectiveness of LSTM heavily relies on the quality and quantity of available data, as well as appropriate model design and training. Therefore, future researchers should consider the specific requirements and limitations of their research topics when deciding whether to utilize LSTM or explore alternative approaches.

10.1 Research Impact and Contributions

The primary contributions of this dissertation are presented below:

- This dissertation contributes to the knowledge of integrating advanced technologies in vehicles for optimizing performance and reducing emissions.
- It highlights the effectiveness of Long Short-Term Memory (LSTM) neural networks in predicting vehicle velocity using data from vehicle-to-infrastructure (V2I) systems.
- The dissertation identifies Model Predictive Control (MPC) as a promising approach for optimizing energy management in hybrid and plug-in hybrid vehicles.
- It showcases the potential of Predictive Optimal Energy Management Systems (POEMS) in enhancing fleet efficiency through advanced driver assistance systems (ADAS) and vehicle-to-everything (V2X) connectivity.
- The dissertation emphasizes the synergistic benefits of combining vehicle-level and infrastructure-level energy optimization techniques for improving overall efficiency.
- It highlights the accuracy and effectiveness of deep neural network approaches, such as Long Short-Term Memory (LSTM) networks, in predicting emissions and fuel consumption in light-duty diesel vehicles.
- The dissertation explores the application of eco-driving concepts in autonomous vehicles, demonstrating their viability and contribution to sustainable transportation.
- The dissertation provides a comprehensive understanding of integrating advanced technologies in vehicles to optimize performance and reduce emissions.

- It lays the foundation for future research and development in the field of intelligent transportation systems, offering insights for innovative solutions to enhance efficiency and sustainability in transportation.

10.2 Impact

This research has a significant impact on various aspects of vehicle improvement and transportation sustainability. It enhances vehicle performance, fuel economy, and emissions reduction through the integration of advanced technologies and predictive systems. The findings provide valuable insights and methodologies for optimizing energy management, resulting in improved efficiency and reduced fuel consumption. By accurately predicting emissions and fuel consumption, the research enables strategies to minimize environmental impact. It also enhances fleet efficiency through the integration of advanced driver assistance systems and energy optimization techniques. The exploration of eco-driving concepts in autonomous vehicles promotes sustainable transportation practices. The research facilitates the practical implementation of advanced technologies, informing industry advancements and policy initiatives. Overall, it contributes to transportation efficiency, sustainability, and a greener future.

10.3 Future Work

Future work of this research may involve refining the predictive models to improve accuracy and robustness in predicting velocity, fuel consumption, and emissions. This could be achieved by incorporating additional variables and exploring different neural network architectures. Integrating real-time data, such as weather conditions and traffic patterns, into the models would optimize vehicle performance in real-world scenarios. The development of adaptive control strategies that dynamically adjust vehicle parameters based on real-time predictions could enhance energy management and eco-driving behaviors. Further testing and validation in diverse driving conditions, vehicle types, and locations would assess the practical applicability of the proposed methodologies. Exploring the integration of emerging technologies like vehicle-to-vehicle communication and autonomous driving capabilities could enhance vehicle optimization. Evaluating the economic and societal impacts of implementing these methodologies, including cost-effectiveness and broader implications for transportation systems and sustainability, would be valuable. Additionally, long-term monitoring and analysis of implemented systems in real-world deployments would provide insights for continuous improvement. By addressing these future research areas, we can advance intelligent transportation systems and contribute to sustainable and efficient transportation solutions.

References

[1] Nicholas Chase, John Maples, and Mark Schipper. Autonomous vehicles: Uncertainties and energy implications. In *2018 EIA Energy Conference, Washington, DC. PowerPoint, June*, volume 5, 2018.

[2] Shaojie Bai, J Zico Kolter, and Vladlen Koltun. An empirical evaluation of generic convolutional and recurrent networks for sequence modeling. March 2018.

[3] Shiva Tarun Chenna. *ARTIFICIAL NEURAL NETWORKS FOR FUEL CONSUMPTION AND EMISSIONS MODELING IN LIGHT DUTY VEHICLES*. PhD thesis, Colorado State University. Libraries.

[4] Greg Schoeninger. Curious inspiration. http://www.curiousinspiration.com/posts/combining-individual-neurons-into-a-feedforward-neural-network. Accessed: 2020-10-30.

[5] C C Chan. The state of the art of electric and hybrid vehicles, 2002.

[6] Md Kalim Amzad Chy, Abdul Kadar Muhammad Masum, Kazi Abdullah Mohammad Sayeed, and Md Zia Uddin. Delicar: A smart deep learning based self driving product delivery car in perspective of bangladesh. *Sensors*, 22:126, December 2021.

[7] Md. Kalim Amzad Chy, Abdul Kadar Muhammad Masum, Kazi Abdullah Mohammad Sayeed, and Md Zia Uddin. Delicar: A smart deep learning based self driving product delivery car in perspective of bangladesh. *Sensors*, 22(1), 2022.

[8] Brian Sauser, Dinesh Verma, Jose Ramirez-Marquez, and Ryan Gove. From TRL to SRL: The concept of systems readiness levels. In *Conference on Systems Engineering Research, Los Angeles, CA*, pages 1–10, 2006.

[9] T Gaikwad, A Rabinowitz, F Motallebiaraghi, T Bradley, and others. Vehicle velocity prediction using artificial neural network and effect of real world signals on prediction window. 2020.

[10] Daniel J Fagnant and Kara Kockelman. Preparing a nation for autonomous vehicles: opportunities, barriers and policy recommendations, 2015.

[11] Harald Waschl, Ilya Kolmanovsky, and Frank Willems. *Control Strategies for Advanced Driver Assistance Systems and Autonomous Driving Functions: Development, Testing and Verification*. Springer, June 2018.

[12] Alicia Birky, Energetics Inc., Columbia, MD (United States), Michael Laughlin, Katie Tartaglia, Rebecca Price, Brandon Lim, and Zhenhong Lin. Electrification beyond light duty: Class 2b-3 commercial vehicles, 2017.

[13] A B Nkoro and Y A Vershinin. Current and future trends in applications of intelligent transport systems on cars and infrastructure. In *17th International IEEE Conference on Intelligent Transportation Systems (ITSC)*, pages 514–519, October 2014.

[14] Soodeh Dadras. Path tracking using fractional order extremum seeking controller for autonomous ground vehicle. In *SAE Technical Paper Series*, number 2017-01-0094, 400 Commonwealth Drive, Warrendale, PA, United States, March 2017. SAE International.

[15] Soodeh Dadras, Homayoun Jamshidi, Sara Dadras, and Thomas Edward Pilutti. Novel stop sign detection algorithm based on vehicle speed profile. In *2019 American Control Conference (ACC)*, pages 3994–3999, July 2019.

[16] Howard B Demuth, Mark H Beale, Orlando De Jess, and Martin T Hagan. *Neural Network Design*. Martin Hagan, USA, 2nd edition, 2014.

[17] F A Bender, M Kaszynski, and O Sawodny. Drive cycle prediction and energy management optimization for hybrid hydraulic vehicles. *IEEE Trans. Veh. Technol.*, 62(8):3581–3592, October 2013.

[18] Teresa Donateo, Damiano Pacella, and Domenico Laforgia. Development of an energy management strategy for plug-in series hybrid electric vehicle based on the prediction of the future driving cycles by ICT technologies and optimized maps, 2011.

[19] C Sun, X Hu, S J Moura, and F Sun. Velocity predictors for predictive energy management in hybrid electric vehicles. *IEEE Trans. Control Syst. Technol.*, 23(3):1197–1204, May 2015.

[20] C Sun, S J Moura, X Hu, J K Hedrick, and F Sun. Dynamic traffic feedback data enabled energy management in plug-in hybrid electric vehicles. *IEEE Trans. Control Syst. Technol.*, 23(3):1075–1086, May 2015.

[21] Qiuming Gong, Yaoyu Li, and Zhong-Ren Peng. Trip-based optimal power management of plug-in hybrid electric vehicles. *IEEE Transactions on Vehicular Technology*, 57(6):3393–3401, 2008.

[22] Amir Rezaei and Jeffrey B Burl. Prediction of vehicle velocity for model predictive control. *IFAC-PapersOnLine*, 48(15):257–262, January 2015.

[23] Q Gong, Y Li, and Z Peng. Trip-Based optimal power management of plug-in hybrid electric vehicles. *IEEE Trans. Veh. Technol.*, 57(6):3393–3401, November 2008.

[24] Mohd Azrin Mohd Zulkefli, Jianfeng Zheng, Zongxuan Sun, and Henry X Liu. Hybrid powertrain optimization with trajectory prediction based on inter-vehicle-communication and vehicle-infrastructure-integration. *Transp. Res. Part C: Emerg. Technol.*, 45:41–63, August 2014.

[25] Tushar D Gaikwad, Zachary D Asher, Kuan Liu, Mike Huang, and Ilya Kolmanovsky. Vehicle velocity prediction and energy management strategy part 2: Integration of machine learning vehicle velocity prediction with optimal energy management to improve fuel economy. Technical report, SAE Technical Paper, 2019.

[26] Stéphanie Lefèvre, Chao Sun, Ruzena Bajcsy, and Christian Laugier. Comparison of parametric and non-parametric approaches for vehicle speed prediction. In *2014 American Control Conference*, pages 3494–3499, June 2014.

[27] Oluwatobi Olabiyi, Eric Martinson, Vijay Chintalapudi, and Rui Guo. Driver action prediction using deep (bidirectional) recurrent neural network. June 2017.

[28] Joe Lemieux and Yuan Ma. Vehicle speed prediction using deep learning. In *2015 IEEE Vehicle Power and Propulsion Conference (VPPC)*, pages 1–5, October 2015.

[29] Fengqi Zhang, Junqiang Xi, and Reza Langari. Real-Time energy management strategy based on velocity forecasts using V2V and V2I communications. *IEEE Trans. Intell. Transp. Syst.*, 18(2):416–430, February 2017.

[30] Chao Sun, Fengchun Sun, Xiaosong Hu, J Karl Hedrick, and Scott Moura. Integrating traffic velocity data into predictive energy management of plug-in hybrid electric vehicles, 2015.

[31] Erik Hellstrom and Mrdjan Jankovic. A driver model for velocity tracking with look-ahead, 2015.

[32] Kuan Liu, Zachary Asher, Xun Gong, Mike Huang, and Ilya Kolmanovsky. Vehicle velocity prediction and energy management strategy part 1: Deterministic and stochastic vehicle velocity prediction using machine learning, 2019.

[33] Christopher Olah. Understanding lstm networks. 2015.

[34] Omer Berat Sezer. LSTM_RNN_Tutorials_with_Demo: LSTM-RNN tutorial with LSTM and RNN tutorial with demo with demo projects such as Stock/Bitcoin time series prediction, sentiment analysis, music generation using Keras-Tensorflow.

[35] Chiou-Jye Huang and Ping-Huan Kuo. A deep CNN-LSTM model for particulate matter (PM2.5) forecasting in smart cities. *Sensors*, 18(7), July 2018.

[36] NVIDIA DRIVE documentation. https://developer.nvidia.com/drive/documentation, March 2018. Accessed: 2021-8-12.

[37] Z D Asher, J A Tunnell, D A Baker, R J Fitzgerald, and others. Enabling prediction for optimal fuel economy vehicle control. 2018.

[38] Amol Arvind Patil, Farhang Motallebiaraghi, Richard Meyer, and Zachary D Asher. Comparison of optimal energy management strategies using dynamic programming, model predictive control, and constant velocity prediction, 2020.

[39] International Energy Agency and International Energy Agency. Key world energy statistics 2016, 2016.

[40] NEXTCAR_Project_Descriptions_FINAL.pdf.

[41] International Energy Agency. *Energy and Climate Change: World Energy Outlook Special Report*. International Energy Agency, 2015.

[42] Sebastian Thrun. Toward robotic cars, 2010.

[43] Mohd Azrin Mohd Zulkefli, Jianfeng Zheng, Zongxuan Sun, and Henry X Liu. Hybrid powertrain optimization with trajectory prediction based on inter-vehicle-communication and vehicle-infrastructure-integration. *Transp. Res. Part C: Emerg. Technol.*, 45:41–63, August 2014.

[44] Z D Asher, A A Patil, V T Wifvat, A A Frank, and others. Identification and review of the research gaps preventing a realization of optimal energy management strategies in vehicles. *SAE Int. J. Alt*, 2019.

[45] Jordan Tunnell, Zachary D Asher, Sudeep Pasricha, and Thomas H Bradley. Toward improving vehicle fuel economy with ADAS. *SAE International Journal of Connected and Automated Vehicles*, 1(12-01-02-0005):81–92, 2018.

[46] D Baker, Z D Asher, and T Bradley. V2V communication based real-world velocity predictions for improved HEV fuel economy. 2018.

[47] Pei Zhang, Fuwu Yan, and Changqing Du. A comprehensive analysis of energy management strategies for hybrid electric vehicles based on bibliometrics. *Renewable Sustainable Energy Rev.*, 48:88–104, August 2015.

[48] Simona Onori, Lorenzo Serrao, and Giorgio Rizzoni. *Hybrid Electric Vehicles: Energy Management Strategies*. Springer, London, 2016.

[49] Wu, G., Qi, X., Barth, M., & Boriboonsomsin, K.. Advanced energy management strategy development for plug-in hybrid electric vehicles. *UC Davis: National Center for Sustainable Transportation.*, May 2016.

[50] Simona Onori, Lorenzo Serrao, and Giorgio Rizzoni. Adaptive equivalent consumption minimization strategy for hybrid electric vehicles, 2010.

[51] H Ali Borhan, H Ali Borhan, Ardalan Vahidi, Anthony M Phillips, Ming L Kuang, and Ilya V Kolmanovsky. Predictive energy management of a power-split hybrid electric vehicle, 2009.

[52] Z D Asher, D A Baker, and T H Bradley. Prediction error applied to hybrid electric vehicle optimal fuel economy. *IEEE Trans. Control Syst. Technol.*, 2017.

[53] Rajesh Rajamani. Vehicle dynamics and control: Springer science & business media, 2011.

[54] Zachary D Asher, David A Trinko, Joshua D Payne, Benjamin M Geller, and Thomas H Bradley. Real-Time implementation of optimal energy management in hybrid electric vehicles: Globally optimal control of acceleration events. *J. Dyn. Syst. Meas. Control*, 142(8), August 2020.

[55] Luigi Del Re, Frank Allgöwer, Luigi Glielmo, Carlos Guardiola, and Ilya Kolmanovsky. *Automotive Model Predictive Control: Models, Methods and Applications*. Springer Science & Business Media, March 2010.

[56] Scott Jason Moura, Hosam K Fathy, Duncan S Callaway, and Jeffrey L Stein. A stochastic optimal control approach for power management in Plug-In hybrid electric vehicles, 2011.

[57] Z D Asher, D A Trinko, and T H Bradley. Increasing the fuel economy of connected and autonomous lithium-ion electrified vehicles. *Behaviour of Lithium-Ion Batteries in*, 2018.

[58] Zachary D Asher, Abril A Galang, Will Briggs, Brian Johnston, Thomas H Bradley, and Shantanu Jathar. Economic and efficient hybrid vehicle fuel economy and emissions modeling using an artificial neural network. In *SAE Technical Paper Series*, number 2018-01-0315, 400 Commonwealth Drive, Warrendale, PA, United States, April 2018. SAE International.

[59] Z D Asher, D A Baker, and T H Bradley. Prediction error applied to hybrid electric vehicle optimal fuel economy. *IEEE Trans. Control Syst. Technol.*, 26(6):2121–2134, November 2018.

[60] Amol Arvind Patil. *Comparison of Optimal Energy Management Strategies Using Dynamic Programming, Model Predictive Control, and Constant Velocity Prediction*. PhD thesis, Western Michigan University, 2020.

[61] Shaobo Xie, Xiaosong Hu, Zongke Xin, and James Brighton. Pontryagin's minimum principle based model predictive control of energy management for a plug-in hybrid electric bus. *Appl. Energy*, 236:893–905, 2019.

[62] H Borhan, A Vahidi, A M Phillips, M L Kuang, I V Kolmanovsky, and S Di Cairano. MPC-Based energy management of a Power-Split hybrid electric vehicle. *IEEE Trans. Control Syst. Technol.*, 20(3):593–603, May 2012.

[63] Lina Fu, Umit Ozguner, Pinak Tulpule, and Vincenzo Marano. Real-time energy management and sensitivity study for hybrid electric vehicles. In *Proceedings of the 2011 American Control Conference*. IEEE, June 2011.

[64] Mike Huang, Shengqi Zhang, and Yushi Shibaike. Real-time long horizon model predictive control of a plug-in hybrid vehicle Power-Split utilizing trip preview. Technical report, SAE Technical Paper, 2019.

[65] Richard Meyer, Raymond A DeCarlo, Peter H Meckl, Chris Doktorcik, and Steve Pekarek. Hybrid model predictive power flow control of a fuel cell-battery vehicle. In *Proceedings of the 2011 American Control Conference*, pages 2725–2731, June 2011.

[66] Richard T Meyer, Raymond A DeCarlo, Peter H Meckl, Chris Doktorcik, and Steve Pekarek. Hybrid model predictive power management of a fuel Cell-Battery vehicle, 2013.

[67] Richard T Meyer, Raymond A DeCarlo, and Steve Pekarek. Hybrid model predictive power management of a battery-supercapacitor electric vehicle. *Asian J. Control*, 18(1):150–165, January 2016.

[68] A Rabinowitz, F M Araghi, T Gaikwad, Z D Asher, and others. Development and evaluation of velocity predictive optimal energy management strategies in intelligent and connected hybrid electric vehicles. *Energies*, 2021.

[69] Other air pollution from transportation. *US Environmental Protection Agency*, 2015.

[70] International Energy Agency and International Energy Agency. CO2 emissions from fuel combustion 2016, 2016.

[71] World Health Organization. *World Health Statistics 2016: Monitoring Health for the SDGs Sustainable Development Goals*. World Health Organization, June 2016.

[72] A E Atabani, Irfan Anjum Badruddin, S Mekhilef, and A S Silitonga. A review on global fuel economy standards, labels and technologies in the transportation sector. *Renewable Sustainable Energy Rev.*, 15(9):4586–4610, December 2011.

[73] C M Martinez, X Hu, D Cao, E Velenis, B Gao, and M Wellers. Energy management in plug-in hybrid electric vehicles: Recent progress and a connected vehicles perspective. *IEEE Trans. Veh. Technol.*, 66(6):4534–4549, June 2017.

[74] S Uebel, N Murgovski, C Tempelhahn, and B Bäker. Optimal energy management and velocity control of hybrid electric vehicles. *IEEE Trans. Veh. Technol.*, 67(1):327–337, January 2018.

[75] Yugong Luo, Tao Chen, and Keqiang Li. Multi-objective decoupling algorithm for active distance control of intelligent hybrid electric vehicle. *Mech. Syst. Signal Process.*, 64-65:29–45, December 2015.

[76] Y Luo, T Chen, S Zhang, and K Li. Intelligent hybrid electric vehicle ACC with coordinated control of tracking ability, fuel economy, and ride comfort. *IEEE Trans. Intell. Transp. Syst.*, 16(4):2303–2308, August 2015.

[77] Q Wang and B Ayalew. A probabilistic framework for tracking the formation and evolution of Multi-Vehicle groups in public traffic in the presence of observation uncertainties. *IEEE Trans. Intell. Transp. Syst.*, 19(2):560–571, February 2018.

[78] Chan-Chiao Lin, Jun-Mo Kang, J.W. Grizzle, and Huei Peng. Energy management strategy for a parallel hybrid electric truck. In *Proceedings of the 2001 American Control Conference. (Cat. No.01CH37148)*, volume 4, pages 2878–2883 vol.4, 2001.

[79] Lorenzo Serrao, Simona Onori, and Giorgio Rizzoni. Ecms as a realization of pontryagin's minimum principle for hev control. In *2009 American Control Conference*, pages 3964–3969, 2009.

[80] Zachary D. Asher, David A. Trinko, Joshua D. Payne, Benjamin M. Geller, and Thomas H. Bradley. Real-time implementation of optimal energy management in hybrid electric vehicles: Globally optimal control of acceleration events. *Journal of Dynamic Systems, Measurement, and Control*, 142(8), 2020.

[81] Jinglai Wu, Jiageng Ruan, Nong Zhang, and Paul D. Walker. An optimized real-time energy management strategy for the power-split hybrid electric vehicles. *IEEE Transactions on Control Systems Technology*, 27(3):1194–1202, 2019.

[82] Cong Liang, Xing Xu, Feng Wang, and Zhiguang Zhou. Coordinated control strategy for mode transition of dm-phev based on mld. *Nonlinear Dynamics*, 103(1):809–832, 2021.

[83] Jordan A. Tunnell, Zachary D. Asher, Sudeep Pasricha, and Thomas H. Bradley. Towards improving vehicle fuel economy with adas. *SAE Technical Paper Series*, 2018.

[84] Zachary D. Asher, Amol A. Patil, Van T. Wifvat, Andrew A. Frank, Scott Samuelsen, and Thomas H. Bradley. Identification and review of the research gaps preventing a realization of optimal energy management strategies in vehicles. *SAE International Journal of Alternative Powertrains*, 8(2), 2019.

[85] David Baker, Zachary Asher, and Thomas Bradley. Investigation of vehicle speed prediction from neural network fit of real world driving data for improved engine on/off control of the ecocar3 hybrid camaro. *SAE Technical Paper Series*, 2017.

[86] David A. Trinko, Zachary D. Asher, and Thomas H. Bradley. Application of pre-computed acceleration event control to improve fuel economy in hybrid electric vehicles. *SAE Technical Paper Series*, 2018.

[87] Q Gong, Y Li, and Z Peng. Power management of plug-in hybrid electric vehicles using neural network based trip modeling. In *2009 American Control Conference*, pages 4601–4606, June 2009.

[88] Tushar Gaikwad, Aaron Rabinowitz, Farhang Motallebiaraghi, Thomas Bradley, Zachary Asher, Lowell Hanson, and Alvis Fong. Vehicle velocity prediction using artificial neural network and effect of real world signals on prediction window. Technical report, SAE Technical Paper, 2020.

[89] David Baker, Zachary D. Asher, and Thomas Bradley. V2v communication based real-world velocity predictions for improved hev fuel economy. *SAE Technical Paper Series*, 2018.

[90] Xuewei Qi, Yadan Luo, Guoyuan Wu, Kanok Boriboonsomsin, and Matthew Barth. Deep reinforcement learning enabled self-learning control for energy efficient driving. *Transportation Research Part C: Emerging Technologies*, 99:67–81, 2019.

[91] K Liu, Z Asher, X Gong, M Huang, and I Kolmanovsky. Vehicle velocity prediction and energy management strategy part 1: Deterministic and stochastic vehicle velocity prediction using machine learning. 2019.

[92] Aaron I Rabinowitz, Tushar Gaikwad, Samantha White, Thomas Bradley, and Zachary Asher. Infrastructure data streams for automotive machine learning algorithms research. Technical report, SAE Technical Paper, 2020.

[93] Andrew A Frank. Control method and apparatus for internal combustion engine electric hybrid vehicles, Apr 2000.

[94] Mohammad Reza Amini, Qiuhao Hu, Hao Wang, Yiheng Feng, Ilya Kolmanovsky, and Jing Sun. Experimental validation of eco-driving and eco-heating strategies for connected and automated hevs. *SAE Technical Paper Series*, 2021.

[95] Xun Gong, Jieyu Wang, Baolin Ma, Liang Lu, Yunfeng Hu, and Hong Chen. Real-time integrated power and thermal management of connected hevs based on hierarchical model predictive control. *IEEE/ASME Transactions on Mechatronics*, 26(3):1271–1282, 2021.

[96] Hao Wang, Mohammad Reza Amini, Qiuhao Hu, Ilya Kolmanovsky, and Jing Sun. Eco-cooling control strategy for automotive air-conditioning system: Design and experimental validation. *IEEE Transactions on Control Systems Technology*, page 1–12, 2020.

[97] J2735: Dedicated short range communications (DSRC) message set dictionary™ - SAE international. https://www.sae.org/standards/content/j2735_200911/. Accessed: 2021-6-14.

[98] Taxonomy and definitions for terms related to driving automation systems for on-road motor vehicles. 2018.

[99] Yuki Kajiwara Ryosuke Okuda and Kazuaki Terashima. A survey of technical trend of adas and autonomous driving. 2014.

[100] Christine Gschwendtner, Simon R. Sinsel, and Annegret Stephan. Vehicle-to-x (v2x) implementation: An overview of predominate trial configurations and technical, social and regulatory challenges. *Renewable and Sustainable Energy Reviews*, 145:110977, 2021.

[101] Cristian Musardo, Giorgio Rizzoni, Yann Guezennec, and Benedetto Staccia. A-ecms: An adaptive algorithm for hybrid electric vehicle energy management. *European Journal of Control*, 11(4):509–524, 2005.

[102] Chao Sun, Hongwen He, and Fengchun Sun. The role of velocity forecasting in adaptive-ecms for hybrid electric vehicles. *Energy Procedia*, 75:1907–1912, 2015.

[103] Weijing Shi, Mohamed Baker Alawieh, Xin Li, and Huafeng Yu. Algorithm and hardware implementation for visual perception system in autonomous vehicle: A survey. *Integration*, 59:148–156, 2017.

[104] Donald E Kirk. *Optimal Control Theory: An Introduction*. Courier Corporation, January 2004.

[105] Namwook Kim, Aymeric Rousseau, and Eric Rask. Autonomie model validation with test data for 2010 toyota prius. *SAE Technical Paper Series*, 2012.

[106] Downloadable dynamometer database: Argonne national laboratory.

[107] S Hochreiter and J Schmidhuber. Long short-term memory. *Neural Comput.*, 9(8):1735–1780, November 1997.

[108] Chris Nicholson. A beginner's guide to lstms and recurrent neural networks. https://pathmind.com/wiki/lstm.

[109] Farhang Motallebiaraghi, Kaisen Yao, Aaron Rabinowitz, Christopher Hoehne, Venu Garikapati, Jacob Holden, Eric Wood, Suren Chen, Zachary Asher, and Thomas Bradley. Mobility energy productivity evaluation of prediction-based vehicle powertrain control combined with optimal traffic management. Technical Report 2022-01-0141, SAE Technical Paper, March 2022.

[110] Energy efficient mobility systems FY 2020 annual progress report. https://www.energy.gov/eere/vehicles/articles/energy-efficient-mobility-systems-fy-2020-annual-progress-report. Accessed: 2021-10-7.

[111] U S Epa and OAR. Inventory of U.S. greenhouse gas emissions and sinks: 1990-2016. January 2018.

[112] Farhang Motallebiaraghi, Aaron Rabinowitz, Shantanu Jathar, Alvis Fong, Zachary Asher, and Thomas Bradley. High-fidelity modeling of light-duty vehicle emission and fuel economy using deep neural networks.

In *SAE Technical Paper Series*, number 2021-01-0181, 400 Commonwealth Drive, Warrendale, PA, United States, April 2021. SAE International.

[113] Yara Hazem Mahmoud, Nicholas E Brown, Farhang Motallebiaraghi, Melinda Koelling, Richard Meyer, Zachary D Asher, Assen Dontchev, and Ilya Kolmanovsky. Autonomous eco-driving with traffic light and lead vehicle constraints: An application of best constrained interpolation. *IFAC-PapersOnLine*, 54(10):45–50, 2021.

[114] Nick Goberville, Md Marsad Zoardar, Johan Rojas, Nicolas Brown, Farhang Motallebiaraghi, Anthony Navarro, and Zachary Asher. Techno-Economic analysis of Fixed-Route autonomous and electric shuttles. *SAE Technical Paper*, pages 01–0061, 2021.

[115] Gino Paganelli, Gabriele Ercole, Avra Brahma, Yann Guezennec, and Giorgio Rizzoni. General supervisory control policy for the energy optimization of charge-sustaining hybrid electric vehicles. *JSAE Review*, 22(4):511–518, October 2001.

[116] K Pandit, D Ghosal, H M Zhang, and others. Adaptive traffic signal control with vehicular ad hoc networks. *IEEE Transactions on*, 2013.

[117] N H Gartner, C Stamatiadis, and P J Tarnoff. Development of advanced traffic signal control strategies for intelligent transportation systems: Multilevel design. *Transp. Res. Rec.*, 1995.

[118] Muhammad Sameer Sheikh, Jun Liang, and Wensong Wang. An improved automatic traffic incident detection technique using a vehicle to infrastructure communication. *Journal of Advanced Transportation*, 2020, January 2020.

[119] T H Chang and J T Lin. Optimal signal timing for an oversaturated intersection. *Trans. Res. Part B: Methodol.*, 2000.

[120] He, Y., Rong, Y., Liu, Z., Du, S. Traffic influence degree of urban traffic emergency based on water wave principle. *Journal of Transportation Systems Engineering and Information Technology*, October 2017.

[121] Eum Han, Hwan Pil Lee, Sangmin Park, Jaehyun (jason) So, and Ilsoo Yun. Optimal signal control algorithm for signalized intersections under a V2I communication environment. *Journal of Advanced Transportation*, 2019, February 2019.

[122] Jiawen Wang, Jiayu Hang, and Xizhao Zhou. Signal timing optimization model for intersections in traffic incidents. *Journal of Advanced Transportation*, 2020, September 2020.

[123] Venu Garikapati, Stan Young, and Yi Hou. Measuring fundamental improvements in sustainable urban mobility: The Mobility-Energy productivity metric, 2019.

[124] Yi Hou, Venu Garikapati, Ambarish Nag, Stanley E Young, and Tom Grushka. Novel and practical method to quantify the quality of mobility: Mobility energy productivity metric. *Transp. Res. Rec.*, 2673(10):141–152, October 2019.

[125] Lulu Guo, Bingzhao Gao, Ying Gao, and Hong Chen. Optimal energy management for HEVs in Eco-Driving applications using Bi-Level MPC. *IEEE Trans. Intell. Transp. Syst.*, 18(8):2153–2162, August 2017.

[126] Ming Li, Xinkai Wu, Xiaozheng He, Guizhen Yu, and Yunpeng Wang. An eco-driving system for electric vehicles with signal control under V2X environment. *Transp. Res. Part C: Emerg. Technol.*, 93:335–350, August 2018.

[127] P Tulpule, V Marano, and G Rizzoni. Effect of traffic, road and weather information on PHEV energy management. 2011.

[128] Yiming He, Mashrur Chowdhury, Yongchang Ma, and Pierluigi Pisu. Merging mobility and energy vision with hybrid electric vehicles and vehicle infrastructure integration. *Energy Policy*, 41:599–609, February 2012.

[129] He Tian, Xu Wang, Ziwang Lu, Yong Huang, and Guangyu Tian. Adaptive fuzzy logic energy management strategy based on reasonable SOC reference curve for online control of plug-in hybrid electric city bus. *IEEE Trans. Intell. Transp. Syst.*, 19(5):1607–1617, May 2018.

[130] Y Shim and C Mollo. A reinforcement learning algorithm for speed optimization and optimal energy management of advanced driver assistance systems and connected vehicles. *SAE international journal of commercial vehicles*, 2021.

[131] Chao Sun, Xinwei Shen, and Scott Moura. Robust optimal ECO-driving control with uncertain traffic signal timing. In *2018 Annual American Control Conference (ACC)*, pages 5548–5553, June 2018.

[132] Rahmi Akçelik and Nagui M Rouphail. Overflow queues and delays with random and platooned arrivals at signalized intersections. *J. Adv. Transp.*, 28(3):227–251, September 1994.

[133] R Akcelik. Extension of the highway capacity manual progression factor method for platooned arrivals. 1995.

[134] Richard Cowan. An improved model for signalised intersections with vehicle-actuated control. *J. Appl. Probab.*, 15(2):384–396, June 1978.

[135] National household travel survey. https://nhts.ornl.gov/. Accessed: 2021-10-12.

[136] F Motallebiaraghi, A Rabinowitz, J Holden, and others. High-Fidelity modeling of Light-Duty vehicle emission and fuel economy using deep neural networks. *SAE Technical*, 2021.

[137] Yanxia Zhang, Haikun Wang, Sai Liang, Ming Xu, Qiang Zhang, Hongyan Zhao, and Jun Bi. A dual strategy for controlling energy consumption and air pollution in china's metropolis of beijing. *Energy*, 81:294–303, March 2015.

[138] World Health Organization. *World Health Statistics 2019: Monitoring Health for the Sdgs, Sustainable Development Goals*. World Health Organization, June 2019.

[139] Federal vehicle standards | center for climate and energy solutions. https://www.c2es.org/content/regulating-transportation-sector-carbon-emissions/, April 2020. Accessed: 2020-6-17.

[140] H Christopher Frey, Kaishan Zhang, and Nagui M Rouphail. Fuel use and emissions comparisons for alternative routes, time of day, road grade, and vehicles based on in-use measurements. *Environ. Sci. Technol.*, 42(7):2483–2489, April 2008.

[141] U S Epa and OAR. Latest version of MOtor vehicle emission simulator (MOVES). May 2016.

[142] Harikishan Perugu. Emission modelling of light-duty vehicles in india using the revamped VSP-based MOVES model: The case study of hyderabad. *Transp. Res. Part D: Trans. Environ.*, 68:150–163, March 2019.

[143] H M Abdul Aziz, H M Abdul Aziz, and Satish V Ukkusuri. A novel approach to estimate emissions from large transportation networks: Hierarchical clustering-based link-driving-schedules for EPA-MOVES using dynamic time warping measures, 2018.

[144] Aaron Brooker, Jeffrey Gonder, Lijuan Wang, Eric Wood, Sean Lopp, and Laurie Ramroth. FASTSim: A model to estimate vehicle efficiency, cost and performance. Technical report, SAE Technical Paper, 2015.

[145] Qiuming Gong, Yaoyu Li, and Zhongren Peng. Power management of plug-in hybrid electric vehicles using neural network based trip modeling. In *2009 American Control Conference*, pages 4601–4606, June 2009.

[146] Tushar Gaikwad, Aaron Rabinowitz, Farhang Motallebiaraghi, Thomas Bradley, Zachary Asher, Alvis Fong, and Rick Meyer. Vehicle velocity prediction using artificial neural network and effect of real world signals on prediction window. Technical Report 2020-01-0729, SAE Technical Paper, April 2020.

[147] P J Shayler, M Goodman, and T Ma. The exploitation of neural networks in automotive engine management systems. *Eng. Appl. Artif. Intell.*, 13(2):147–157, April 2000.

[148] Viktor Rausch, Andreas Hansen, Eugen Solowjow, Chang Liu, Edwin Kreuzer, and J Karl Hedrick. Learning a deep neural net policy for end-to-end control of autonomous vehicles. In *2017 American Control Conference (ACC)*, pages 4914–4919, May 2017.

[149] S Lange, F Ulbrich, and D Goehring. Online vehicle detection using deep neural networks and lidar based preselected image patches. In *2016 IEEE Intelligent Vehicles Symposium (IV)*, pages 954–959, June 2016.

[150] Chenxi Ding, Wuhong Wang, Xiao Wang, and Martin Baumann. A neural network model for driver's Lane-Changing trajectory prediction in urban traffic flow, 2013.

[151] Asif Raza and Ming Zhong. An optimized hybrid Lane-Based Short-Term urban traffic forecasting using artificial neural network and locally weighted regression models, 2018.

[152] G J Thompson, C M Atkinson, N N Clark, T W Long, and E Hanzevack. Technical note: Neural network modelling of the emissions and performance of a heavy-duty diesel engine. *Proc. Inst. Mech. Eng. Pt. D: J. Automobile Eng.*, 214(2):111–126, February 2000.

[153] J M Alonso, F Alvarruiz, J M Desantes, L Hernandez, V Hernandez, and G Molto. Combining neural networks and genetic algorithms to predict and reduce diesel engine emissions. *IEEE Trans. Evol. Comput.*, 11(1):46–55, February 2007.

[154] G Najafi, B Ghobadian, T Tavakoli, D R Buttsworth, T F Yusaf, and M Faizollahnejad. Performance and exhaust emissions of a gasoline engine with ethanol blended gasoline fuels using artificial neural network. *Appl. Energy*, 86(5):630–639, May 2009.

[155] Zachary D Asher, Abril A Galang, Will Briggs, Brian Johnston, Thomas H Bradley, and Shantanu Jathar. Economic and efficient hybrid vehicle fuel economy and emissions modeling using an artificial neural network. 2018.

[156] Oludare Isaac Abiodun, Aman Jantan, Abiodun Esther Omolara, Kemi Victoria Dada, Nachaat Abdelatif Mohamed, and Humaira Arshad. State-of-the-art in artificial neural network applications: A survey. *Heliyon*, 4(11):e00938, November 2018.

[157] RDE PEMS real driving emissions portable emissions measurement systems - micro-PEMS, nano-PEMS. https://www.globalmrv.com/pems-axionrs-2, February 2019. Accessed: 2021-8-13.

[158] H Christopher Frey, Kaishan Zhang, and Nagui M Rouphail. Vehicle-specific emissions modeling based upon on-road measurements. *Environ. Sci. Technol.*, 44(9):3594–3600, May 2010.

[159] Morgan Maynard. *Neural Networks: Introduction to Artificial Neurons, Backpropagation and Multilayer Feedforward Neural Networks with Real-World Applications*. Independently Published, May 2020.

[160] Alex Graves and Jürgen Schmidhuber. Framewise phoneme classification with bidirectional LSTM and other neural network architectures, 2005.

[161] D Mandic and Jonathon Chambers. *Recurrent neural networks for prediction: learning algorithms, architectures and stability*. Wiley, Chichester, August 2001.

[162] U S Epa and OAR. MOVES and other mobile source emissions models. February 2016.

[163] U S Usepa. Environmental protection agency (2014). user guide for MOVES2014. EPA report. Technical report, EPA-420-B-14-055. Office of Transportation and Air Quality, 2014.

[164] Mohamadreza Farzaneh, Gokhan Memisoglu, and Kiavash Kianfar. Optimal deployment of emission reduction technologies for large fleets, 2012.

[165] Josh Patterson and Adam Gibson. *Deep Learning: A Practitioner's Approach*. "O'Reilly Media, Inc.", July 2017.

[166] Farhang Motallebi Araghi, Aaron Rabinwoitz, Chon Chia Ang, Sachin Sharma, Parth Kadav, Richard T. Meyer, Thomas Bradley, Zachary D. Asher. Identifying and assessing research gaps for energy efficient control of electrified autonomous vehicle Eco-Driving. In Sudeep Pasricha Vipin Kumar Kukkala, editor, *Machine Learning and Optimization Techniques for Automotive Cyber-Physical Systems*. Springer, July 2023.

[167] Norbert Mundorf, Colleen A Redding, and Songtao Bao. Sustainable transportation and health. *Int. J. Environ. Res. Public Health*, 15(3), March 2018.

[168] Aaron Rabinowitz, Farhang Motallebi Araghi, Tushar Gaikwad, Zachary D Asher, and Thomas H Bradley. Development and evaluation of velocity predictive optimal energy management strategies in intelligent and connected hybrid electric vehicles. *Energies*, 14(18):5713, September 2021.

[169] Electric vehicle benefits and considerations. https://afdc.energy.gov/fuels/electricity_benefits.html. Accessed: 2022-5-17.

[170] Heejung Jung. Fuel economy of Plug-In hybrid electric and hybrid electric vehicles: Effects of vehicle weight, hybridization ratio and ambient temperature. *World Electric Vehicle Journal*, 11(2):31, March 2020.

[171] Probhas Bose and Dipak Kumar Mandal. The future has arrived, are we ready for EV? *IOP Conf. Ser.: Mater. Sci. Eng.*, 1080(1):012004, February 2021.

[172] Matteo Muratori, Marcus Alexander, Doug Arent, Morgan Bazilian, Pierpaolo Cazzola, Ercan M Dede, John Farrell, Chris Gearhart, David Greene, Alan Jenn, Matthew Keyser, Timothy Lipman, Sreekant Narumanchi, Ahmad Pesaran, Ramteen Sioshansi, Emilia Suomalainen, Gil Tal, Kevin Walkowicz, and

Jacob Ward. The rise of electric vehicles—2020 status and future expectations. *Prog. Energy Combust. Sci.*, 3(2):022002, March 2021.

[173] Salma Ahmad, Mohd Khan, and Others. Tesla: Disruptor or sustaining innovator. *Journal of Case Research*, 10(1), 2019.

[174] Arvid Linde. *Electric Cars – The Future is Now!* Veloce Publishing Ltd, 2010.

[175] Yan Zhou, Michael Wang, Han Hao, Larry Johnson, Hewu Wang, and Han Hao. Plug-in electric vehicle market penetration and incentives: a global review. *Mitig. Adapt. Strateg. Glob. Chang.*, 20(5):777–795, June 2015.

[176] Iqbal Husain. *Electric and Hybrid Vehicles: Design Fundamentals, Second Edition*. CRC Press, June 2011.

[177] Council on Future Mobility & Electrification. 2020 report. Technical Report 1, Michigan Office of Future Mobility and Electrification, March 2020.

[178] Wards Auto. Powering up electric vehicles key part of michigan future plans, October 2020.

[179] Ingrid Malmgren. Quantifying the societal benefits of electric vehicles. *World Electric Vehicle Journal*, 8(4):996–1007, December 2016.

[180] Albert G Boulanger, Andrew C Chu, Suzanne Maxx, and David L Waltz. Vehicle electrification: Status and issues. *Proc. IEEE*, 99(6):1116–1138, June 2011.

[181] Oscar Mauricio Forero Camacho, Per Bromand Norgard, Ningling Rao, and Lucian Mihet-Popa. Electrical vehicle batteries testing in a distribution network using sustainable energy, 2014.

[182] Oscar Mauricio Forero Camacho and Lucian Mihet-Popa. Fast charging and smart charging tests for electric vehicles batteries using renewable energy. *Oil & Gas Science and Technology – Revue d'IFP Energies nouvelles*, 71(1):13, 2016.

[183] Fuad Un-Noor, Sanjeevikumar Padmanaban, Lucian Mihet-Popa, Mohammad Nurunnabi Mollah, and Eklas Hossain. A comprehensive study of key electric vehicle (EV) components, technologies, challenges, impacts, and future direction of development. *Energies*, 10(8):1217, August 2017.

[184] Chan-Chiao Lin, Huei Peng, J W Grizzle, and Jun-Mo Kang. Power management strategy for a parallel hybrid electric truck. *IEEE Trans. Control Syst. Technol.*, 11(6):839–849, November 2003.

[185] Guang Wu, Xing Zhang, and Zuomin Dong. Powertrain architectures of electrified vehicles: Review, classification and comparison. *J. Franklin Inst.*, 352(2):425–448, February 2015.

[186] Nadine Rauh, Thomas Franke, and Josef F Krems. Understanding the impact of electric vehicle driving experience on range anxiety. *Hum. Factors*, 57(1):177–187, February 2015.

[187] Z D Asher, V Wifvat, A Navarro, S Samuelsen, and T Bradley. The importance of HEV fuel economy and two research gaps preventing real world implementation of optimal energy management. 2017.

[188] Zachary D Asher, Amol A Patil, Van T Wifvat, Andrew A Frank, Scott Samuelsen, and Thomas H Bradley. Identification and review of the research gaps preventing a realization of optimal energy management strategies in vehicles. *SAE Int. J. Alt. Power.*, 8(2), November 2019.

[189] Xiangrui Zeng and Junmin Wang. A two-level stochastic approach to optimize the energy management strategy for fixed-route hybrid electric vehicles. *Mechatronics*, 38:93–102, September 2016.

[190] D L Hibberd, A H Jamson, and S L Jamson. The design of an in-vehicle assistance system to support eco-driving. *Transp. Res. Part C: Emerg. Technol.*, 58:732–748, September 2015.

[191] Min Zhou, Hui Jin, and Wenshuo Wang. A review of vehicle fuel consumption models to evaluate eco-driving and eco-routing. *Transp. Res. Part D: Trans. Environ.*, 49:203–218, December 2016.

[192] Aishwarya Panday and Hari Om Bansal. A review of optimal energy management strategies for hybrid electric vehicle. *Int. J. Veh. Technol.*, 2014:1–19, November 2014.

[193] Shaik Amjad, S Neelakrishnan, and R Rudramoorthy. Review of design considerations and technological challenges for successful development and deployment of plug-in hybrid electric vehicles. *Renewable Sustainable Energy Rev.*, 14(3):1104–1110, April 2010.

[194] Fengqi Zhang, Lihua Wang, Serdar Coskun, Hui Pang, Yahui Cui, and Junqiang Xi. Energy management strategies for hybrid electric vehicles: Review, classification, comparison, and outlook. *Energies*, 13(13):3352, June 2020.

[195] Chao Yang, Mingjun Zha, Weida Wang, Kaijia Liu, and Changle Xiang. Efficient energy management strategy for hybrid electric vehicles/plug-in hybrid electric vehicles: review and recent advances under intelligent transportation system. *IET Intel. Transport Syst.*, March 2020.

[196] Fengqi Zhang, Xiaosong Hu, Reza Langari, and Dongpu Cao. Energy management strategies of connected HEVs and PHEVs: Recent progress and outlook. *Prog. Energy Combust. Sci.*, 73:235–256, July 2019.

[197] Z D Asher, D A Baker, and T H Bradley. Prediction error applied to hybrid electric vehicle optimal fuel economy. *IEEE Trans. Control Syst. Technol.*, 2017.

[198] N Sulaiman, M A Hannan, A Mohamed, E H Majlan, and W R Wan Daud. A review on energy management system for fuel cell hybrid electric vehicle: Issues and challenges. *Renewable Sustainable Energy Rev.*, 52:802–814, December 2015.

[199] Andrew F Burke and Gene E Smith. Impacts of use-pattern on the design of electric and hybrid vehicles. In *SAE Technical Paper Series*, number 810265, 400 Commonwealth Drive, Warrendale, PA, United States, February 1981. SAE International.

[200] Harpreetsingh Banvait, Sohel Anwar, and Yaobin Chen. A rule-based energy management strategy for plug-in hybrid electric vehicle (PHEV). In *2009 American Control Conference*, pages 3938–3943, June 2009.

[201] Yongpeng Shen, Gaorui Ge, Ankang Liu, and Zhufeng Zheng. Operation of an ICE/PM/TTRB APU in a range extender electric vehicle Power-Train. In *2019 IEEE Innovative Smart Grid Technologies - Asia (ISGT Asia)*, pages 3205–3210, May 2019.

[202] A A Frank and A Francisco. Ideal operating line CVT shifting strategy for hybrid electric vehicles. Technical report, July 2002.

[203] Qi Li, Weirong Chen, Yankun Li, Shukui Liu, and Jin Huang. Energy management strategy for fuel cell/battery/ultracapacitor hybrid vehicle based on fuzzy logic. *Int. J. Electr. Power Energy Syst.*, 43(1):514–525, December 2012.

[204] Li Jun, Zou Faming, Tu Xiong, Liu Biao, and Wang Wenbin. Simulation research on PHEV based on fuzzy logic control strategies. *Journal of Chongqing Jiao Tong University (Natural Science)*, 32(2):329–333, 2013.

[205] Mohamad Faizrizwan Mohd Sabri, Kumeresan A Danapalasingam, and Mohd Fua'ad Rahmat. Improved fuel economy of Through-the-Road hybrid electric vehicle with fuzzy Logic-Based energy management strategy. *Int. J. Fuzzy Syst.*, 20(8):2677–2692, December 2018.

[206] Nicolas Denis, Maxime R Dubois, and Alain Desrochers. Fuzzy-based blended control for the energy management of a parallel plug-in hybrid electric vehicle. *IET Intel. Transport Syst.*, 9(1):30–37, February 2015.

[207] Ping Li, Yang Li, Yuying Wang, and Xiaohong Jiao. An intelligent logic Rule-Based energy management strategy for Power-Split plug-in hybrid electric vehicle. In *2018 37th Chinese Control Conference (CCC)*, pages 7668–7672, July 2018.

[208] Richard T Meyer. Distributed switched optimal control of an electric vehicle. *Energies*, 13(13):3364, July 2020.

[209] M Abotabik and R T Meyer. Switched optimal control of a Heavy-Duty hybrid vehicle. *Energies*, 2021.

[210] Jichao Liu, Yangzhou Chen, Wei Li, Fei Shang, and Jingyuan Zhan. Hybrid-Trip-Model-Based energy management of a PHEV with Computation-Optimized dynamic programming. *IEEE Trans. Veh. Technol.*, 67(1):338–353, January 2018.

[211] Chan-Chiao Lin, Jun-Mo Kang, J W Grizzle, and Huei Peng. Energy management strategy for a parallel hybrid electric truck, 2001.

[212] R Bellman. Dynamic programming. *Science*, 153(3731):34–37, July 1966.

[213] G Rousseau, D Sinoquet, and P Rouchon. Constrained optimization of energy management for a Mild-Hybrid vehicle. *Oil & Gas Science and Technology - Revue de l'IFP*, 62(4):623–634, 2007.

[214] X Wei, L Guzzella, V I Utkin, and G Rizzoni. Model-Based fuel optimal control of hybrid electric vehicle using variable structure control systems, 2007.

[215] Lorenzo Serrao and Giorgio Rizzoni. Optimal control of power split for a hybrid electric refuse vehicle. In *2008 American Control Conference*, pages 4498–4503, June 2008.

[216] Yongchang Du, Yue Zhao, Qinpu Wang, Yuanbo Zhang, and Huaicheng Xia. Trip-oriented stochastic optimal energy management strategy for plug-in hybrid electric bus. *Energy*, 115:1259–1271, November 2016.

[217] Binhao Liu, Liang Li, Xiangyu Wang, and Shuo Cheng. Hybrid electric vehicle downshifting strategy based on stochastic dynamic programming during regenerative braking process. *IEEE Trans. Veh. Technol.*, 67(6):4716–4727, June 2018.

[218] Thomas Leroy, Jérémy Malaizé, and Gilles Corde. Towards real-time optimal energy management of HEV powertrains using stochastic dynamic programming. In *2012 IEEE Vehicle Power and Propulsion Conference*, pages 383–388. ieeexplore.ieee.org, October 2012.

[219] Xueqin Lü, Yinbo Wu, Jie Lian, Yangyang Zhang, Chao Chen, Peisong Wang, and Lingzheng Meng. Energy management of hybrid electric vehicles: A review of energy optimization of fuel cell hybrid power system based on genetic algorithm. *Energy Convers. Manage.*, 205:112474, February 2020.

[220] Maciej Wieczorek and Mirosław Lewandowski. A mathematical representation of an energy management strategy for hybrid energy storage system in electric vehicle and real time optimization using a genetic algorithm. *Appl. Energy*, 192:222–233, April 2017.

[221] Zeyu Chen, Rui Xiong, Kunyu Wang, and Bin Jiao. Optimal energy management strategy of a plug-in hybrid electric vehicle based on a particle swarm optimization algorithm. *Energies*, 8(5):3661–3678, April 2015.

[222] Zeyu Chen, Rui Xiong, and Jiayi Cao. Particle swarm optimization-based optimal power management of plug-in hybrid electric vehicles considering uncertain driving conditions. *Energy*, 96:197–208, February 2016.

[223] A Rezaei, J B Burl, and B Zhou. Estimation of the ECMS equivalent factor bounds for hybrid electric vehicles. *IEEE Trans. Control Syst. Technol.*, 2017.

[224] Yuanjian Zhang, Liang Chu, Zicheng Fu, Chong Guo, Di Zhao, Yukuan Li, Yang Ou, and Lei Xu. An improved adaptive equivalent consumption minimization strategy for parallel plug-in hybrid electric vehicle. *Proc. Inst. Mech. Eng. Pt. D: J. Automobile Eng.*, 233(6):1649–1663, May 2019.

[225] Z Chen, Y Liu, M Ye, Y Zhang, Z Chen, and G Li. A survey on key techniques and development perspectives of equivalent consumption minimisation strategy for hybrid electric vehicles. *Renewable Sustainable Energy Rev.*, 151:111607, November 2021.

[226] Zachary D Asher, David A Trinko, Joshua D Payne, Benjamin M Geller, and Thomas H Bradley. Real-Time implementation of optimal energy management in hybrid electric vehicles: Globally optimal control of acceleration events. *J. Dyn. Syst. Meas. Control*, 142(8), August 2020.

[227] Shaobo Xie, Xiaosong Hu, Shanwei Qi, Xiaolin Tang, Kun Lang, Zongke Xin, and James Brighton. Model predictive energy management for plug-in hybrid electric vehicles considering optimal battery depth of discharge. *Energy*, 173:667–678, April 2019.

[228] Richard T Meyer, Raymond A DeCarlo, and Steve Pekarek. Hybrid model predictive power management of a battery-supercapacitor electric vehicle. *Asian J. Control*, 18(1):150–165, January 2016.

[229] R T Meyer, R A DeCarlo, and S Pekarek. Hybrid model predictive power management of a battery-supercapacitor electric vehicle. *Asian J. Control*, 2016.

[230] Richard T Meyer, Scott C Johnson, Raymond A DeCarlo, Steve Pekarek, and Scott D Sudhoff. Hybrid electric vehicle fault tolerant control. *J. Dyn. Syst. Meas. Control*, 140(2), September 2017.

[231] Dimitri P Bertsekas. *Dynamic Programming and Optimal Control*. Athena Scientific, 1995.

[232] Kris Braekers, Katrien Ramaekers, and Inneke Van Nieuwenhuyse. The vehicle routing problem: State of the art classification and review. *Comput. Ind. Eng.*, 99:300–313, September 2016.

[233] E W Dijkstra. A note on two problems in connexion with graphs. *Numer. Math.*, 1(1):269–271, December 1959.

[234] Eva Ericsson, Hanna Larsson, and Karin Brundell-Freij. Optimizing route choice for lowest fuel consumption–potential effects of a new driver support tool. *Transp. Res. Part C: Emerg. Technol.*, 14(6):369–383, 2006.

[235] Kanok Boriboonsomsin, Matthew J Barth, Weihua Zhu, and Alexander Vu. Eco-Routing navigation system based on multisource historical and Real-Time traffic information. *IEEE Trans. Intell. Transp. Syst.*, 13(4):1694–1704, December 2012.

[236] Lei Zhu and Yi-Chang Chiu. Transportation routing map abstraction approach: Algorithm and numerical analysis. *Transp. Res. Rec.*, 2528(1):78–85, January 2015.

[237] Lei Zhu. *Routing map topology analysis and application.* PhD thesis, 2014.

[238] Matthew Barth, Kanok Boriboonsomsin, and Alex Vu. Environmentally-Friendly navigation. In *2007 IEEE Intelligent Transportation Systems Conference*, pages 684–689, September 2007.

[239] Ove Andersen, Christian S Jensen, Kristian Torp, and Bin Yang. EcoTour: Reducing the environmental footprint of vehicles using eco-routes. In *2013 IEEE 14th International Conference on Mobile Data Management*, volume 1, pages 338–340, June 2013.

[240] Bin Yang, Chenjuan Guo, Christian S Jensen, Manohar Kaul, and Shuo Shang. Stochastic skyline route planning under time-varying uncertainty. In *2014 IEEE 30th International Conference on Data Engineering*, pages 136–147, March 2014.

[241] Jacopo Guanetti, Yeojun Kim, and Francesco Borrelli. Control of connected and automated vehicles: State of the art and future challenges. *Annu. Rev. Control*, 45:18–40, January 2018.

[242] Matej Kubicka, Jan Klusacek, Antonio Sciarretta, Arben Cela, Hugues Mounier, Laurent Thibault, and S I Niculescu. Performance of current eco-routing methods, 2016.

[243] Tomas Jurik, Arben Cela, Redha Hamouche, Rene Natowicz, Abdellatif Reama, Silviu-Iulian Niculescu, and Jerome Julien. Energy optimal Real-Time navigation system, 2014.

[244] Zhonghao Sun and Xingshe Zhou. To save money or to save time: Intelligent routing design for plug-in hybrid electric vehicle. *Transp. Res. Part D: Trans. Environ.*, 43:238–250, March 2016.

[245] Zhiqian Qiao and Orkun Karabasoglu. Vehicle powertrain connected route optimization for conventional, hybrid and plug-in electric vehicles. December 2016.

[246] Giovanni De Nunzio, Antonio Sciarretta, Ibtihel Ben Gharbia, and Luis Leon Ojeda. A constrained Eco-Routing strategy for hybrid electric vehicles based on Semi-Analytical energy management. In *2018 21st International Conference on Intelligent Transportation Systems (ITSC)*, pages 355–361, November 2018.

[247] Arian Houshmand and Christos G Cassandras. Eco-Routing of Plug-In hybrid electric vehicles in transportation networks. In *2018 21st International Conference on Intelligent Transportation Systems (ITSC)*, pages 1508–1513, November 2018.

[248] Zachary D Asher, David A Trinko, and Thomas H Bradley. Increasing the fuel economy of connected and autonomous Lithium-Ion electrified vehicles. In Gianfranco Pistoia and Boryann Liaw, editors, *Behaviour of Lithium-Ion Batteries in Electric Vehicles: Battery Health, Performance, Safety, and Cost*, pages 129–151. Springer International Publishing, Cham, 2018.

[249] Pierre Michel, Dominik Karbowski, and Aymeric Rousseau. Impact of connectivity and automation on vehicle energy use. Technical report, SAE Technical Paper, 2016.

[250] S Mandava, K Boriboonsomsin, and M Barth. Arterial velocity planning based on traffic signal information under light traffic conditions. In *2009 12th International IEEE Conference on Intelligent Transportation Systems*, pages 1–6. ieeexplore.ieee.org, October 2009.

[251] J Potvin-Bernal, B Hansma, B Donmez, P Lockwood, and L H Shu. Influencing greater adoption of Eco-Driving practices using an associative graphical display. *J. Mech. Des.*, 142(3), January 2020.

[252] Fengqi Zhang, Xiaosong Hu, Reza Langari, and Dongpu Cao. Energy management strategies of connected HEVs and PHEVs: Recent progress and outlook. *Prog. Energy Combust. Sci.*, 73:235–256, July 2019.

[253] Katherine R Davis, Charles M Davis, Saman A Zonouz, Rakesh B Bobba, Robin Berthier, Luis Garcia, and Peter W Sauer. A Cyber-Physical modeling and assessment framework for power grid infrastructures. *IEEE Trans. Smart Grid*, 6(5):2464–2475, September 2015.

[254] Ragunathan Rajkumar, Insup Lee, Lui Sha, and John Stankovic. Cyber-physical systems: The next computing revolution. In *Design Automation Conference*, pages 731–736. ieeexplore.ieee.org, June 2010.

[255] Jairo Giraldo, Esha Sarkar, Alvaro A Cardenas, Michail Maniatakos, and Murat Kantarcioglu. Security and privacy in Cyber-Physical systems: A survey of surveys. *IEEE Design Test*, 34(4):7–17, August 2017.

[256] Christof Ebert and Capers Jones. Embedded software: Facts, figures, and future. *Computer*, 42(4):42–52, April 2009.

[257] Anupam Chattopadhyay and Kwok-Yan Lam. Security of autonomous vehicle as a cyber-physical system. In *2017 7th International Symposium on Embedded Computing and System Design (ISED)*, pages 1–6. ieeexplore.ieee.org, December 2017.

[258] Baiyu Chen, Zhengyu Yang, Siyu Huang, Xianzhi Du, Zhiwei Cui, Janki Bhimani, Xin Xie, and Ningfang Mi. Cyber-physical system enabled nearby traffic flow modelling for autonomous vehicles. In *2017 IEEE 36th International Performance Computing and Communications Conference (IPCCC)*, pages 1–6. ieeexplore.ieee.org, December 2017.

[259] Hassan Abid, Luong Thi Thu Phuong, Jin Wang, Sungyoung Lee, and Saad Qaisar. V-Cloud: vehicular cyber-physical systems and cloud computing. In *Proceedings of the 4th International Symposium on Applied Sciences in Biomedical and Communication Technologies*, number Article 165 in ISABEL '11, pages 1–5, New York, NY, USA, October 2011. Association for Computing Machinery.

[260] Corey D Harper, Chris T Hendrickson, Sonia Mangones, and Constantine Samaras. Estimating potential increases in travel with autonomous vehicles for the non-driving, elderly and people with travel-restrictive medical conditions. *Transp. Res. Part C: Emerg. Technol.*, 72:1–9, November 2016.

[261] Aniruddh Mohan, Shashank Sripad, Parth Vaishnav, and Venkatasubramanian Viswanathan. Trade-offs between automation and light vehicle electrification. *Nature Energy*, June 2020.

[262] Nicholas A Goberville, Parth Kadav, and Zachary D Asher. Tire track identification: A method for drivable region detection in conditions of Snow-Occluded lane lines. Technical report, SAE Technical Paper, 2022.

[263] Karen A Robinson, Ian J Saldanha, and Naomi A Mckoy. Development of a framework to identify research gaps from systematic reviews, 2011.

[264] Francisca Rosique, Pedro J Navarro, Carlos Fernández, and Antonio Padilla. A systematic review of perception system and simulators for autonomous vehicles research. *Sensors*, 19(3), February 2019.

[265] Brian Paden, Michal Čáp, Sze Zheng Yong, Dmitry Yershov, and Emilio Frazzoli. A survey of motion planning and control techniques for Self-Driving urban vehicles. *IEEE Transactions on Intelligent Vehicles*, 1(1):33–55, March 2016.

[266] Xiaohui Li, Zhenping Sun, Dongpu Cao, Zhen He, and Qi Zhu. Real-Time trajectory planning for autonomous urban driving: Framework, algorithms, and verifications. *IEEE/ASME Trans. Mechatron.*, 21(2):740–753, April 2016.

[267] John C Mankins. Technology readiness assessments: A retrospective. *Acta Astronaut.*, 65(9):1216–1223, November 2009.

[268] Robert Shishko. Optimizing technology investments: A broad mission model approach. In *AIAA Space 2003 Conference & Exposition*, AIAA SPACE Forum. American Institute of Aeronautics and Astronautics, September 2003.

[269] Xianfeng Terry Yang, Ke Huang, Zhehao Zhang, Zhao Alan Zhang, and Fang Lin. Eco-Driving system for connected automated vehicles: Multi-Objective trajectory optimization. *IEEE Trans. Intell. Transp. Syst.*, 22(12):7837–7849, December 2021.

[270] Zhengwei Bai, Peng Hao, Wei Shangguan, Baigen Cai, and Matthew J Barth. Hybrid reinforcement Learning-Based Eco-Driving strategy for connected and automated vehicles at signalized intersections. January 2022.

[271] J Fleming, X Yan, C Allison, N Stanton, and others. Real-time predictive eco-driving assistance considering road geometry and long-range radar measurements. *IET Intel. Transport Syst.*, 2021.

[272] Chao Sun, Jacopo Guanetti, Francesco Borrelli, and Scott J. Moura. Optimal eco-driving control of connected and autonomous vehicles through signalized intersections. *IEEE Internet of Things Journal*, 7(5):3759–3773, 2020.

[273] Sangjae Bae, Yongkeun Choi, Yeojun Kim, Jacopo Guanetti, Francesco Borrelli, and Scott J. Moura. Real-time ecological velocity planning for plug-in hybrid vehicles with partial communication to traffic lights. *CoRR*, abs/1903.08784, 2019.

[274] Balazs Nemeth, András Mihály, and Péter Gáspár. Design of fault-tolerant cruise control in a hierarchical framework for connected automated vehicles. pages 1–6, 09 2021.

[275] Abhishek Jandial, Pierre Merdrignac, Oyunchimeg Shagdar, and Laurent Fevrier. Implementation and evaluation of intelligent roadside infrastructure for automated vehicle with i2v communication. In Anis Laouiti, Amir Qayyum, and Mohamad Naufal Mohamad Saad, editors, *Vehicular Ad-hoc Networks for Smart Cities*, pages 3–18, Singapore, 2020. Springer Singapore.

[276] Jorge Vargas, Suleiman Alsweiss, Onur Toker, Rahul Razdan, and Joshua Santos. An overview of autonomous vehicles sensors and their vulnerability to weather conditions. *Sensors*, 21(16), August 2021.

[277] Ekim Yurtsever, Jacob Lambert, Alexander Carballo, and Kazuya Takeda. A survey of autonomous driving: Common practices and emerging technologies. *CoRR*, abs/1906.05113, 2019.

[278] Shreshta Rajakumar Deshpande, Shobhit Gupta, Abhishek Gupta, and Marcello Canova. Real-Time Eco-driving Control in Electrified Connected and Autonomous Vehicles Using Approximate Dynamic Programming. *Journal of Dynamic Systems, Measurement, and Control*, 144(1), 01 2022. 011111.

[279] Lei Kang, Bozhao Qi, Dan Janecek, and Suman Banerjee. Ecodrive: A mobile sensing and control system for fuel efficient driving. In *Proceedings of the 21st Annual International Conference on Mobile Computing and Networking*, MobiCom '15, page 358–371, New York, NY, USA, 2015. Association for Computing Machinery.

[280] Raj Rajkumar, Junfeng Zhao, Chen Fang Chang, and Jeffrey Gonder. Corroborative evaluation of the real-world energy saving potentials of inforich eco-autonomous driving (iread) system. 4 2020.

[281] Jongryeol Jeong, Dominik Karbowski, Namdoo Kim, Jihun Han, Kevin Stutenberg, Miriam Di Russo, and Julien Grave. Vehicle-in-the-loop workflow for the evaluation of energy-efficient automated driving controls in real vehicles. Technical report, 2022.

[282] Technical report.

[283] Jiaqi Ma, Jia Hu, Ed Leslie, Fang Zhou, Peter Huang, and Joe Bared. An eco-drive experiment on rolling terrains for fuel consumption optimization with connected automated vehicles. *Transportation Research Part C: Emerging Technologies*, 100:125–141, 2019.

[284] Sangjae Bae, Yeojun Kim, Yongkeun Choi, Jacopo Guanetti, Preet Gill, Francesco Borrelli, and Scott J. Moura. Ecological Adaptive Cruise Control of Plug-In Hybrid Electric Vehicle With Connected Infrastructure and On-Road Experiments. *Journal of Dynamic Systems, Measurement, and Control*, 144(1), 01 2022. 011109.

[285] Ziran Wang, Yuan-Pu Hsu, Alexander Vu, Francisco Caballero, Peng Hao, Guoyuan Wu, Kanok Boriboonsomsin, Matthew J Barth, Aravind Kailas, Pascal Amar, Eddie Garmon, and Sandeep Tanugula. Early findings from field trials of Heavy-Duty truck connected Eco-Driving system. In *2019 IEEE Intelligent Transportation Systems Conference (ITSC)*, pages 3037–3042, October 2019.

[286] Mohammad Reza Amini, Qiuhao Hu, Hao Wang, Yiheng Feng, Ilya Kolmanovsky, and Jing Sun. Experimental Validation of Eco-Driving and Eco-Heating Strategies for Connected and Automated HEVs. pages 2021–01–0435, April 2021.

[287] Zhen Yang, Yiheng Feng, Xun Gong, Ding Zhao, and Jing Sun. Eco-Trajectory planning with consideration of queue along congested corridor for hybrid electric vehicles. *Transp. Res. Rec.*, 2673(9):277–286, September 2019.

[288] Samantha White. *Physical validation of predictive acceleration control on A parallel Hybrid Electric Vehicle*. PhD thesis, Colorado State University, 2022.

[289] Farhang Motallebiaraghi, Aaron Rabinowitz, Johan Fanas Rojas, Parth Kadav, Damon A Miller, Thomas Bradley, Rick Meyer, and Zachary Asher. Autonomous eco-driving evaluation of an electric vehicle on a chassis dynamometer. Technical Report 2023-01-0715, SAE Technical Paper, April 2023.

[290] 5g-enabled connected car to lead the automotive market by 2025. https://circuitdigest.com/article/5g-enabled-connected-car-lead-automotive-market-by-2025. Accessed: 2023-5-30.